Georgia Institute of Technology Team ARES

120 North Ave NW Atlanta GA 30332

Project Hermes

March 14, 2016

Table of Contents

1. Summary

1.1. Team Summary

Team Summary	
School Name	Georgia Institute of Technology
Mailing Address	North Avenue NW, Atlanta GA 30332
Team Name	Team Autonomous Rocket Equipment System (A.R.E.S.)
Project Title	Hermes
Launch Vehicle Name	Skyron
Project Lead	Victor R.
Safety Officer	Stephen K
Team Advisors	Dr. Eric Feron
NAR Section	Primary: Southern Area Launch vehiclery (SoAR) #571
NAR Contact, Number & Certification Level	Primary Contact: Joseph Mattingly
	NAR/TRA Number: 92646
	Certification Level: Level 2
	Secondary: Jorge Blanco

1.2. Launch Vehicle Summary

The *Skyron* launch vehicle features a resilient design that allows the completion of all the mission success criteria with a maximum 38% mass increase and an AeroTech L1390 motor. The current design however, utilizes an AeroTech L910 motor accounting for a total mass of roughly 25lb. Team A.R.E.S. successfully developed a modular design that integrates six subsystems performing their task independently with dedicated power supplies if necessary. The priority of the launch vehicle, other than achieving the system level requirements, is to ensure the safe performance of each component. The recovery system is comprised of a dual deployment system with redundant flight systems that ensure the descent rate of the launch vehicle is below 16ft/s, maintaining the total kinetic energy at impact below 75ft-lbf.

1.3. AGSE Summary

Team ARES' Autonomous Ground Support Equipment (AGSE) mission will be to secure the payload, raise the launch vehicle, and insert the igniter. The AGSE weighs 35 lbs, has a 10 ft. by 2 ft. base, and a starting height of 26 in. At full extension, the AGSE will be 10 ft. tall. The Robotic Payload Delivery System (RPDS), using servo motors, will deliver and secure the payload inside the launch vehicle. The Rocket Erection System (RES) will use a lead screw and acme nut design to raise the launch vehicle from a horizontal position to a position 5 degrees from the vertical. The Motor Ignition System (MIS) will use a rack and pinion system to insert the igniter. All functions of the AGSE will be controlled by an Arduino Uno. Electronics will be housed in the Electronics Containment Unit (ECU).

2. Changes Made Since CDR

2.1. Launch Vehicle Changes

Table 1: Launch Vehicle Changes

Subsystem	Design Change	Justification
GPS Bay	An independent section was created within the nosecone for the GPS, it will be insulated with aluminum foil to prevent signal interference.	The GPS transmit signals at 900MHz that pose a risk of signal interference with other subsystems.
Avionics Bay	New avionics bay configuration and fastening method.	Allows for better user interface and better accommodation of the electronics
ATS	Design was refined and finalized with high torque servo motors and 3D printed flaps	Allows for lower design complexity and eliminates possible points of failure.

Booster	Motor selection finalized as Cesaroni L910	Appropriate mission performance obtained with new selection
Recovery	Parachute resizing to reduce ground impact velocity	Total kinetic energy needed to be reduced due to the increased mass of the finalized design

2.2. AGSE Changes

Table 2: AGSE Changes

Subsystem	Change	Justification
RES	Spool and pulley system replaced by lead screw and threaded rod design	Less torque required from motor, and more stability during movement
RPDS	Claw design changed	Eliminate interference from screws
RES	Angle supports and more rails on the ground	Increase stability by increasing contact area with ground. Reduce bending in rails during RES actuation
RPDS	Servo motor mounts redesigned	Easier 3D printing and support removable, and tighter fit with servos
MIS	Ball bearings changed to slotted guide	Reduce unwanted motion during actuation
MIS	Added a launch vehicle stop to the launch vehicle rail	Keep the launch vehicle from shifting too far down the rail
ECU	Changed design and material from wood to acrylic	More compact, accessible, visible, and aesthetically pleasing

2.3. Flight System Changes

- No significant changes to the flight system computer, however the ATS is now using servo motors to control the flap direction

2.4. Project Plan Changes

Updated date to accurately reflect the status of the project

3. Launch Vehicle Criteria

3.1. Launch Vehicle Overview

The launch vehicle's purpose is to demonstrate the ability to retain a standard payload, effectively launch it one mile above ground level, and safely recover it. Skyron's design guarantees that it will be completely reusable by simply replacing the motor, and still manage to accomplish all the mission success criteria. The launch vehicle also features low complexity interfaces for the AGSE, as well as an efficient pre-launch systems check interface.

A 5 inch G12 fiberglass airframe provides a sufficiently wide platform to house every subsystem within independent sections. The platform also provides the structural integrity necessary to maintain high safety standards considering the incisions required for the interfaces of subsystems such as the ATS and the Payload Bay. A subscale test flight involving a 4 inch diameter launch vehicle occurred on November 21, 2015 to demonstrate the functionality of the launch vehicle design, as well as the effective integration of every subsystem. The full scale test flight occurred on March 12, 2016 with the objective of fulfilling the systems level success criteria, as well as ensure the safe operation throughout all phases of flight. The launch vehicle must demonstrate full capability to deploy the recovery system and maintain full structural integrity.
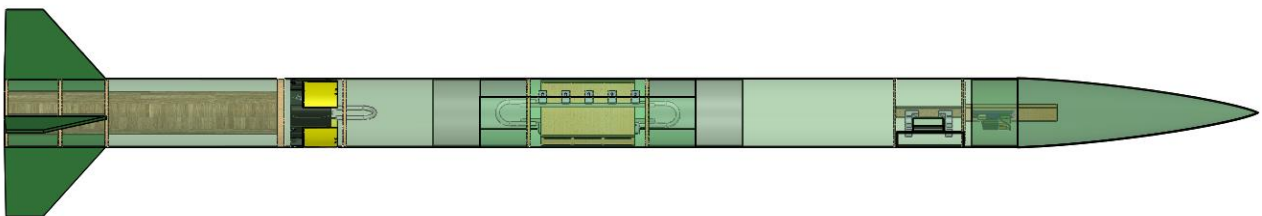
Figure 1: Side view of launch vehicle without recovery subsdyytem

3.2. Launch Vehicle Features

3.2.1. Nosecone GPS

The Nosecone GPS section of the Launch Vehicle consists of two primary parts- a bulkhead and a board that houses the Eggfinder GPS on the left side and the battery holder on the other side. Both the bulkhead and the board were laser cut from 1/4th inch thick plywood. The bulkhead had two slots which were 1" apart and each slot had a length of 1"and a width of 0.125". The GPS board of length 6.75" easily slid into the slots which provided it extra vertical stability. At first, the GPS board could not fit inside the slots due to a discrepancy between the thickness of the plywood and the width of the slots, hence the width was doubled to account for this discrepancy. Additionally, two holes of diameter 0.1" were constructed on the left side of the board at a distance of 2.9" from each other to accommodate for the Eggfinder GPS (.9"w x 2.25" l x .3"h). Four more holes were drilled on the right side for the inclusion of the 9V battery holder. Finally, the slotted bulkhead was epoxied with the upper bulkhead of the Launch Vehicle.
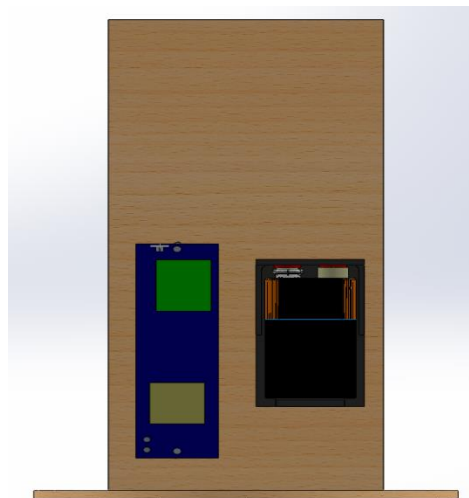
Figure 2: Bulkhead and Board with Eggfinder GPS, 9V Battery Holder and 9V Batteries
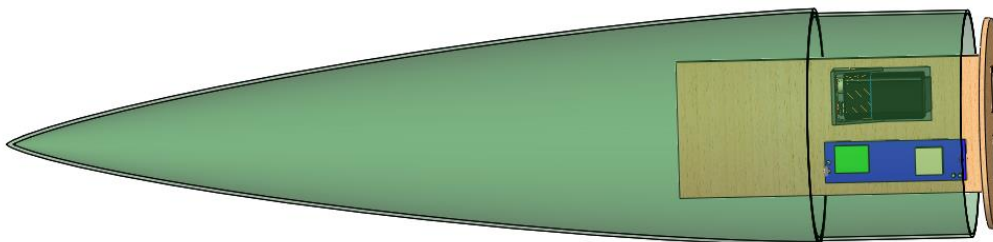
Figure 3: Side View of Nosecone GPS section
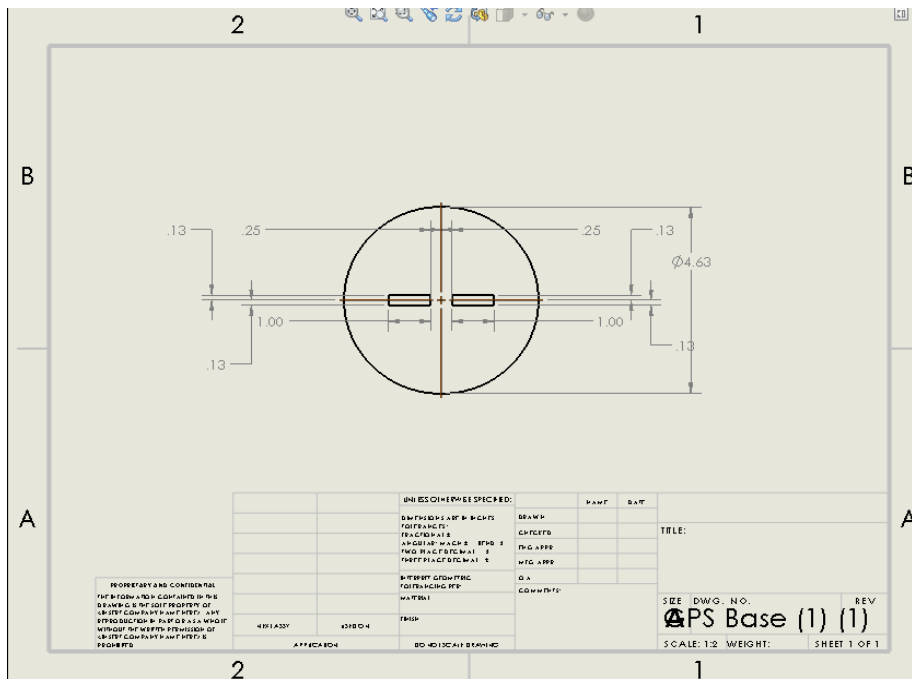
Figure 4: Engineering Drawing of Bulkhead
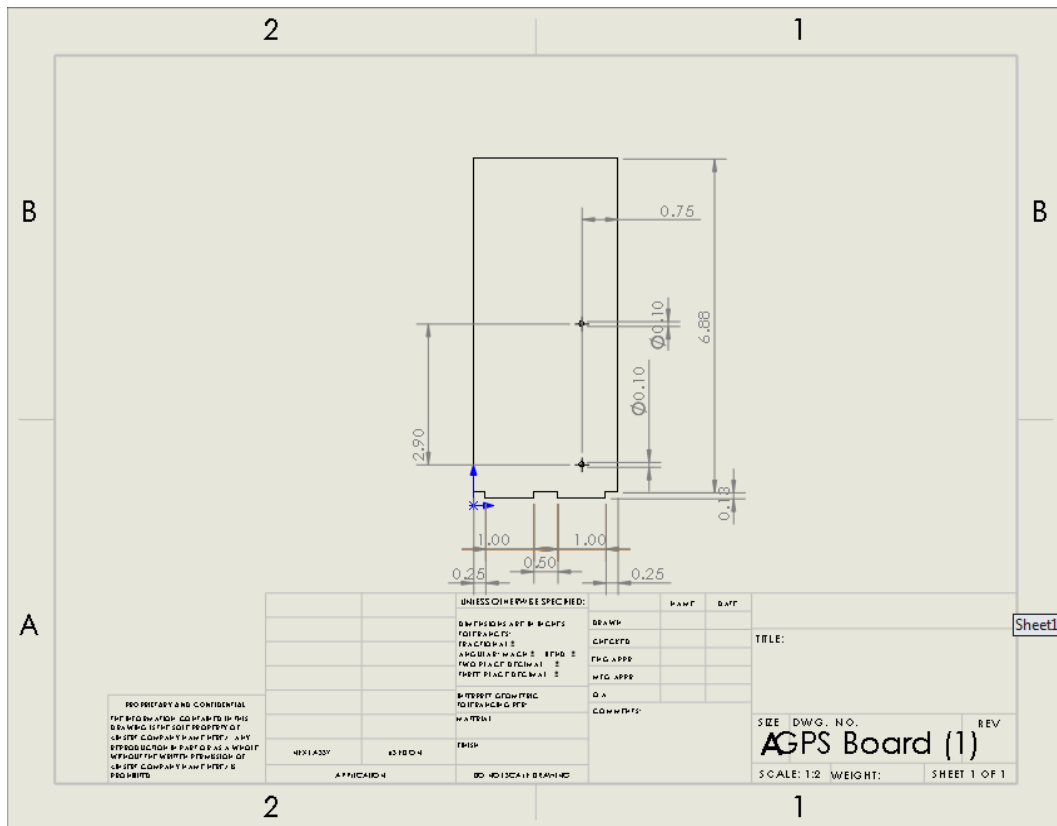
Figure 5: Engineering drawing of GPS board

3.2.2. Payload Section

Skyron's payload section is located just below the nosecone and houses the payload bay as well as the main parachute for the recovery system. Its primary purpose is to securely hold and transport a payload throughout the duration of the flight. The payload bay is constructed of two 0.25" plywood bulkheads connected by a rectangular sheet of 0.125" plywood. The rectangular base is joined to the two bulkheads by a series of slots as well as with the application of wood glue. Two payload locks, made of 3D printed ABS plastic, are attached to the rectangular base with four screws and nuts. On the fuselage enclosing the payload bay, a small 3 x 5" door is cut to allow easy access to the payload. The door rotates about a small hinge and is locked shut with magnets. This simple but effective design has plentiful structural integrity and provides a great foundation for the GPS section as well as U – bolts for the recovery system.

Figure 6: Solidworks Payload Section Assembly both top and bottom
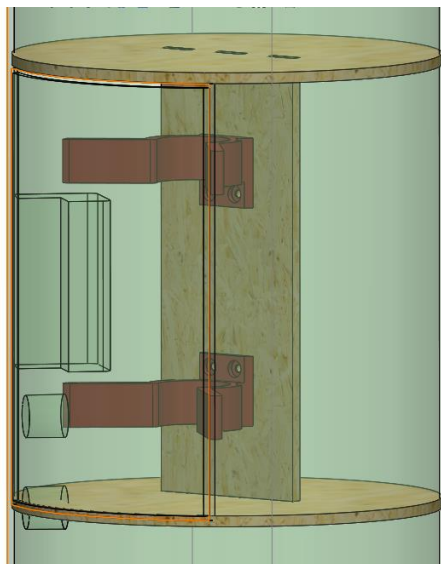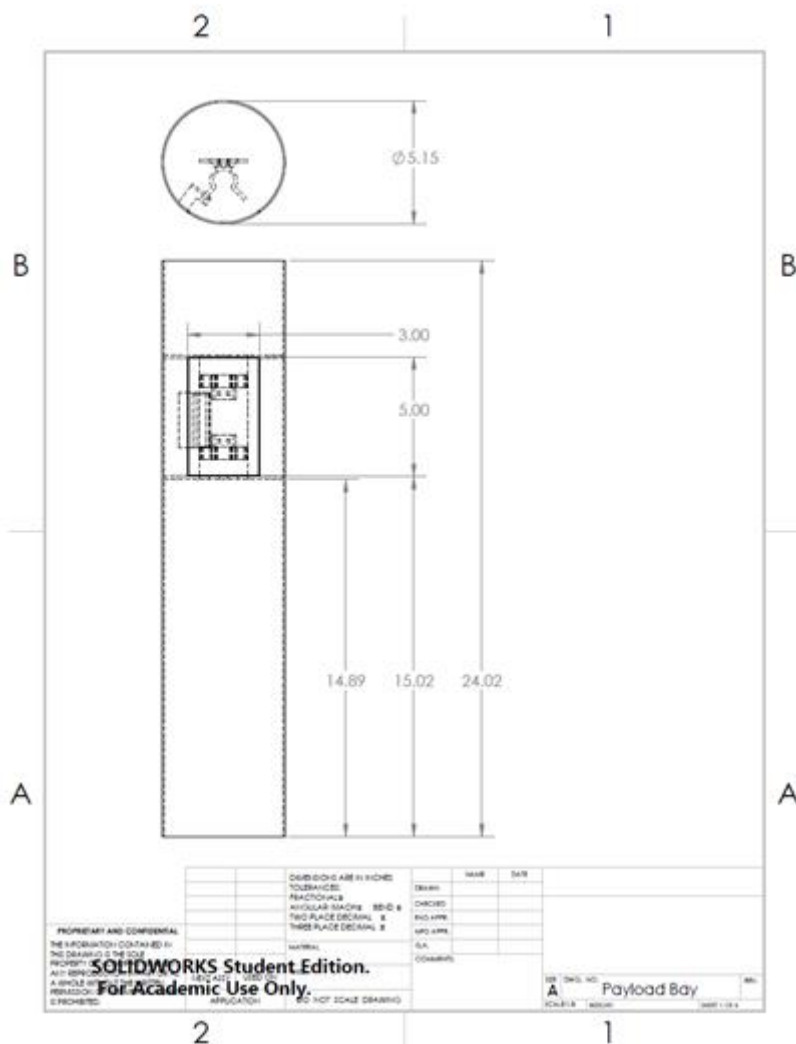
Figure 7: Payload Section Dimensions
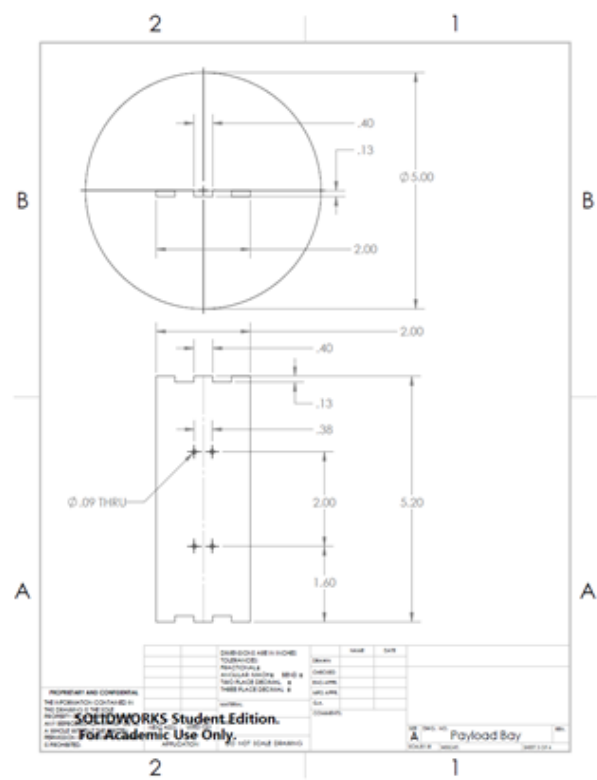
Figure 8: Payload Bulkheads and inner diameter

Figure 9: Payload Lock Dimensions
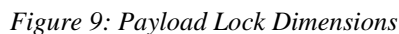
3.2.3. Avionics Bay

Skyron's avionics bay houses the following avionics mission critical components- stratologgers, accelerometer, MBED microcontroller and various 9V alkaline batteries to power the the entire avionics unit and the ATS. It also contains the main and drogue parachutes as well as blasting caps to deploy these parachutes. A complete component list can be found below in Table 3. With such a large number of electric components, the design process included making   Since this section has a large number of electronic equipment, the design of the avionics bay must include important safety and security features so that the electronics are not compromised during flight, installation and/or recovery.

The airframe of the avionics bay is constructed from G12 fiberglass tubes. The Avionics Bay measures 16.3 inches in length and is attached to the rest of the launch vehicle using G12 fiberglass couplers. One of the primary features of the Avionics bay that distinguishes it from other sections of the launch vehicle is its removable airframe section. The removable airframe section allows the operator to access the launch vehicle's electronics without completely disassembling it. The fixed half of the airframe is held in place by screws, which connect the plate to the rest of the launch

vehicle. The tabs which are 10 in number are epoxied to the inside the launch vehicle to prevent them from disrupting the airflow over the launch vehicle during flight. The tabs were 3D-printed out of ABS plastic. This plastic was chosen for its rigidity, high melting point and low response to deformations. The tabs are 0.52" inch long and 0.05" inch in thickness. They are curved to match the inner diameter of the airframe. Both the fixed portion of the airframe and the tabs have ⅛" holes 5 on each side of the airframe.

The avionics bay consists of a board system manufactured out of 2 vertical avionics ⅛" plywood boards on which the avionics equipment described in are securely screwed on. Additionally, the 2 slotted backboards are made of plywood and are epoxied to the inner diameter of the 2 airframe sections of the avionics bay to hold the avionics boards in the axial and lateral directions. The avionics boards are 7" in length and 4.72" in width and the slotted backboards are 7" in length (same as avionics board) and 1.38" in width.

Table 4: List of avionics components with quantity and functions

Name (x number)	Function
Stratologger SL100 x 2	Altimeter - used to receive and record altitude
MMA8452Q- Accelerometer x 1	Accelerometer - used to receive and record acceleration
mbed LPC 1768 x 1	Microcontroller - used to receive sensor data to compute and control the ATS
9V Alkaline Batteries x 6	Used to power all Avionics components and ATS
AAA battery x 1	Power supply for mbed

!Unexpected End of Formula
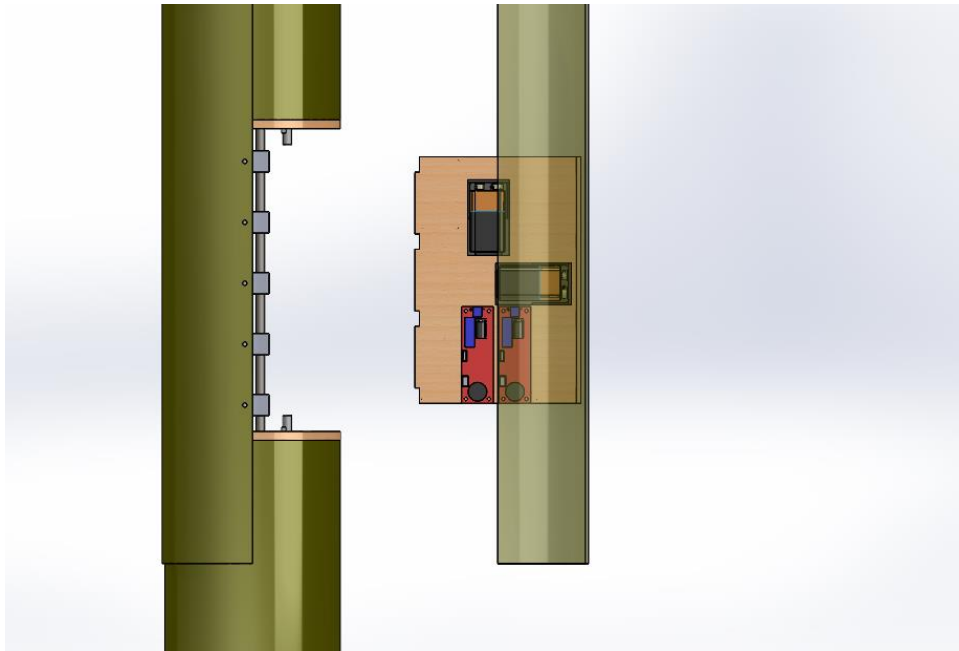
Figure 10: Avionics board placement on detachable airframe
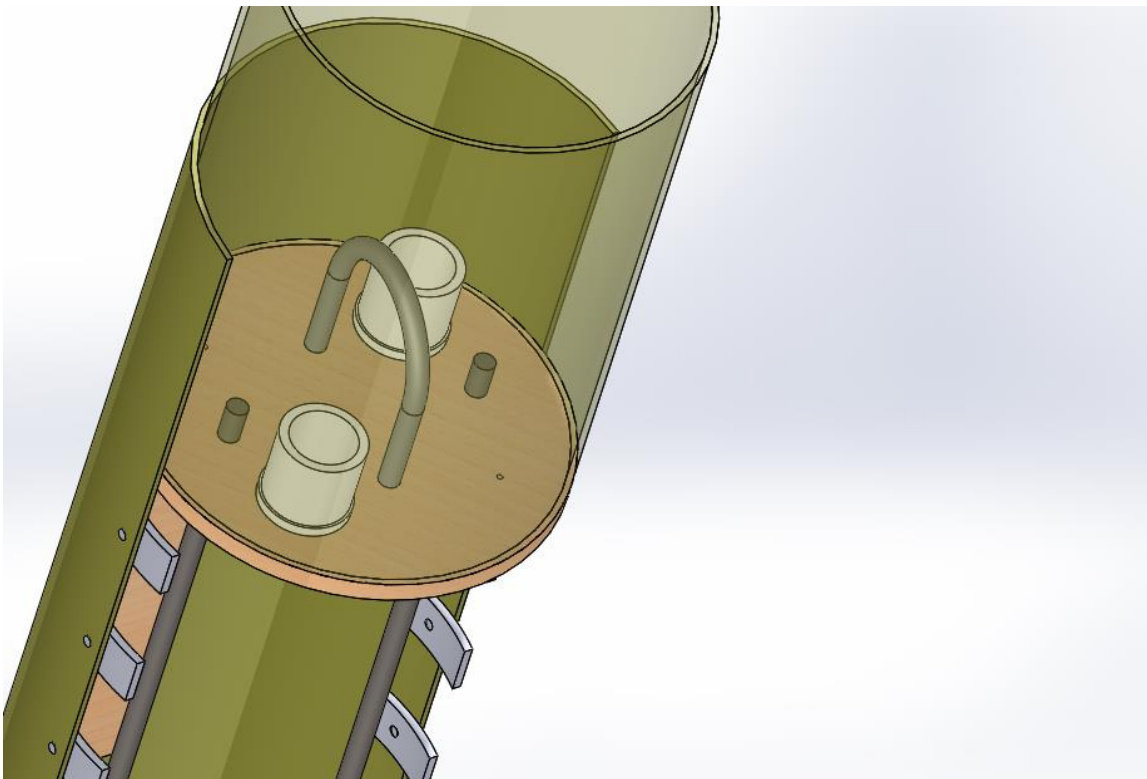
Figure 11: Upper bulkhead location on avionics bay with U-bolt and blasting caps
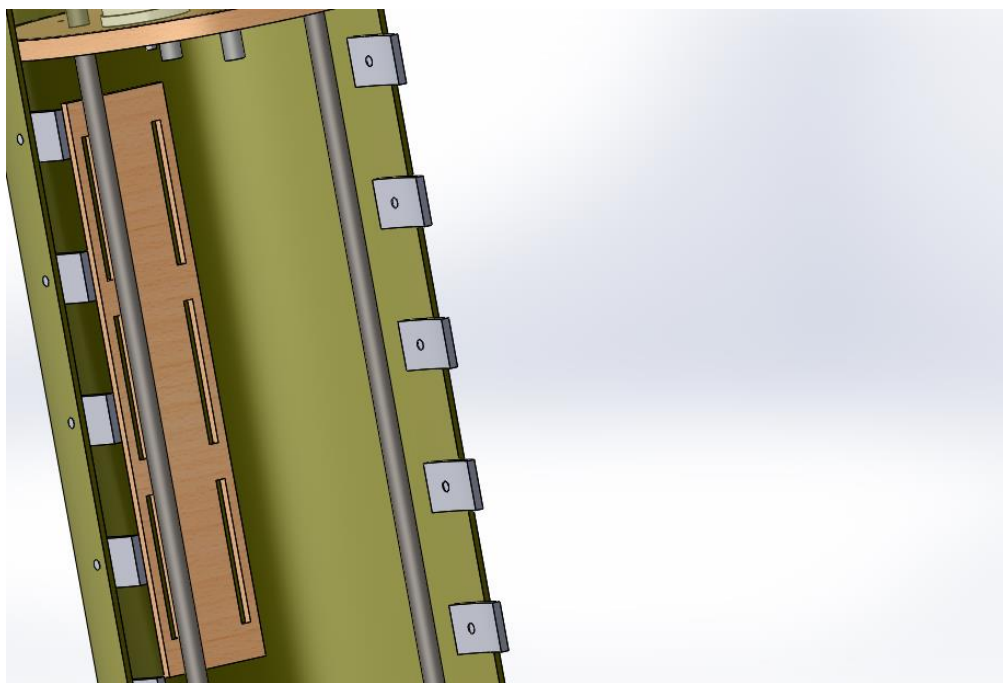
Figure 12: Fixed airframe section with threaded rods, tabs and slotted backboard
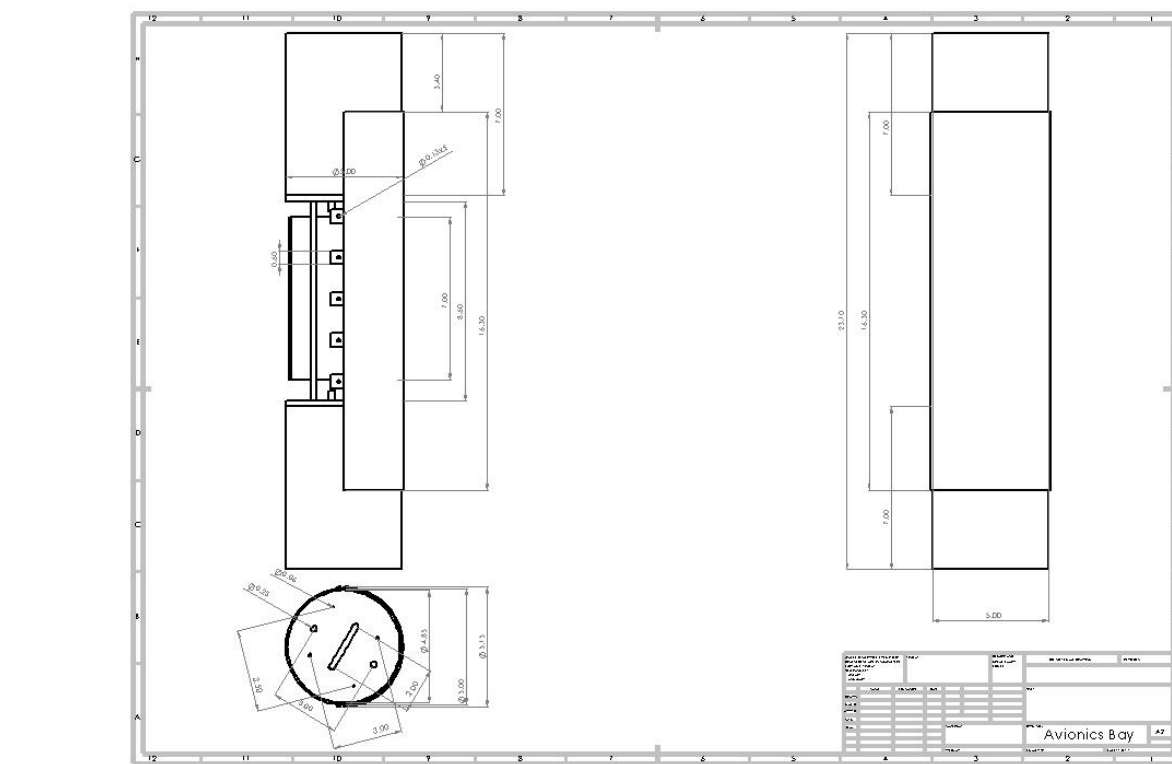
Figure 13: Engineering Drawing of Avionics Bay

3.2.4. Booster Section

The booster section (Figure 14) houses the Cessaroni L910 Motor. Skyron's propulsion system will be contained within an AeroTech Pro75/3840 3G casing, which is cross compatible with CTI 75in motors. A spacer will have to be incorporated to the assembly given that the Cessaroni L910 is a 2 grain motor. A complete list of the booster section components can be found below in Table 5. The thrust plate, which will hold the motor and the motor casing in place and prevent the motor from travelling straight through the launch vehicle, is manufactured from ½" plywood. The centering rings were manufactured out of ¼" plywood using a laser cutter based off SolidWorks models. Plywood was selected over fiberglass due to its light weight, reliability, and cost. The motor mount tube, which houses the motor in the motor casing, was manufactured out of a cardboard tube with an outer diameter of 3.189 inches. During manufacturing, the centering rings were epoxied to the motor mount tube. To ensure the centering rings were at the correct height on the motor tube, a model fin was used to align the centering rings with the fin slots.
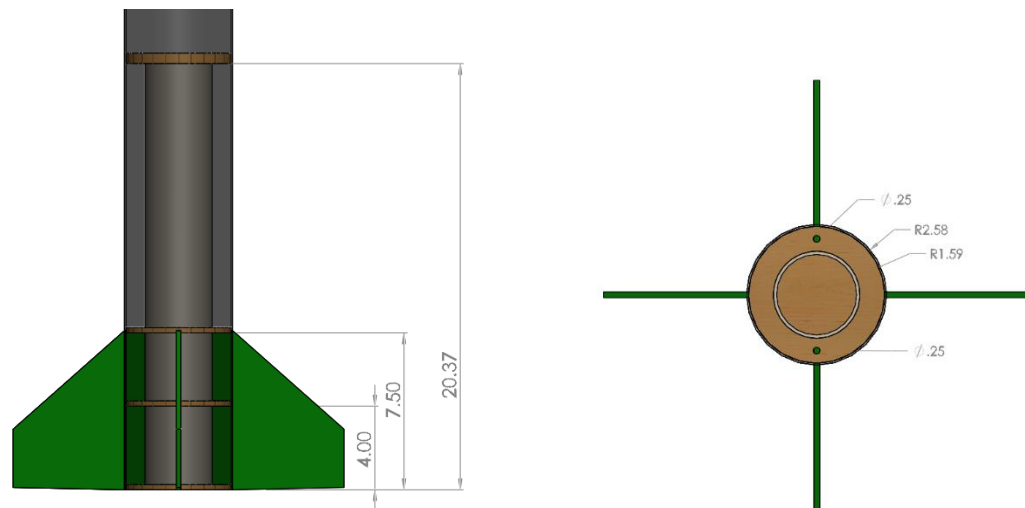
Figure 14: Booster Section
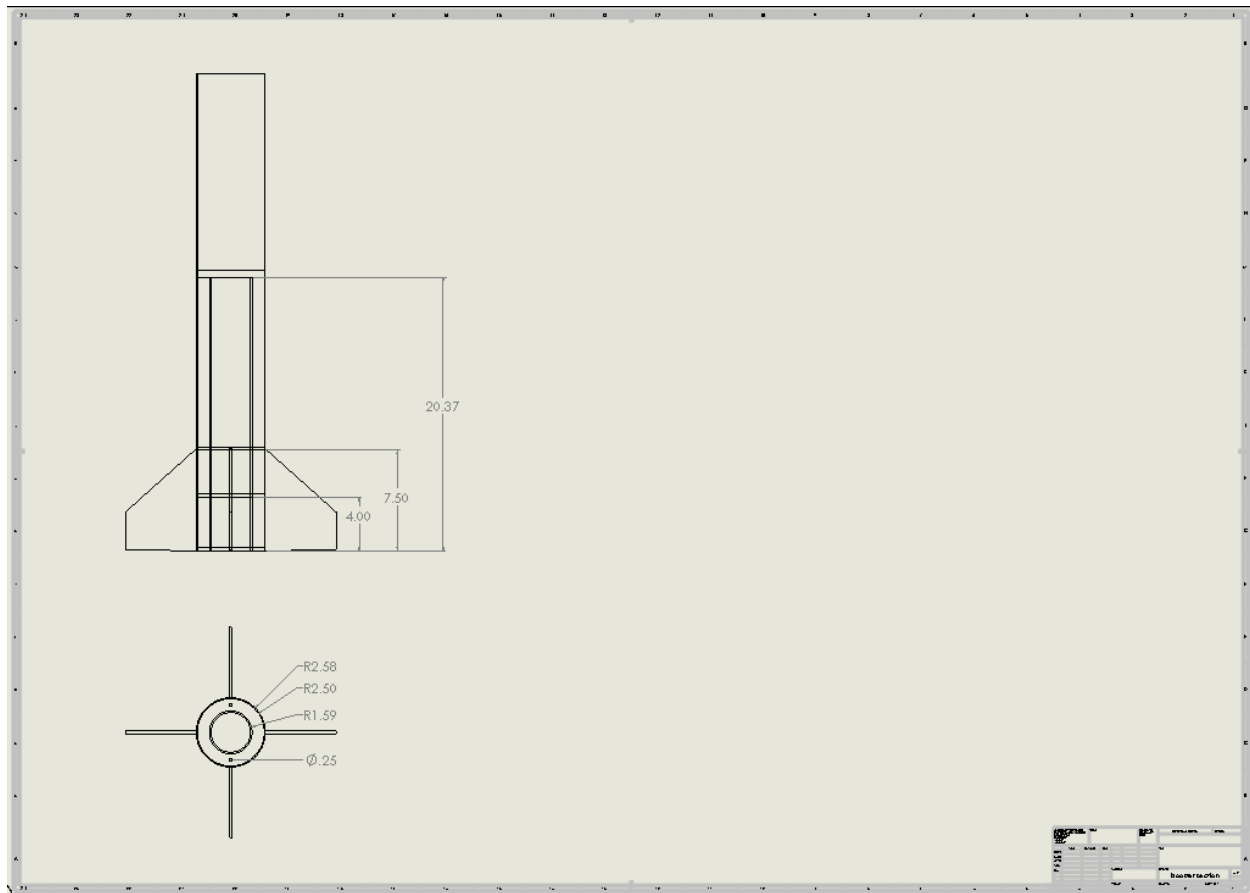
Figure 15: Engineering Drawing Booster Section

Figure XX: Booster Section - Engineering Drawing

Table 5: Booster Section Components

Freeform G12 Fin Set	Cessaroni L910 Motor
Cardboard Inner Tube	G12 Fiberglass Airframe
Centering Ring (Bottom)	Thrust Plate
Motor Retention System	Aerotech Pro75/3840 3G Motor Casing
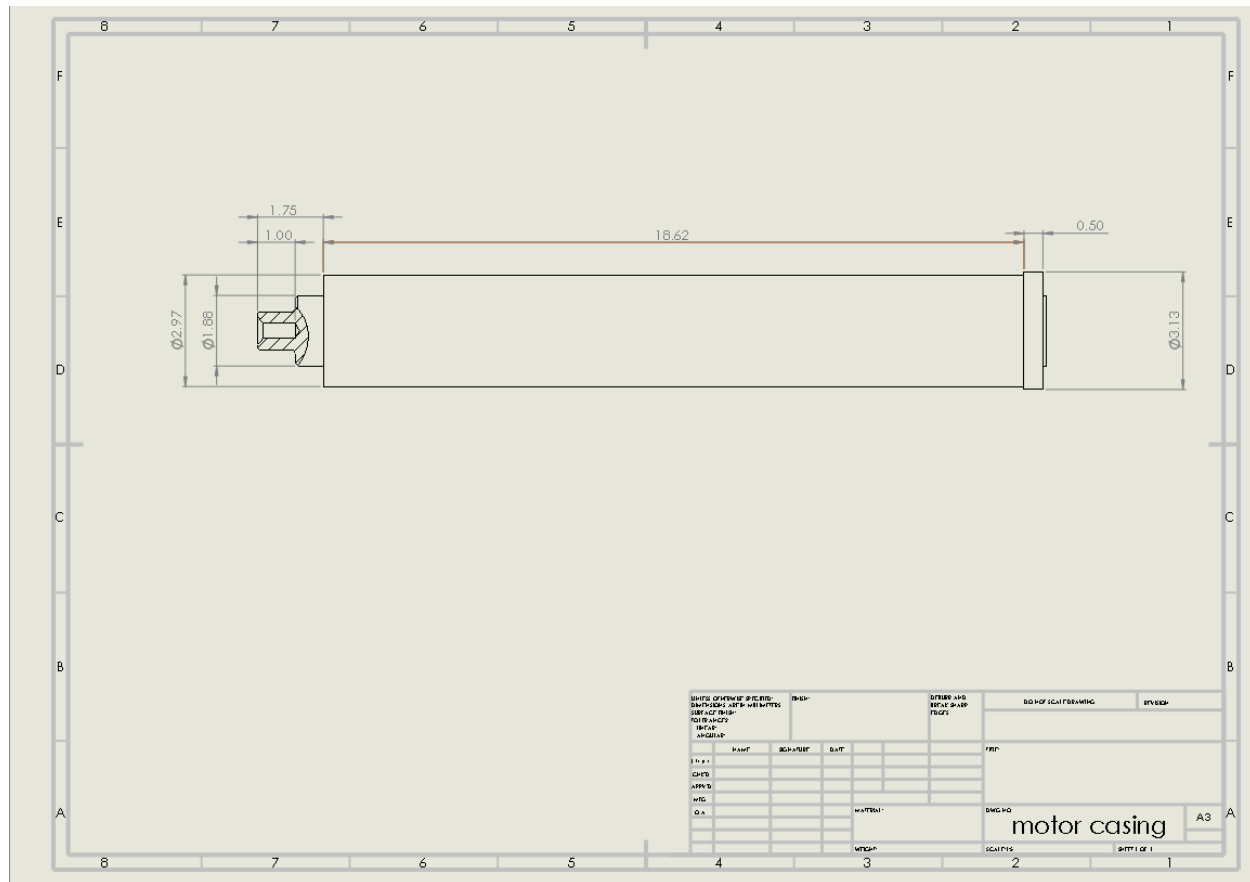
Figure 16: AeroTech Pro75/3840 3G motor casing Dimensions

3.2.5. Fins

The fins will be made using G10 Fiberglass as the material of choice. Initially, the fins were attempted to be made with a smooth airfoil shape in order to improve the aerodynamics of the fin. Due to complications in the sanding process, it was determined that the smooth airfoil shape would be unreasonable for the fins. The main problem came from the fact that G10 Fiberglass is not one solid material, but multiple layers on top of each other. During sanding, it was assumed that the layers would begin to peel apart from one another.
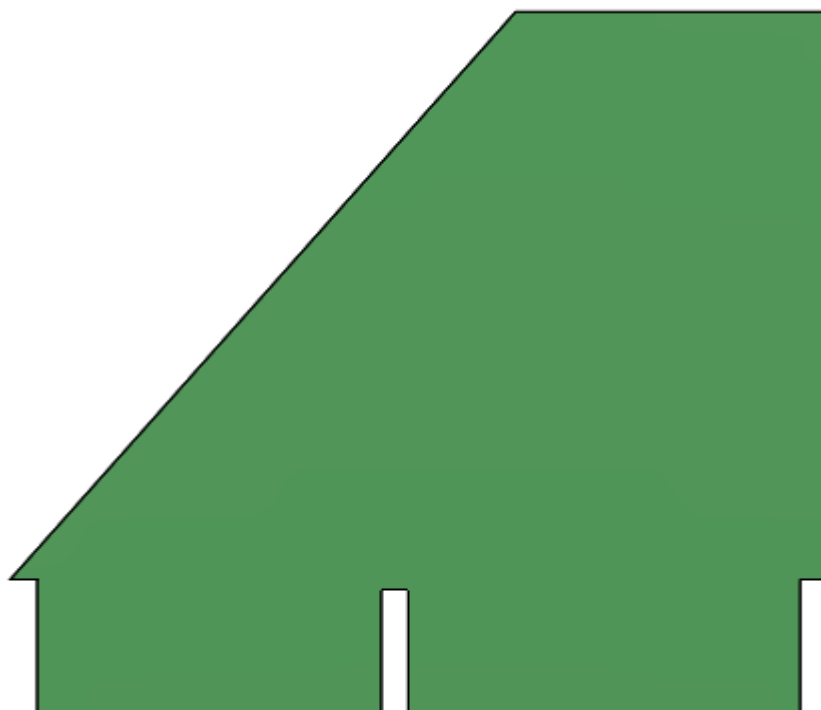
Figure 17: Launch Vehicle Fin

Table 6: LV Fin dimensions

Parameter	Value
Overall Length	93.6 in
Booster Section	35.5 in
Avionics Section	16.1 in
Payload Section	24 in
Body Diameter	5 in
Nose Cone Length	18 in
Fin Height	5.3 in
Fin Root Chord	7.5 in
Fin tip Chord	3.1 in

Table 7: Parameters of the launch vehicle

Parameter	Value
Payload Bay	6.2 in
GPS Module	3 in
Avionics Bay	9.1 in
ATS	6 in
Motor Casing	25.8 in
Couplers	7 in
Bulkheads & Centering Rings (Thickness)	0.25 in

The fin has a clipped delta fin shape which was determined as the most viable option for a rocket with four fins. With four fins, the stability of the rocket will increase as opposed to using only three fins (stability is expected increase by slightly over 50%). The fin flutter speed was calculated using the Flutter Boundary Equation published in NACA Technical Paper 4197:

$$V_f = a \sqrt{\frac{G}{\frac{1.337 AR^3 P(\lambda + 1)}{2(AR + 2)(\frac{t}{c})^3}}}$$

The corresponding variables for our fin are listed in Table XX located below. The fin flutter speed was calculated to be 1326.109 mph. Comparing Vf to our maximum velocity Vmax of 552.148 mph (0.72 Mach), Skyron will not experience the unstable effects of fin flutter. Exceeding the fin flutter speed would exponentially amplify the oscillations and rapidly increase the energy in the fins.

Table (). Fin dimensions

Variable	Unit
Speed of Sound, a	1105.26 ft/sec
Pressure, P	13.19 lb/in^2
Temperature, T	48.32 Fahrenheit
Shear Modulus, G	425,000 psi
Taper Ratio,	0.3627

Tip Chord	7 cm or 2.75591 in
Root Chord	19.3 cm or 7.598 in
Thickness	0.318 cm or 0.1252 in
Fin Area	55.23 in^2
Span	13.4 cm or 5.275591 in
Aspect Ratio	0.50392

3.2.6. Apogee Targeting System

3.2.6.1. Mechanism

The Apogee Targeting System (ATS) has been modified from the previous lead-screw design in the Critical Design Review due to a change in motor selection and resulting changes in the dimensions of the ATS section of the booster body tube.

The ATS consists of four Tower Pro MG995 servo motors, each individually powered by one 9V battery. The servos will each rotate a metal rectangular arm (Figure 18) when needed to extend the 3D printed tabs (Figure 19) and decrease the apogee. The rotation of the servos will be determined by the mBed microcontroller and the software's control algorithm. The arms' rotations will push the ATS tabs to a maximum extension of forty-five degrees about their hinges as seen in Figure 20. The ATS tab extension will increase the drag of the Skyron, thereby decreasing the apogee. The tab hinges are located 24.85 inches from the bottom of the launch vehicle and are centered between the fins to lessen any turbulent effects on the flow over the fins created in the tabs' wakes as seen in Figure21. The servos are each secured and aligned by a 3D printed servo mount (Figure 22). By using an alignment piece (Figure 23) that was 3D-printed to create equal spacing between the servo mounts, we ensure that the servos are aligned with grooves in the 3D printed tabs as seen in Figure 23.

Figure 18: ATS Arm Attached to Servo

Figure 19: ATS Tab - Engineering Drawing
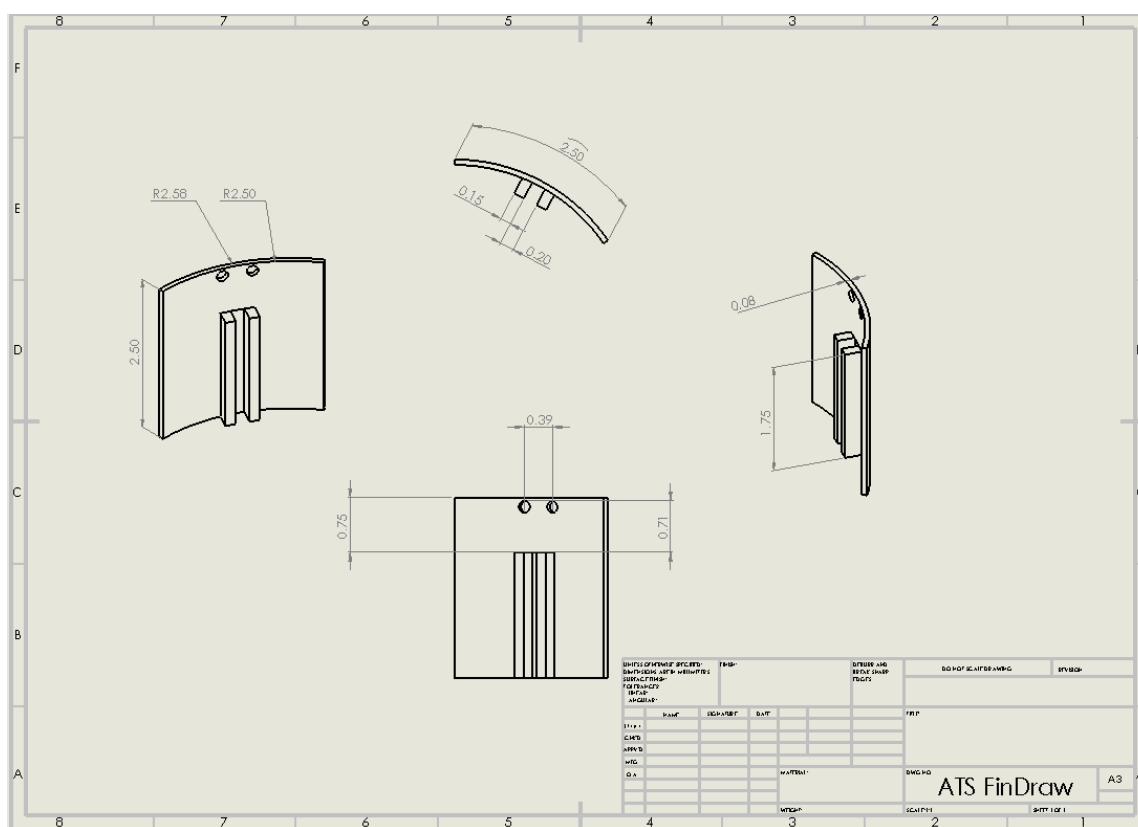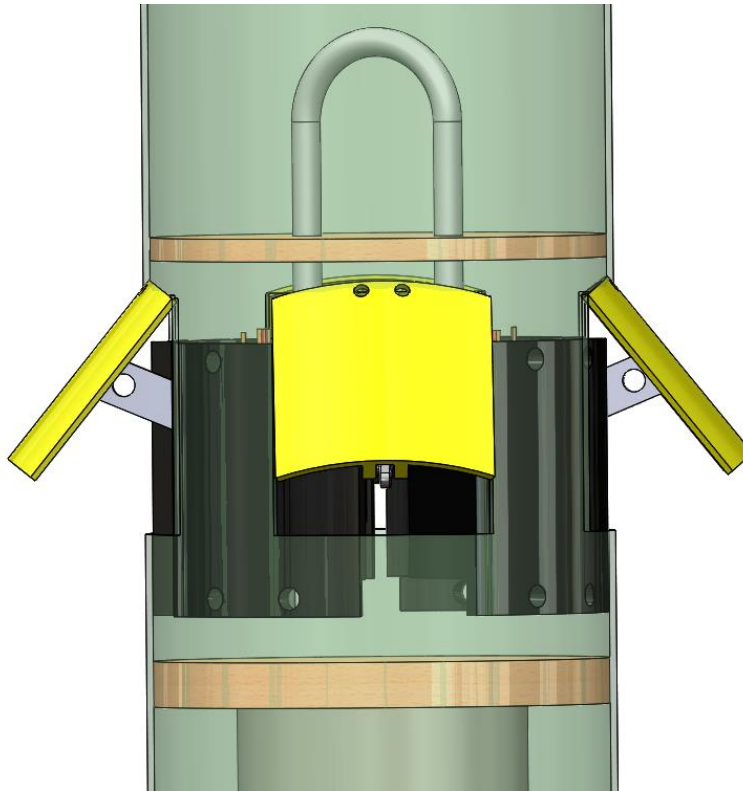
Figure 20: ATS Tabs fully deployed to 45 degrees, side view
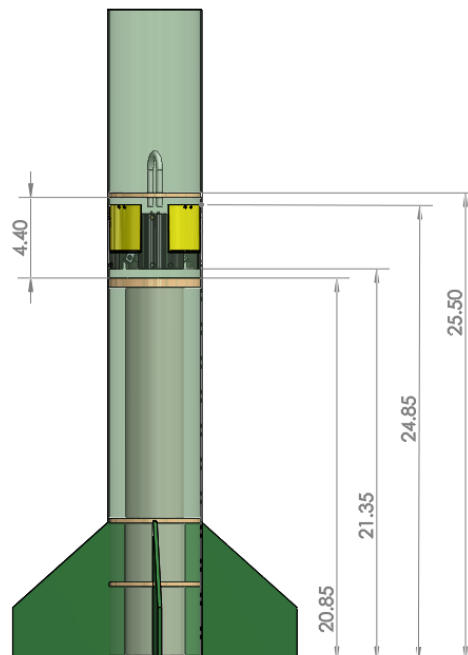
Figure 21: ATS Placement in Booster Section
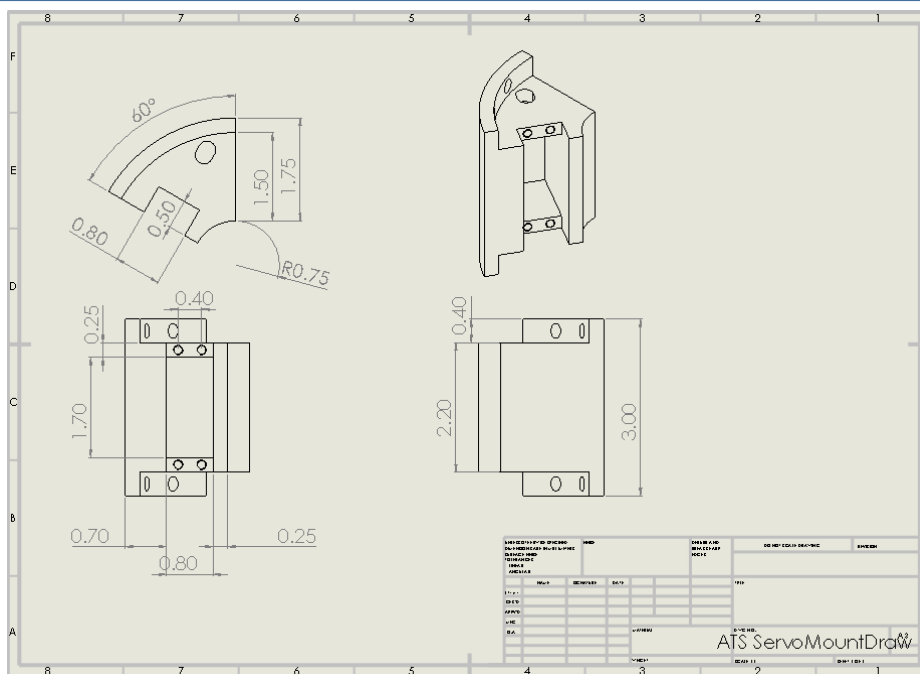
Figure 22: Servo Mount - Engineering Drawing
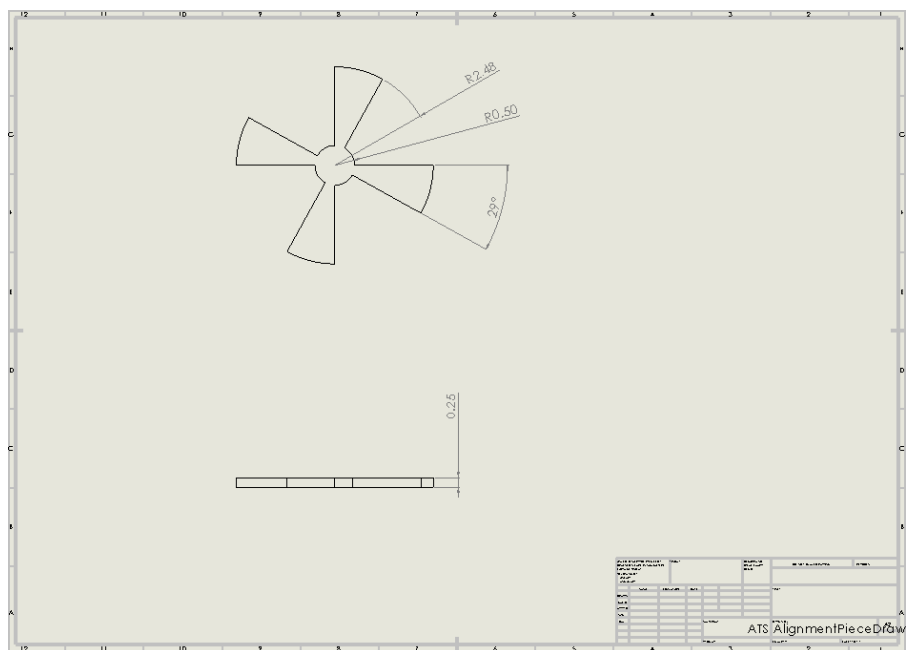
Figure 23: ATS Alignment piece - Engineering Drawing

Figure 24: Servo and Servo Mount Placement
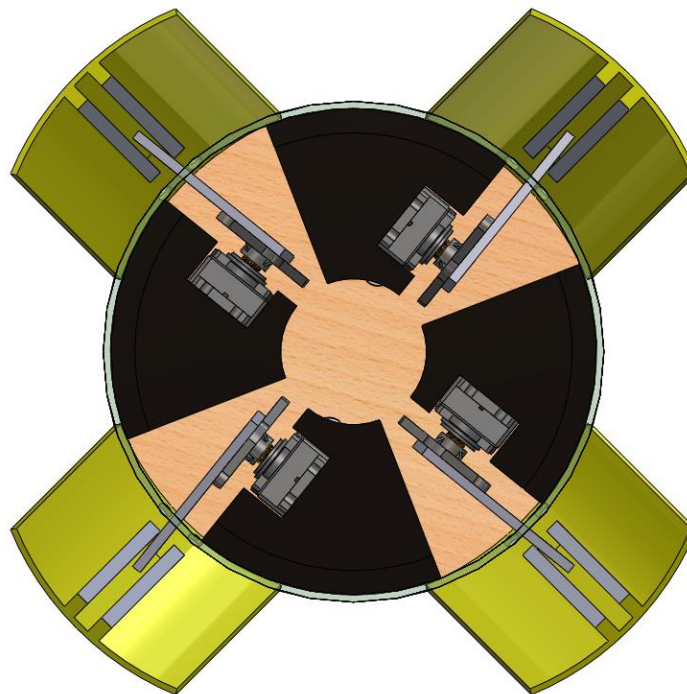
Figure 25: Fully Deployed ATS bottom view
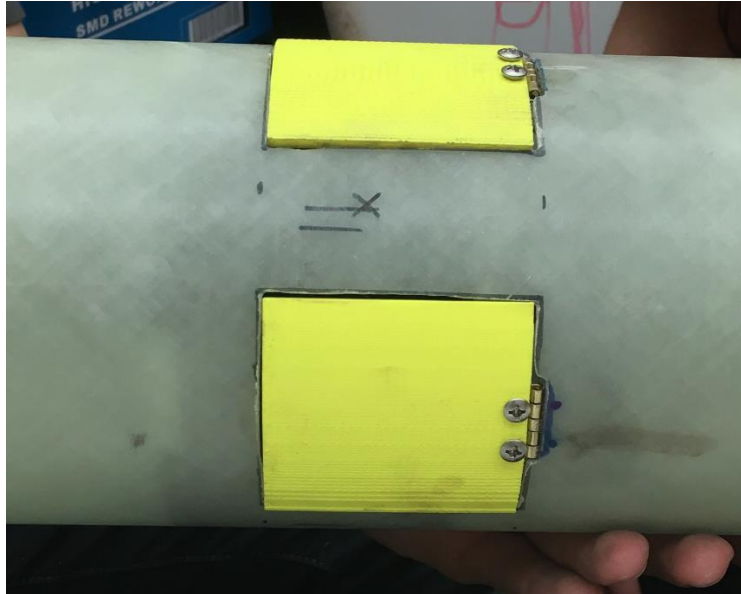
Figure 26: Fully retracted ATS tabs

3.2.6.2. Electronics

The ATS function will be controlled by the 32-bit ARM microcontroller, which is being used as the flight computer. Based on the the flight systems software's control algorithm, a PWM out (pulse-width modulated) will be sent to the 4 servo motors telling them whether to actuate the flaps or not. If the output of the microcontroller to a motor is a '1', then the servo motor will actuate a flap. If the output is '0', then a motor will retract a flap. The control algorithm outputs a '1' or a '0' based on the control algorithm shown in Figure 27, which shows the control is based on a the change in height of the rocket added to the derived change in velocity.

```
s = (lambda * delta_h) + delta_v;
*control = (sign(s) + 1)/2;
```
Figure 27: controlling flaps equations.

3.2.6.3. Power

Each of the four MG995 servo motors are individually powered by a 9 Volt battery located in the battery casing in the avionics bay. To connect the ATS system to the battery housing, the PWM cables are encased in a heat shrink tube and run along the edge of the inner diameter of the fuselage from holes through the servo mounts and up to the avionics bay. The PWM cables are designed to

separate when a significant tension force is applied when the first separation occurs at apogee. The cables are protected by the insulating material as well as the heat shrink tube to prevent their malfunction after multiple test flights

3.2.7. Recovery System

A dual deployment recovery system will be used on the launch vehicle in order to maintain an acceptable drift profile, as well as to mitigate the impact Kinetic Energy on landing. This is done in order to minimize structural damage to the launch vehicle assembly and ensure that Skyron is recoverable. A main parachute of 80" in diameter and a drogue of 30" in diameter was found to limit the impact KE values to under 75ft-lbf for the largest sections of the launch vehicle. In addition to this parachutes were also selected to support the weight of the launch vehicle. Parachutes will be made of rip-stop nylon and secured to U-bolts via 30 kevlar shock cords of total length 30ft. The parachutes will then be carefully folded and packed into their various pressurized housing compartment where they will be sealed off from other section of the launch vehicle and fireproofed using NOMEX shielding.

Ejection charge calculations were done and the size of the shear force needed to separate each compartments was determined so that efficient deployment occurs upon reaching projected altitudes.
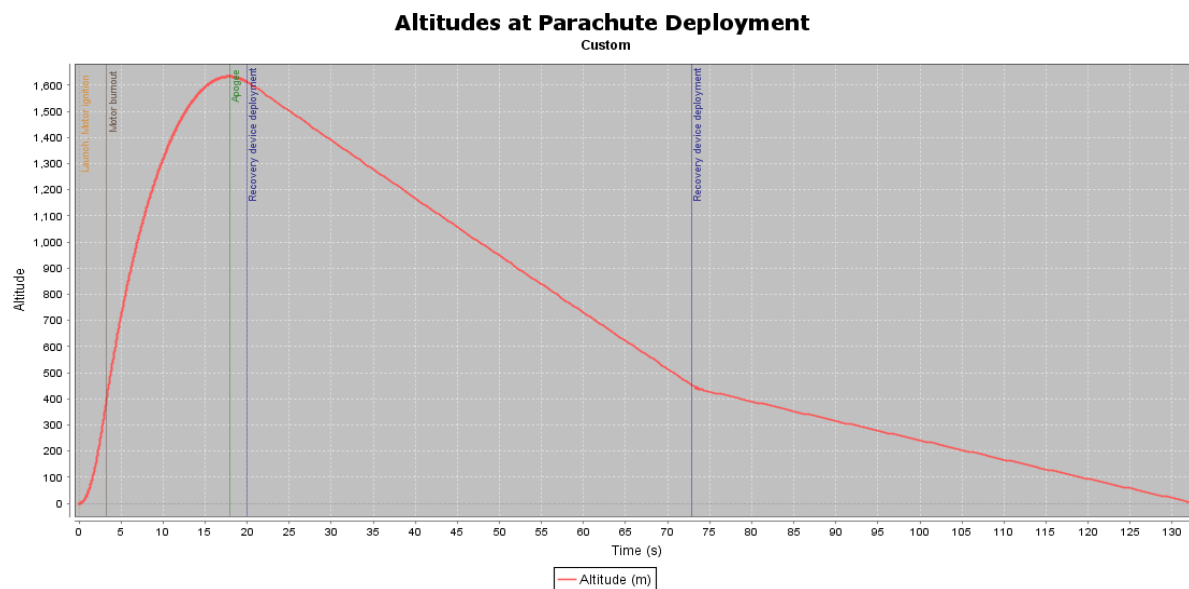
Figure 28: Altitude at Parachute Deployment for ideal wind speeds

3.2.8. Final Motor Selection

Despite originally using a Cesaroni L990 in the Critical Design Review, Team ARES ultimately opted for a Cesaroni L910. The decision to switch motors was based on two main factors: the L910's geometry and its influence on the launch vehicle's overall flight profile.

The team chose the Cesaroni L910 as a replacement based on two factors.–Most importantly, however, the change facilitated the placement of the Apogee Targeting System in the upper booster section. The L910 is shorter by 30cm, and this change in motor length significantly loosened the geometric constraints on the ATS placement and overall dimensions of the system.

Nevertheless, the L910 motor's average thrust was 907.1 N, leaving the launch vehicle with a new projected apogee of 1.04 miles. More dimensions and information about the L910 motor can be found in Table 8. Thus, despite substantial differences in geometry and thrust profiles, the Cesaroni L910 proved a more efficient path towards mission success. The official Cesaroni L910 thrust curve is seen below in Figure 29.

Table 8: L910

Cesaroni L910	
Diameter	75.00 mm
Length	35.0 cm
Propellant Weight	2.616 kg
Overall Weight	1.270 kg
Average Thrust	907.1 N
Maximum Thrust	1086.1 N
Total Impulse	2,856.1 N-s
Specific Impulse	229 s
Burn Time	3.2 s
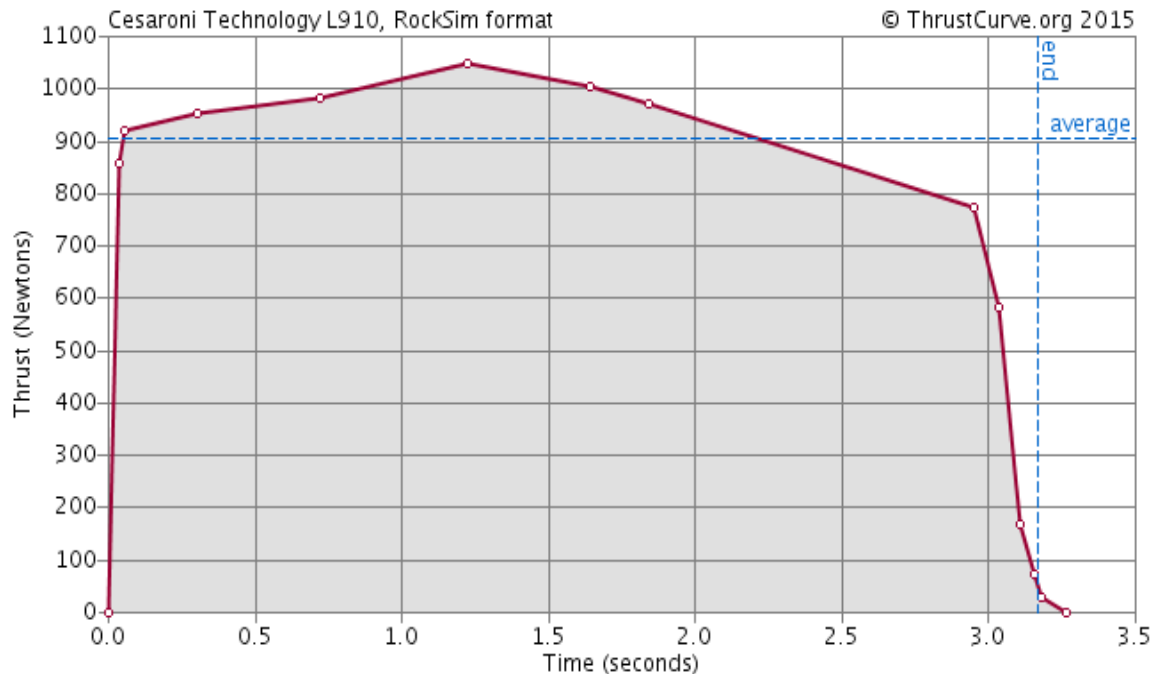
Figure 29: Cesaroni L910 thrust profile

3.3. Structural Elements

3.3.1. Structure Components Analysis

The main structural components of the Skyron are the body tubes, couplers, nose cone, fins, bulkheads, centering rings, and thrust plate. The body tubes, couplers, nosecone, and fins are made out of G12 fiberglass. G12 fiberglass is being used for its high ultimate breaking point and its ductility, which allows the launch vehicle to have more flexibility. This means the launch vehicle, especially thin structures such as the fin, is more likely to stay intact during a soft or hard landing without cracking as compared to previously used materials, like carbon fiber. The bulkheads, centering rings, and thrust plate of the launch vehicle were manufactured with plywood. The bulkheads and centering rings were made of 1/4 inch plywood and the thrust plate of 1/2 inch plywood. Plywood is much cheaper than fiberglass and it can meet expected standards of performance at maximum thrust. The use of plywood has also been proven to be more efficient in use with the machinery we have at hand, such as with the laser cutter, since we have already cut bulkheads, centering rings, and thrust plates using plywood for the subscale and full-scale test launches in relatively short time.

3.3.2. Thrust Plate Analysis

The Motor Retention Plate, which will hold the motor in place and prevent the motor from travelling straight through the launch vehicle, will be manufactured from ½ " plywood. To ensure that the maximum thrust of the motor does not penetrate and create enough displacement to cause problems, we simulated the stress on the motor retention plate using Finite Element Analysis. Finite Element Analysis (FEA) is a numerical technique used for finding approximate solutions to partial differential equations. This technique is useful for theoretical analysis of design components. Solidworks utilizes this technique to perform basic FEA, and was used to analyze the thrust plate, shown in Figure 30.
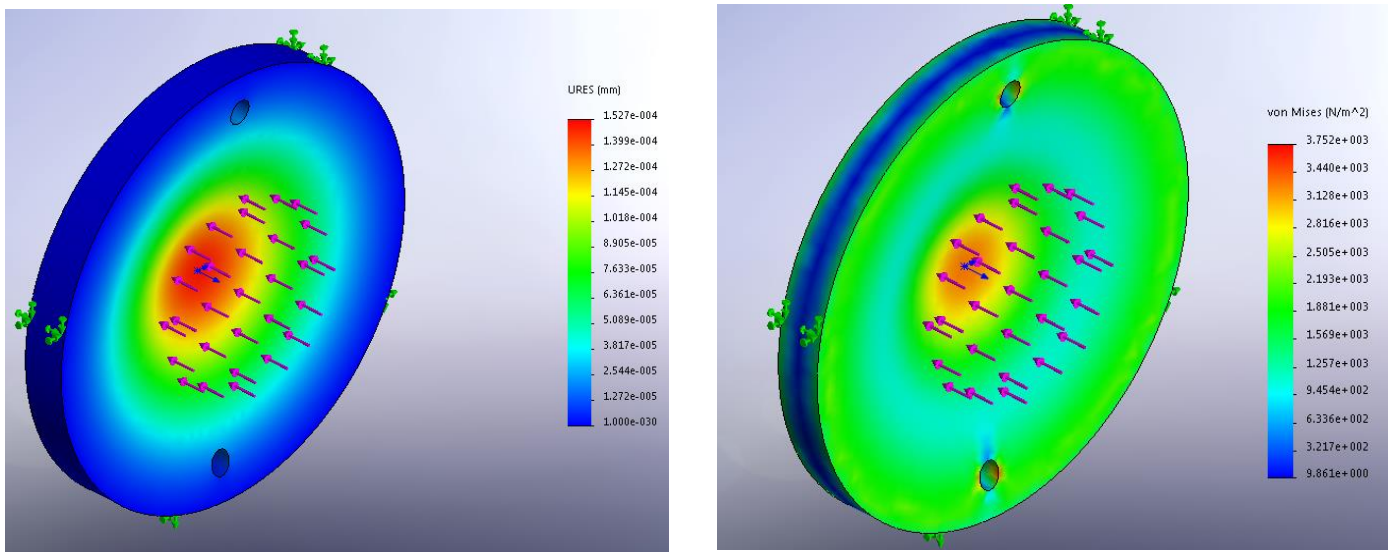
Figure 30: FEA Thrust Plate

The force applied corresponds to the maximum thrust the L910 can produce, which is 244.16 lbf. The maximum displacement of the thrust plate was 0.01 inches with a maximum stress of 375 N/m^2. The figures were scaled to emphasize the displacement.

3.4. Mass Breakdown

3.4.1. Skyron Mass Breakdown

All of the components of the Skyron and their relative masses are listed in Table 9 and in Figure 31 with the following subsections, Structures, Recovery, Propulsion, ATS, or Avionics. Each component was divided into their relative subsystem in a logical fashion, such as the nosecone, body tube sections, and fin masses being included in the Structures subsystem because they are main structural elements or the drogue and main parachute masses being included in the Recovery subsystem because they are vital recovery components.

Table 9: Mass Breakdown

Subsystem	Component	Units	Mass/Unit (g)	Total
	Nosecone	1	681	681
	Upper Section	1	886	886
	Avionics Section	1	594	594
	Booster Section	1	1310	1310
	Coupler	2	215	430
	Fin	4	225.5	902
	Centering Ring (1/4")	3	27.4	82.2
	Thrust Plate (1/2")	1	103	103
	Bulkheads (1/4")	5	47.5	237.5
	Inner Tube	1	65.9	65.9
	U-Bolt (w/ nuts)	4	21.6	86.4
	Payload Bay Board	1	14.45	14.45
Structures	Payload Retainers	2	3.2	6.4
Recovery	Drogue Parachute	1	36.3	36.3

	Main Parachute	1	173	173
	Blasting Caps	4	5.4	21.6
Propulsion	Motor (L910)	1	2615.8	2615.8
ATS	ATS Housing	4	20.5	82
	ATS Guide Rails (4"x0.25")	4	21	84
	12V DC 6000RPM Electric Motor	4	64	256
	9V Battery	8	45.6	364.8
Avionics	Insulator	1	7	7
	Terminal Blocks	3	2	6
	mBed IPC 1768	1	12	12
	Altimeter SL 100	2	12.75	25.5
	Hbridge (Motor Driver)	2	1	2
	GPS Eggfinder	1	20	20
	Breakout Pins (long)	2	2.8	5.6
	PVC Guide Rails (1.5"x0.5")	2	6.8	13.6
	Threaded Guide Rails (4"x0.25")	2	18.95	37.9

Raw Total	9161.95
Total w/ Error Margin (25%)	11452.4375
Total w/o Propellant	10083.4375
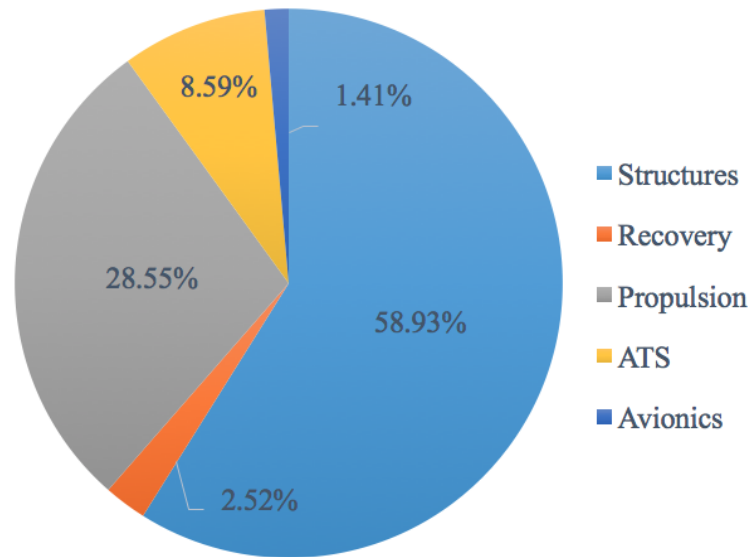
Figure 31: Visual representation of the subsystems and their relative mass percentages

3.5. Mission Performance

3.5.1. Mission Performance Overview

3.5.2. Mission Performance Criteria

The target is to achieve an apogee of 1 mile (5280 ft) as stated in the student launch handbook. Skyron is designed such that the launch vehicle could reach a higher altitude. This overshoot provides a margin for any adverse flight conditions. The apogee targeting system will deploy to ensure that Skyron does not exceed its goal.

3.5.3. Mission Performance Predictions

The flight model predictions were all carried out in OpenRocket. Figure XY and XW, show the flight profiles of Skyron with a 5 mph and 10 mph wind speed respectively. With a 5 mph wind, the launch vehicle will achieve apogee at 1642 m (5390 ft) at 17.8 seconds after ignition. With a 10 mph wind, the launch vehicle is predicted to reach apogee in 17.6 seconds at an altitude of 1629 m (5344 ft).

3.5.4. Aerodynamics Analysis

3.5.4.1. Problem Statement and Motivation

The drag effect of the fluid flow around the launch vehicle cannot be determined with a closed form solution because of the turbulent flow that would be generated which could affect the stability of the launch vehicle. With the objective of answering these questions, a Computational Fluid Dynamics (CFD) analysis of a model of the launch vehicle was conducted in Ansys Fluent R16.1. Computational Fluid Dynamic (CFD) analysis of the launch vehicle involved using numerical analysis and algorithms to solve and analyze fluid flows around the launch vehicle.

Condition	*Values*
Motor	Cessaroni L910
Total Mass	10.842 kg
Launch Rod	3.05 m
Angle	5°

Table XY: Parameters used during flight simulations
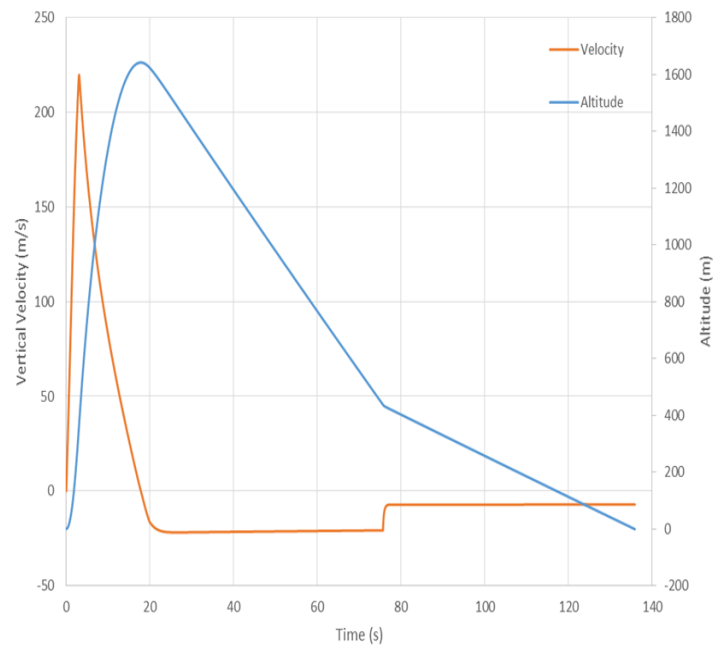
Figure XY: Flight profile at 5 mph wind speed
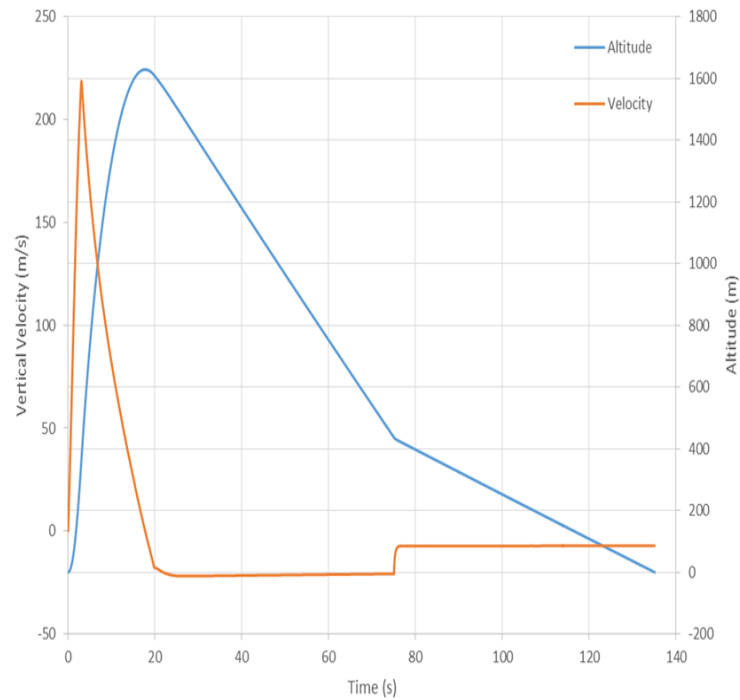
Figure XZ: Flight profile at 10 mph wind speed

The OpenRocket design utilized a Cessaroni L910 engine and a predicted mass of 10.842. The weight analysis takes into account a 25 percent error margin to account for excess mass generated during the manufacturing process.

3.5.4.2. Mesh Definition and Statistics

The process involved dividing the volume occupied by the fluid into uniform discrete cells (creating the mesh). The boundary conditions were also defined by specifying fluid behaviour and properties at the boundaries. The solution domain was defined assuming lateral symmetry of the launch vehicle in order to reduce required computing resources.
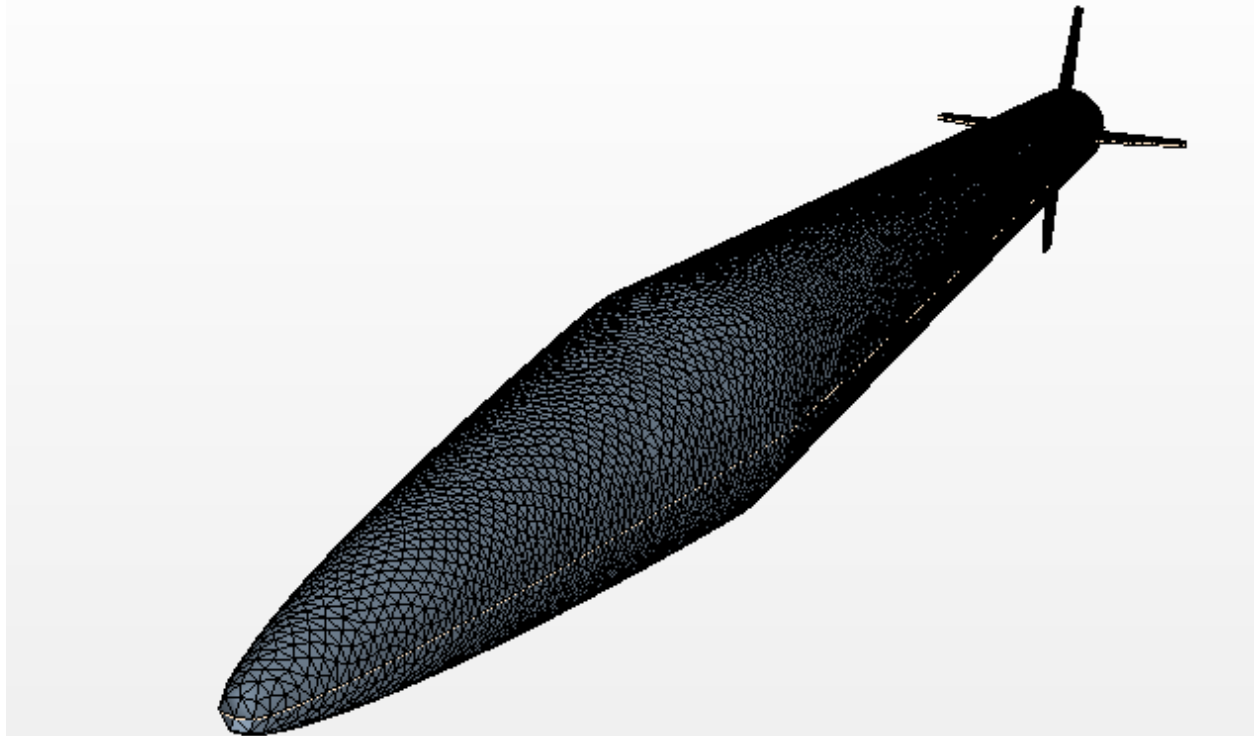
Figure B. Mesh around the launch vehicle
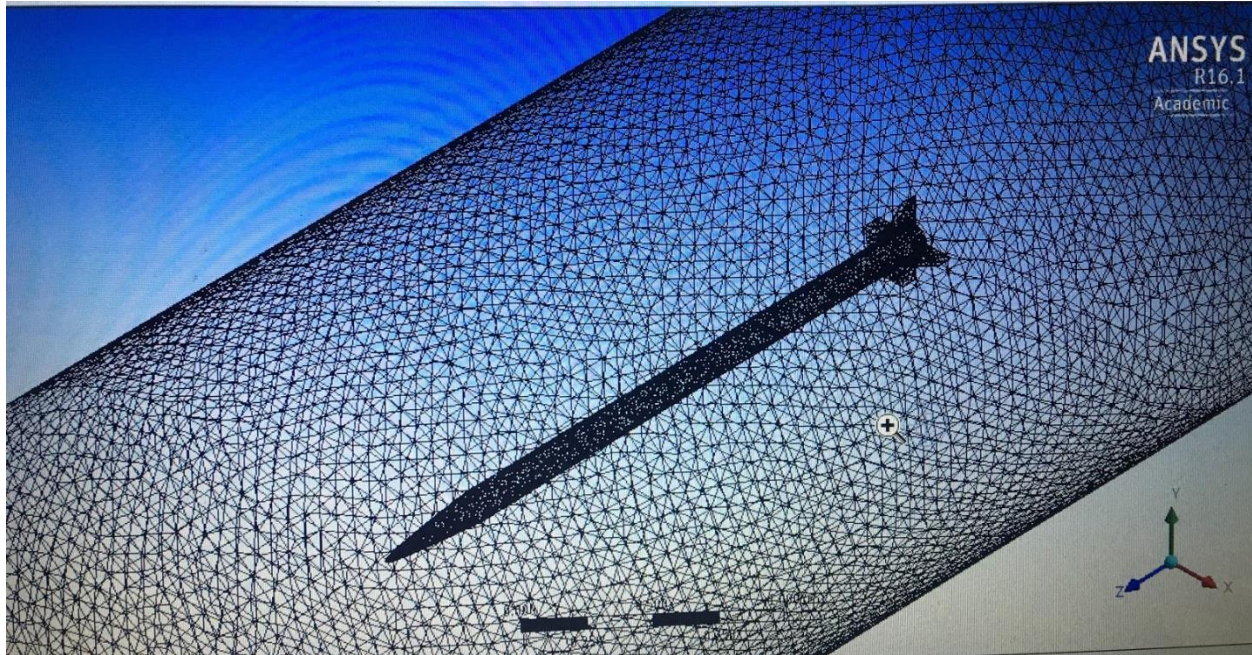
Figure X. Mesh around launch vehicle body

The size of the mesh was heavily constrained by limited computing resources available. Relevant statistics of the computer used for the simulation are listed in Table A. The memory available posed a critical limitation on the size of the mesh.

Table A: Statistics of computer used in meshing and simulation

Processor	Intel Core i5-4200
RAM	8.00 GB
Operating system	Windows 10

        3.5.4.3.Physics Setup

The simulation was conducted at a velocity of 222 m/s at standard sea level temperature and pressure. A density-based k-omega SST model was used with an energy equation to account for compressibility effects. A pressure-far-field boundary condition was applied to the far-field boundary layer and a symmetry boundary condition was applied to the symmetry plane. The solution converged with a continuity of 8.8e-2.
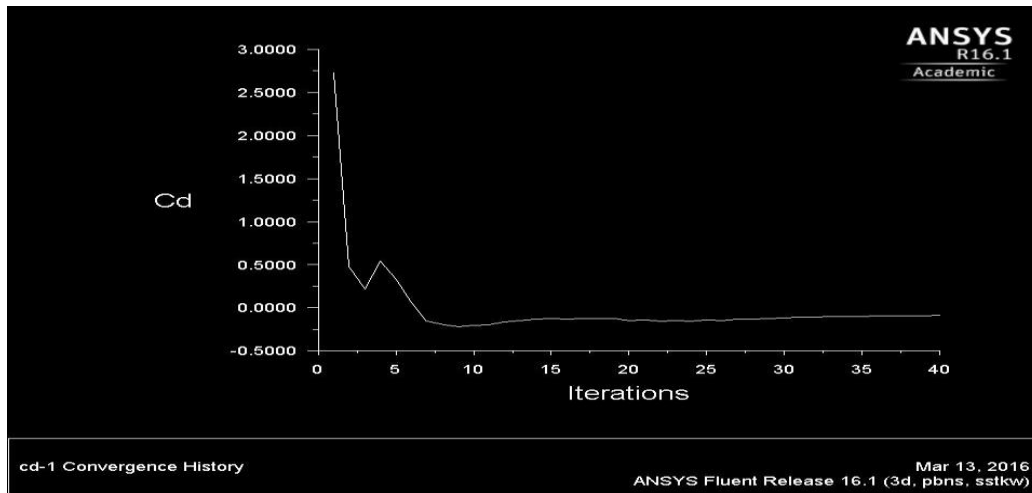
Figure A. Plot of CD-convergence history

Table 6: Force Results for launch vehicle and fins

Reference Area(in²)	Drag force(lbf)	Drag Coefficient(~)
513	1343	0.6

Velocities obtained from the ground and test flight that was carried out on the launch vehicle were used to calculate drag acting at different stages of the mission. Equation 3 below was used to calculate the drag. The drag coefficient (C_D) used was the drag coefficient obtained from the flight simulation, the surface area(A) was 0.330967, density(rho) was 1.225kg/m³ .

$$D=0.5(rho)(v^2)(A)(C_D) \tag{3}$$

Figure 7 below displays a plot of drag obtained against time. The data obtained matches results expected from theoretical knowledge.
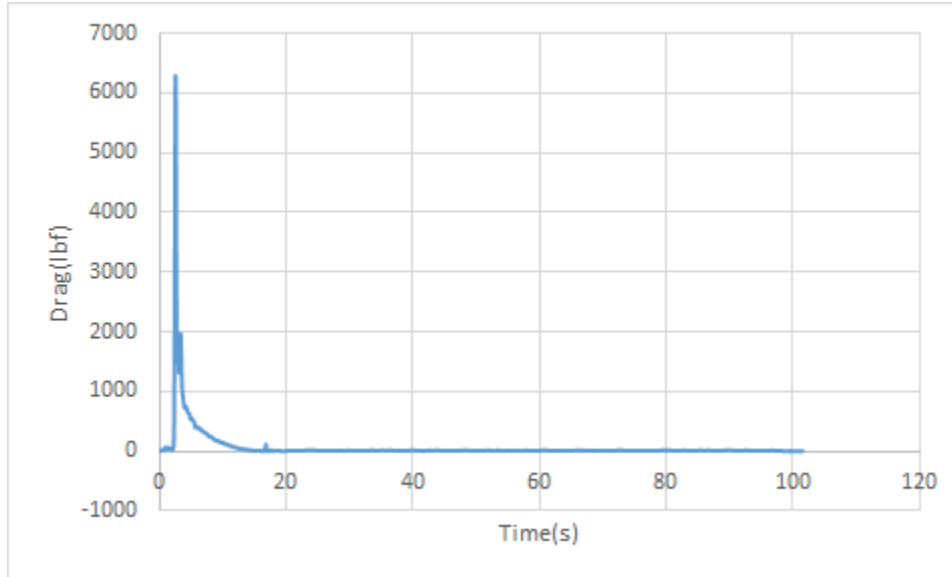
Figure 7. Plot of Drag against time

Faulty data logged by the altimeter accounted for the extraneous data points shown in figure 7 above.

3.5.5. Aerodynamics Locations

Our target stability is between 2 and 3 cal (launch vehicle diameters) and an OPENROCKET vehicle simulation was run to ensure that this stability is maintained throughout the duration of the flight to apogee. The locations of the center of gravity and center of pressure are also displayed below in Figure X. Finally, as seen in Figure Y, the stability margin was within 2-3 in any of the wind conditions.

The average stability for the flight at Mach 0.3 is 2.13 and thus the launch vehicle can be said to be stable.
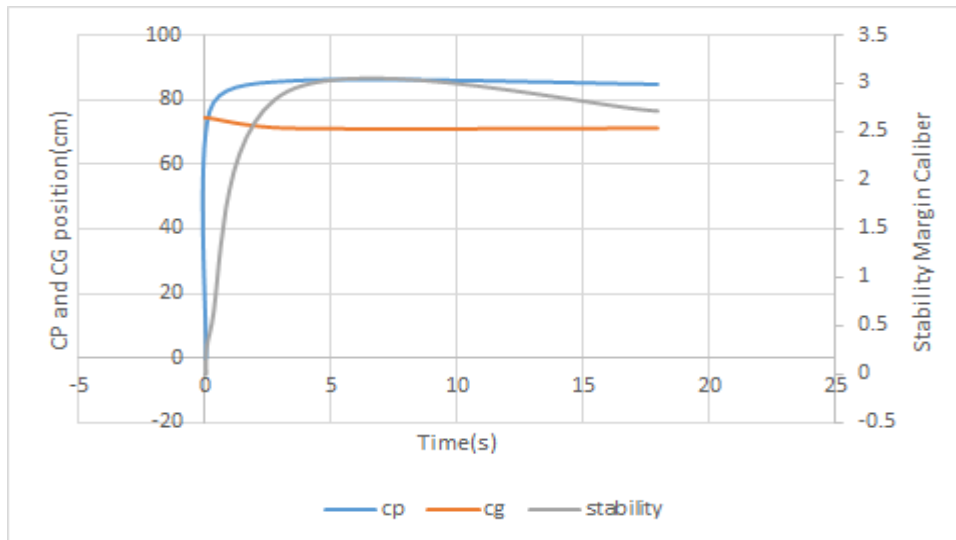
Figure X: Stability margin, CG, CP with 5mph wind
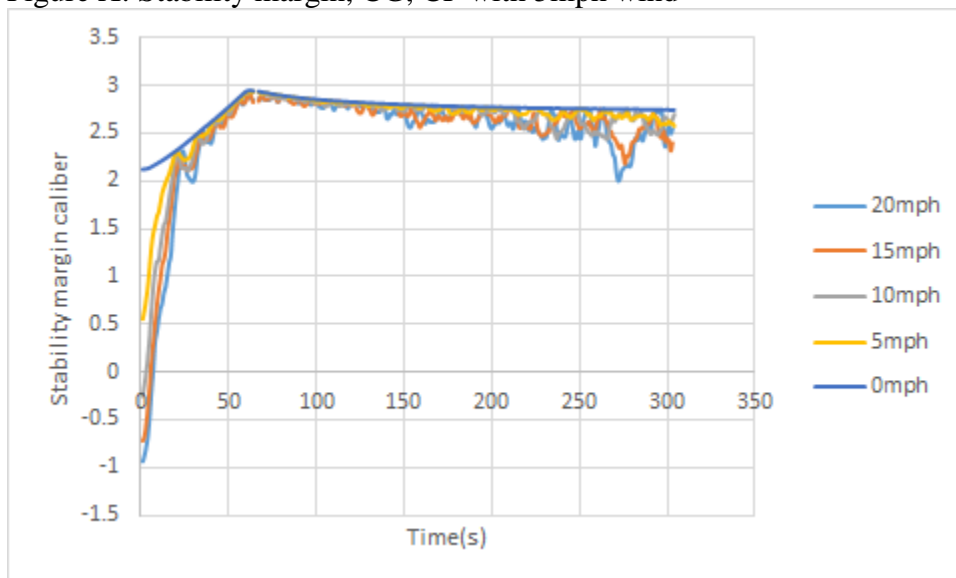
Figure Y. Stability margin with varying wind speeds

3.5.6. Kinetic Energy Breakdown

The definition of a safe landing velocity being that each individual component must not possess more than 75 ft− lbf of kinetic energy at landing. The Kinetic Energy through the various stages of the mission were calculated using velocities found from the OPENROCKET vehicle simulation that was performed. Equation X was used to calculate the kinetic energy at each stage of the mission. The stages that were analysed are: liftoff, burnout, apogee, recovery device deployment, and landing.

$$\text{Kinetic Energy} = 0.5\ (m)(v^2) \qquad\qquad (X)$$

By inserting the determined values, where m is the mass and v is velocity, the kinetic energy of the launch vehicle at each stage is displayed in Table X.

3.5.7. Drift Profile
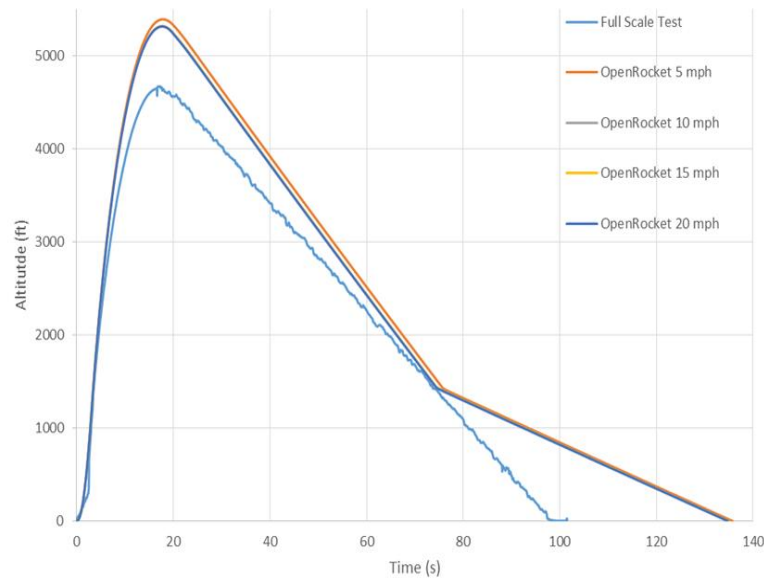
Figure : Display of altitude for the OpenRocket predictions against the full scale data
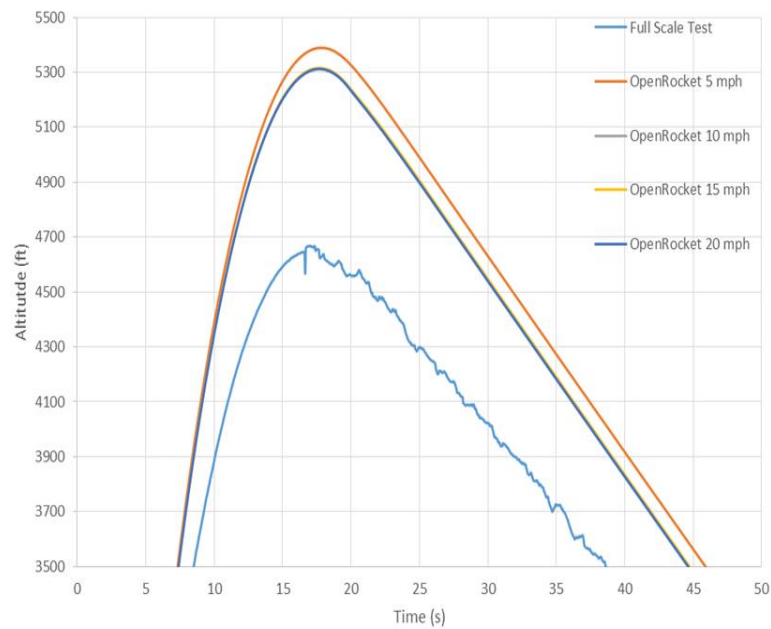
Figure : Display of the max apogee difference between full scale data and OpenRocket predictions
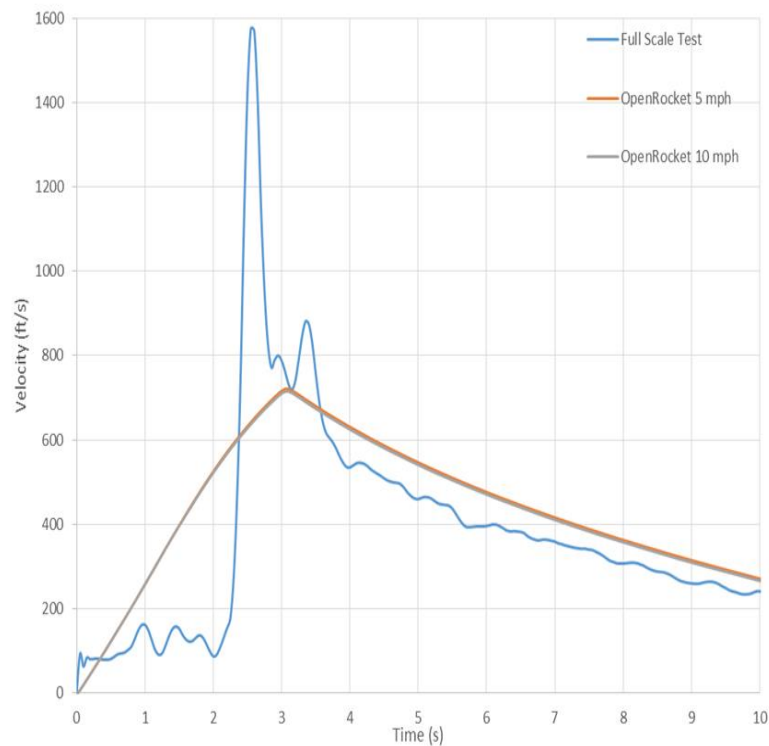
Figure : Burnout velocity comparison of full scale launch data and OpenRocket predictions

3.5.8. Apogee Targeting System

3.5.8.1. Apogee Targeting System Predictions

The general form of our simulink model is shown in Figure XX. The Simulink model aims to simulate the program and assist in the motor selection process. Furthermore, the simulink model allows us to design the controller for this system.
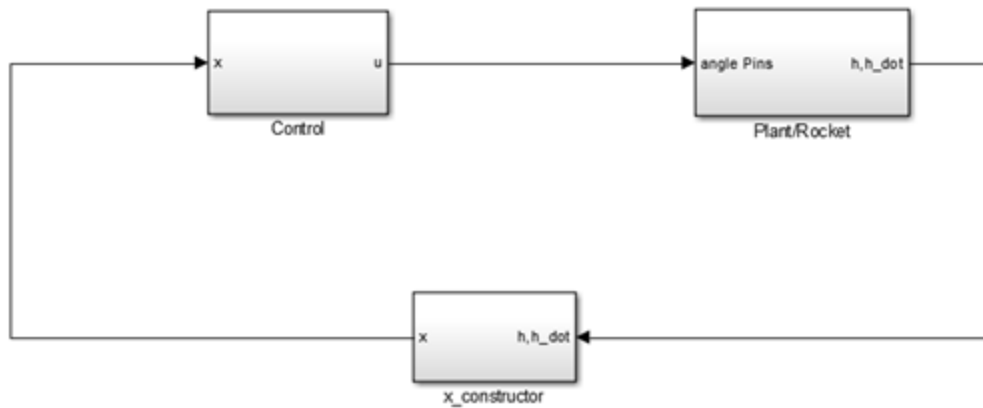
Figure XX. The controller and the system block, designed in Simulink.

We have implemented a Simulink model for the equations of the launch vehicle, shown in Figure YY. Briefly, we have: weight, engine thrust, flap drag, and launch vehicle drag. All of these forces are acting on the launch vehicle. So, we created these forces, summed them (with the adequate projection) and then due to Newton's 2nd law we know that this net sum equals the mass of the launch vehicle times its acceleration.
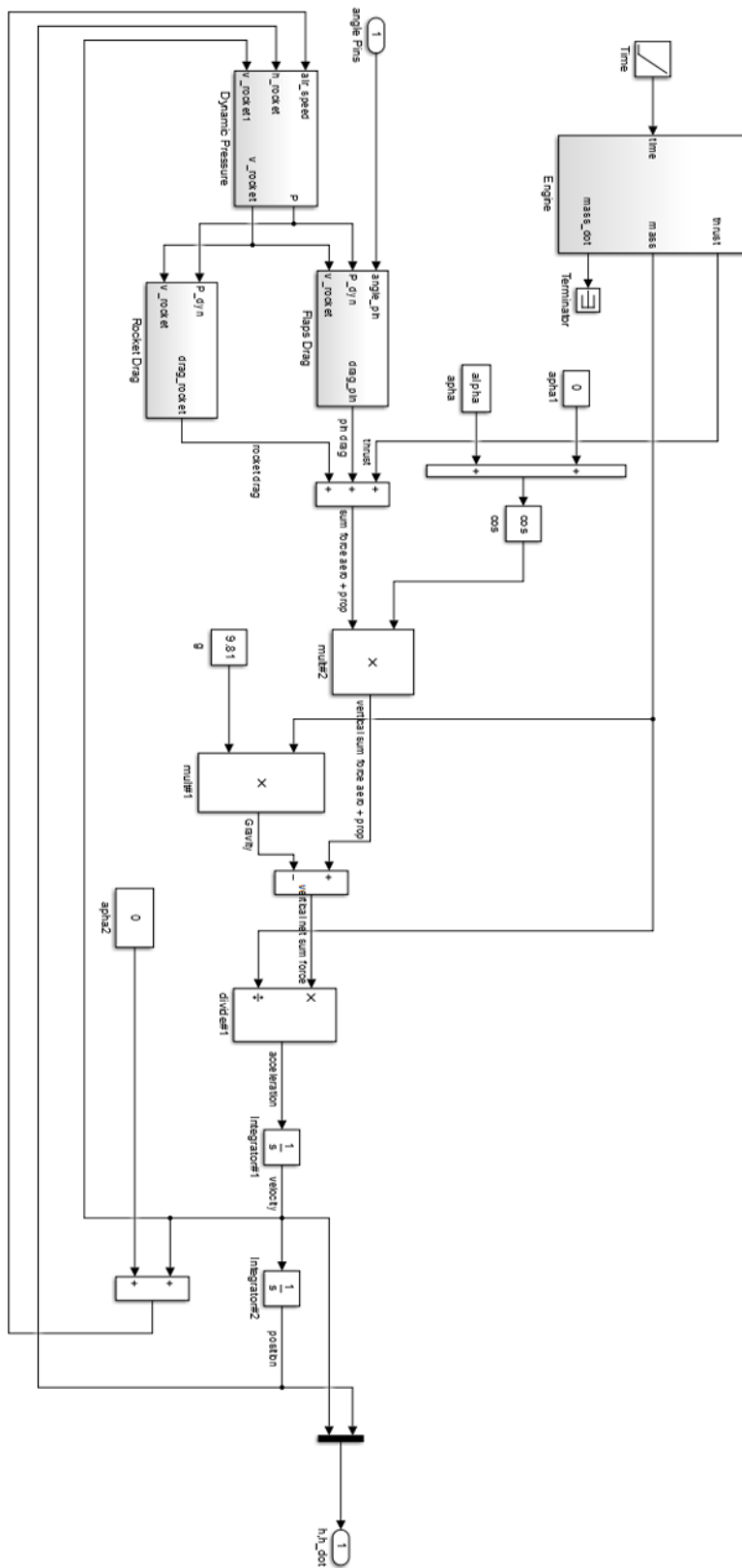
To model the engine mass and the propellant lost during flight, a function was created dependent on time, shown in Figure ZZ. From this function we are then able to compute the mass ejected by the motor since launch and the thrust level.
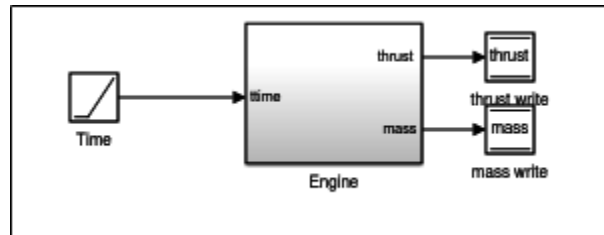
Figure ZZ. Simulink model of the engine.

The objective of control in this model is to reach the exact apogee using flaps. Indeed, the flaps are going to be extended depending on the relative position of the rocket and a "nominal" trajectory pre generated by simulation. The nominal trajectory is generated using the equation of the motion of the launch vehicle: then we know that in the absence of perturbation it is exactly the motion that the rocket should have and so we know that this trajectory is perfectly doable by the system, Please see below in Figure AA an example of a nominal trajectory used for launch.
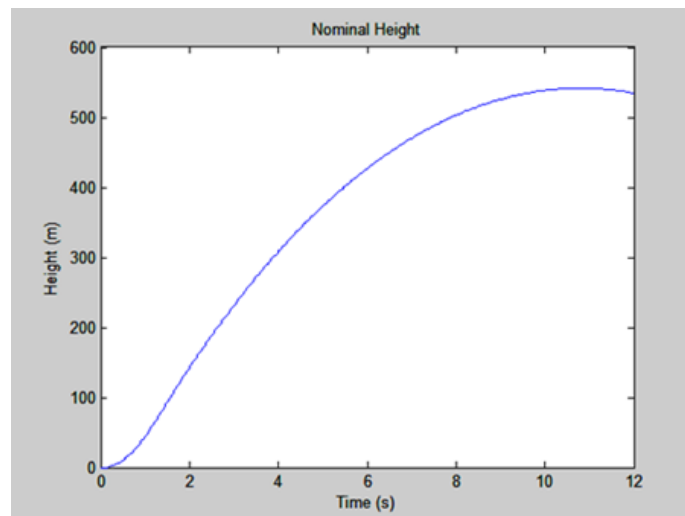
Figure AA. The nominal trajectory simulation used during launch.

Once this nominal trajectory generated, we implement a controller such that the error between the current altitude and the nominal altitude goes to zero as t goes to infinity.

For that, we will use here a system of flaps. The control authority we have here is therefore: either extend the flaps or create more drag, either not extend the flaps or create less drag. With this technique the rocket will then be able to reach an apogee that is close to the one we want even with the presence of perturbation.

3.6. Recovery Subsystem

3.6.1. Recovery System Overview

The goal of the recovery system is to minimize the descent velocity of the launch vehicle while also limiting the downrange drift. Minimizing the descent velocity reduces the launch vehicle's impact energy with the ground .A dual deployment recovery system will be used to mitigate wind conditions at the launch site.

The drogue parachute will be housed in the compartment connecting the booster and payload which has a diameter of 5 inches and length of 9 inches. The main parachute will be located between the payload section and the nose cone of dimension 5 inches in diameter and 12 inches in length. See Figure XX for parachute locations.
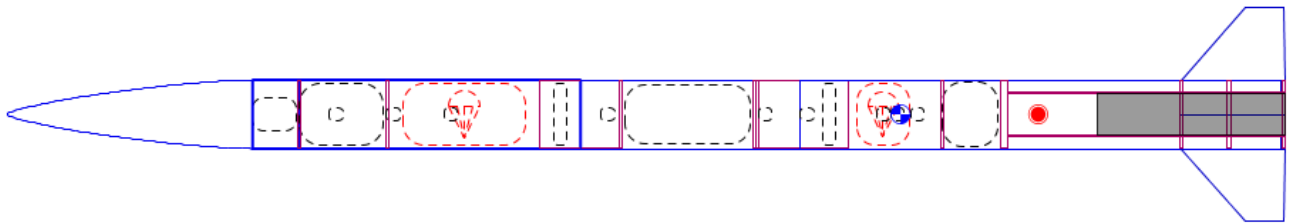
Figure XX: Parachute Placements

The launch vehicle will be armed on the launch pad using arming switches, for independent altimeters and ejection charges. Both parachutes are made of rip-stop nylon.

A bulkhead in the rear payload section will house the ejection wells and also serve to reduce the effects of the impulse from the gun powder blast. The drogue parachute's retention mechanics includes a U Bolt placed between the two ejection wells on the underside of the payload section, as well as a U Bolt in the booster section thrust plate. In addition, there is a shock cord connecting the booster section and main rocket body together. At deployment, the ejection charges will separate the booster section from the main rocket, releasing the drogue parachute. Figure XX shows a view of the drogue compartment.

Figure XX: Drogue Compartment

The main parachute's ejection wells will be placed such that the impulse is imparted on the payload section and the nose cone is separated from the main rocket pulling the main parachute out. Shock cords will connect the main parachute to the nose cone and the payload section of the launch vehicle, ensuring that the all sections remain together during descent. Figure XX shows a detailed view of the main parachute compartment and assembly.

Figure XX: Main Parachute Compartment

The parachute housings are made of G10 fiberglass, and the bulkheads under the main chute is made of plywood. U –bolts will be drilled into the bulkheads, and will be used to attach the shock cords. The U-bolts are made of stainless steel and will be drilled into the bulkheads in order to attach the shock chords. 4-1/16''Nylon shear pins will be used to ensure that the main and drogue chute compartments stay together until separation is required and parachutes are deployed. PVC end caps will be used to direct the ejection charges in order to protect the casing from thermal shock, and a NOMEX shield will protect the parachutes.

3.6.2. Parachutes Analysis

The parachute sizes were selected in order to ensure the impact K.E. remains below the 75lbf-ft limit.

$$E = 1/2mv^2$$

A ground hit velocity of less than 22ft/s is needed to achieve such limitations and ensure structural soundness of structural elements exposed to high stress at impact such as the fins. The kinetic energies of the separate sections are given in Table X.

The parachutes were sized using equation X as a guide, as well as iterating through parachute sizes in OpenRocket to obtain the minimum terminal velocity. The main parachute is 6.67 ft in diameter while the drogue is 2.5ft in diameter.

$$\text{Diameter} = (2/V_{etrminal})*((sqrt(2)W)/rho*pi*C_D)$$

Table XX: Parachute Sizes

Properties	*Main Parachute*	*Drogue Parachute*

Diameter (ft)	10	2.5
Surface Area(ft²)	78.54	4.9
Estimated C_D	0.8	0.8
Target Descent (ft/s)	16.54	62

Table XX: Kinetic Energy at Landing

Launch Vehicle Section	Weight (lb)	Velocity (ft/s)	Kinetic Energy (ft-lbf)
Upper Section	6.52	15.54	24.45
Avionics Bay	3.62	15.54	13.57
Booster Section	8.65	15.54	32.44

Redundant black powder charges will be used to eject the parachutes. The container housing the parachutes are pressurized in order to ensure the chutes deploy.

Black powder masses were calculated using equation XX with variables defined in Table XX. Volume, V is set by the design of the launch vehicle, while the gas constant, R and temperature, T are known for black powder.

A pressurization value of 10 psig and 9 psig was used as a structural maximum for the main and drogue chutes respectively. The mass of black powder used directly depends on the dimension of the housings which were estimated to be 5 inches in diameter, and 12 inches and 9 inches for the main and drogue.

$$W = \Delta P * V / RT$$

The results are shown in Table XX. The compartment will be held together by 3 Nylon shear pins of diameter 4-1/16'' and tensile yield strength of 12 ksi. From equation XX a force of 155 pounds will be needed to separate each compartment.

$$F = (\sigma \pi d^2)/4$$

Table XX: Ejection charge equation variables

	Description	Units
W	Weight of the black powder in pound mass	$454 * W_{grams}$

V	Volume of the container to be pressurized	in^3
ΔP	Pressure Differential	psi
R	Gas Combustion Constant for black powder	22.16ft*lbf/lbm*R
T	Gas Combustion Temperature	3307 R

Table XX: Black Powder Charge

	Main Parachute	Drogue Parachute
Total Pressurization (psia)	24.7	23.7
Pressure at Deployment Altitude (psia)	14.43	13.9
Differential Pressure (psia)	10.27	9.8
Amount of Black Powder(g)	1.20	0.81

3.6.3. Safety and Failure Analysis

The table below details the safety and failure analysis for the Recovery subsystem. The parachutes are the main components of interest in the analysis.

Phase	Description	Failure Mode	Hazard
Construction	Parachutes will be secured in their individual sections using an insulated material to prevent the ignition of the nylon.	Insulation material fails to prevent nylon from igniting. Parachutes will fail to deploy; likely resulting in failure of recovering the rocket.	With the parachutes failing to deploy, the rocket will gain momentum as it falls back to the ground posing as a possible threat for anything in the vicinity of the crash site.
Assembly	Parachutes will be attached and secured to the rocket via-shock cords which are connected to U-bolts	Parachutes are not secured correctly resulting in failure of deployment during descent.	See Construction Hazard

	installed onto the centering rings.		
Launch	Parachutes deploy.	Parachutes fail to deploy	See Construction Hazard
Recovery	Rocket is successfully recovered.	Parts or entire rocket cannot be recovered.	See Construction Hazard

3.7. Full Scale Test Flight
3.7.1. Full Scale Recovery System Test

Each compartment underwent testing for feasibility. The tests were conducted to verify black powder calculations for both the drogue and main parachute compartment. For testing to be considered successful the criteria listed in Table XX had to be met. The test is considered a failure if none of the criteria are met or if one of the failure mode occurs listed in Table XX occurs.

Table XX: Recovery Testing Success Criteria

Success Criteria	*Risk Level*	*Mitigation*
Ejection Charge Ignites	Low	Keep personnel a safe distance away
Shear Pins Break	Low	Keep personnel a safe distance away
The launch vehicle moves half the distance of the shock cords	Medium	Keep personnel a safe distance away

Table XX: Recovery Testing Failure Modes

Failure Criteria	*Risk Level*	*Mitigation*
Bulkheads or couplers shatter due to charge.	Medium	Keep personnel a safe distance away
The shear pins do not break and launch vehicle compartments remains connected	Low	Keep personnel a safe distance away

The NOMEX cloth fails and parachutes burn	Medium	Properly folding parachutes
Black powder fails to ignite	Low	Redundant ignition system

During full scale flight tests the drogue deployed at around 16 seconds into the flight which was within the range of expected deployment time. A signal was sent for the main to be deploy at 88 seconds into flight, as within the expected range, however, the parachute failed to deploy. The drogue chute thus passed the feasibility test and matched the black powder calculation for separation and shearing. The main parachute experienced a failure mode. Further investigation is needed to account for the failure.

3.7.2. Flight Data

3.7.3. Apogee Targeting System Effectiveness

Based on the design criteria for the ATS, we were able to successfully convert the Solidworks model to a working mechanical system integrated into the booster section. We were also able to verify the validity of our modular design from the successful integration of the various components. The servo motors were selected based on their holding torque and RPM to withstand the calculated theoretical force on the tabs during flight. Based on our calculations, the servo needs to be able to withstand a torque of 2.90 kg-cm at maximum angle of deployment and at maximum velocity. The servos that we selected were rated at 10kg-cm, and should be able to withstand applied loads within reasonable deviation.

Our full scale test launch was used to determine the effectiveness of the launch vehicle design and to give us a base value for the actual launch vehicle apogee. The test allows a perfection on the simulation and model.

3.8. Electrical Elements

3.8.1. Recovery System Electronics

The Stratologger CF is the only electrical element used to record the flight data. This altimeter records data at a rate of 20 samples per second and stores it for

Later use. They also include a Data I/0 connector which allows for real-time altimeter data to be sent to the onboard flight computer. This altimeter is functional up to an altitude of 100,000 feet and will be used to deploy the main and drogue parachutes upon reaching specified altitude.

3.8.2. Apogee Targeting System Electronics

The Apogee Targeting System electronic parts consists of 2 main sections: the controller and the actuator. For the controller, a mBed microcontroller was used. For the actuator, four MG995 High Torque Servo motor are used for the motor system which are controlled by mbed which is for the micro-control system.

An mbed LPC1768 is used for the micro-control system. The reason mBed is used for this project is that comparing to other digital boards, such as Arduino Board which contains 14 digital pins, has more ports and pins. The mBed used for this project has 26 digital pins (p5 - p30, which can be used as digital in and digital out interfaces) which means that it can drive more digital elements. The mBed and its pin layout are depicted in Figure XX1 below. This mBed has a 32-bit ARM Cortex-M3 core running at 96MHz. It includes 512 KB Flash, 32 KB RAM and lots of interfaces.
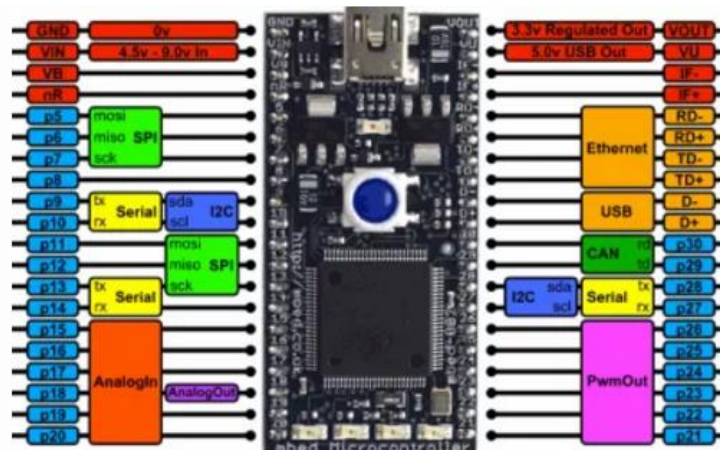
Figure XX1: mBed NXP LPC1768 Microcontroller interfaces and locations

The MG995 High Torque motor is an all metal gears motor. It has dimension 40 × 19 × 43 mm, and weight 69 g. The operation speed is 0.17 sec / 60 degrees at 4.8 V with no load, and 0.13 sec / 60 degrees at 6.0 V with no load. In the design, there will be 9 V power supply for each motor, so the rotation speed of the motor will be faster than the data listed above in the launch. Also, the stall torque of one MG995 motor is 13 kg-cm (180.5 oz-in) at 4.8 V and 15 kg-cm (208.3 oz-in) at 6 V. Figure XX1 shows one of the MG995 High Torque motor.

Figure XX2: MG995 High Torque Motor

3.9. Launch Vehicle Verification

3.9.1. Mission Success Criteria and Verification

Mission Success Criteria	Design feature to satisfy that requirement	Verification Method	Status
Reach an altitude of 5,280 ft. with a precision of 5%	The A.T.S. will deploy during cruise flight to adjust the flight profile curve to match a real-time ideal projection of the rocket's trajectory.	Testing, Analysis	In Progress
Full structural integrity must be maintained.	Robust materials were selected for the components of the launch vehicle that will be subjected to high-stress environments.	Inspection	Completed
The payload must be secured throughout flight	A payload bay with secure payload holders will provide sufficient force to prevent detachment due to vibrations.	Inspection	Completed
The launch vehicle must pass a full systems check prior to launch	Accessible interfaces for all electronics housed within the launch vehicle.	Testing	In Progress

3.8.2 Mission Requirements and Verification

Table XX: Project Mission Requirements

Requirement	Design Feature to Satisfy Requirement	Verification Method	Status
Vehicle altimeter will report an apogee altitude of 5,280 feet AGL.	Low-mounted electric-controlled fins will be extended and retracted in reaction to altimeter readings to control drag and limit altitude.	Analysis	Completed
Launch vehicle will be designed to be recoverable and reusable within the day of initial launch.	Vehicle will be constructed of fiberglass to resist fractures and ensure stability.	Designed, Testing	Completed
Vehicle will be prepared within 2 hours and will be able to maintain launch-ready position for at least 1 hour.	Compartmentalized design with standard assembly procedure.	Testing	Completed
The launch vehicle shall have a maximum of four (4) independent sections.	Three (3) sections include: payload, avionics, and booster	Designed	Completed
The vehicle will be limited to a single stage, solid motor propulsion system, delivering an impulse of no more than 5,120 Newton-seconds.	Single-staged design that utilizes a single "L" impulse classification motor.	Design Review	Completed
Team must launch and recover both a subscale and full scale model prior to each CDR and FRR respectively.	Efficient Recovery System with redundancies to ensure successful operation.	Execution	Completed
The launch vehicle shall stage the deployment of its recovery devices, where a drogue parachute is deployed at apogee and a main parachute is deployed at a much lower altitude.	Redundant altimeters programmed to deploy at specific altitudes.	Designed, Testing	Completed

At landing, the launch vehicle shall have a maximum kinetic energy of 75 ft-lbf.	Optimization of parachute sizing for the total mass of the launch vehicle	Testing	Completed
The recovery system will contain redundant altimeters, each with their own power supply and dedicated arming switch located on the exterior of the rocket airframe	Install a master key-switch at the rear of the avionics bay to close all circuits simultaneously, and independent compartment for sensors and power supply.	Designed	Completed
Each detachable section of the vehicle and payload must contain an electronic tracking device and continue transmission to the ground throughout flight and landing.	Independent GPS compartment with transmission capabilities and ground station with receiving capabilities.	Designed	Completed

3.10. Testing

Fin static Test

Recovery System Ground Test

Altimeter Testing

3.11. Workmanship

The heavy machinery involved in the manufacturing process was made up of the following: laser cutters, a waterjet cutter, a CNC mill, a Dimension Elite 3D printer, an Afinia H480 3D printer, a chopsaw and a bandsaw. Power tools used included electric drills and a Dremel. For all machines, various preventive measures and visual verifications were made before initiating largely irreversible processes, as detailed below.

Team ARES manufactured the launch vehicle's components to the highest standard possible by taking steps to physically ensure design correctness. Examples of these steps included: manually confirming the dimensions of any prefabricated material upon their delivery; preceding any permanent laser-powered cut with a low-power etch; visually verifying the alignment of markings when drilling holes for threaded rods, bolts, and other components; and carefully measuring everything multiple times, verifying measurements by using various tools where possible.

3.11.1. Launch Vehicle Body Tubes

The Skyron's main outer structural component is its airframe, composed of fiberglass body tubes. The airframe is divided into three body tubes interconnected by two couplers. The nosecone is connected to the upper body tube, while there are four fins attached to the bottom body tube (booster section). Again, all of these components are manufactured from G12 fiberglass -- the reason behind this material's selection can be found in Section 3.3.1.

Starting from the bottom, the body tubes are divided into three sections named the booster section, avionics section, and upper section. The length of the booster section is 35.5 inches, that of the avionics bay is 16.1 inches, and that of the upper section is 24 inches. The coupler that connects the booster section and avionics section is 7 inches long, while the coupler that connects the avionics bay and the upper section is 6 inches long.

3.11.2. Bulkheads

The launch vehicle's bulkheads, centering rings, and thrust plates served various purposes which ranged from motor retention to providing additional surface area for epoxying, hosting various bolts, or providing support for other components or electronics. Independent of their mixed purposes, all of these were all manufactured out of ½ inch and ¼ inch plywood sheets. The manufacturing process for them specifically consisted of first developing CAD models of the bulkheads, which could later be used to export DXF files for vector cutting. These DXF files were later imported into the Trotec Speedy 300 laser cutters at the Georgia Tech Invention Studio and AE Maker Space.

The reasons behind using laser cutters for this manufacturing process were the following: first of all, the laser cutters were the only CNC-enabled cutting machinery available to the team. The CNC technology enabled the laser cutter to cut with tremendous precision, ensuring that the bulkheads would have the exact dimensions that they were intended to have. Furthermore, laser cutting smaller holes allowed the team to avoid of utilizing a power drill, thus minimizing the risk of making a mistake and causing irreversible damage to the component.
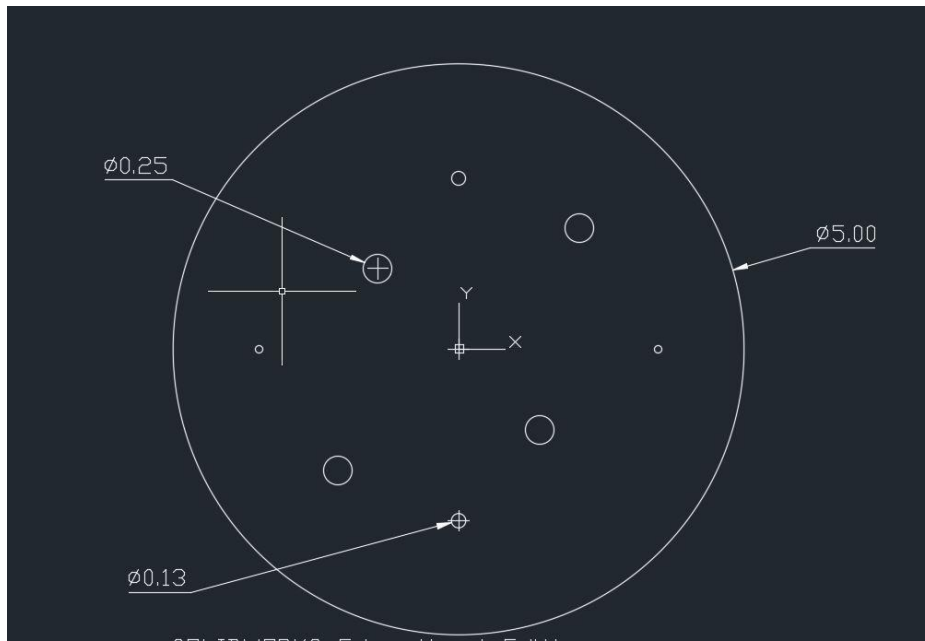
Figure XX: Avionics Bay Bulkhead drawing

3.11.3. Fins

Team ARES manufactured its launch vehicle's fins out of ⅛ inch G12 fiberglass sheets. In order to cut them efficiently and successfully, the Invention Studio's waterjet cutter was selected due to its high reliability. The greatest risk is the delamination of the material, so necessary precautions were taken. First of all, the waterjet's settings were set to operating conditions for a "brittle material" lowering the pressure of the jet. A step further was taken by reducing the jet's cutting speed to a quarter of its nominal operating speed. To prevent the fin from falling into the water tank, the fin design accommodated small structural tabs that would later be removed, as well as clamps all around the material.
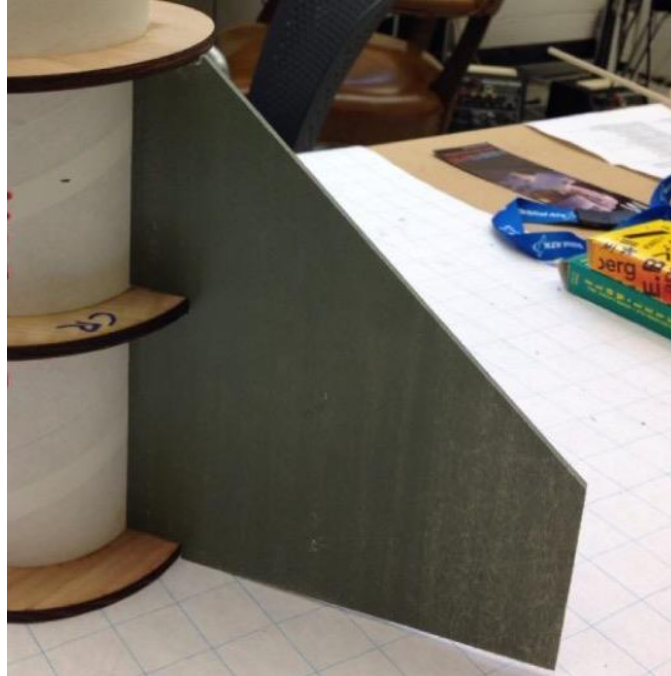
Figure XX: Image of a fully manufactured fiberglass fin.

3.11.4. Apogee Targeting System

The servo mounts and tabs were printed in a Dimension Elite 3D Printer out of ABSplus thermoplastic based on our SolidWorks models. We then cut holes out of the fiberglass body tube for the tabs using a standard jigsaw. After we were done using the jigsaw to cut rough outlines for the holes, we then used a metal file and dremel to smooth the holes and get the tabs flush with the body tube.

After the holes were cut in the body tube, we bolted the hinges on the tabs to the inside of the body tube. We then bolted the servos into the servo mounts and epoxied the servo horns to the metal arm attachments. After the epoxy on the servo arms had hardened, we screwed the servo arms into the servos and the glued the servo mounts to the plastic alignment piece with Gorilla Glue. Finally, we slid the servo mounts into the body tube and epoxied them to the inside of the body tube.

3.12.   Payload Integration

3.12.1. Justification

The payload section is confined within the 5" fiberglass airframe just below the nosecone GPS section. The payload bay will be integrated by attaching a plywood base to two plywood bulkheads. The rectangular base has three small teeth at each end that fit into their own respective slots in the circular bulkheads. Wood glue will be used to ensure the pieces don't fall apart or the geometry isn't altered when considerable force is applied. Small screws and nuts fasten the payload locks to the frame of the payload bay. The design of the locks allow the payload to easily snap into place but also firmly grasps it so the payload cannot move. The sturdy fiberglass fuselage also prevents the payload frame from experiencing any damage even after a severe impact. Since the payload section has great structural integrity, it is additionally used as a mount for the GPS unit and recovery systems.

3.12.2. Payload Integration Process

To manufacture the frame for the payload section, a laser cutter machine referenced CAD files to cut the bulkheads and payload base. The two circular bulkheads were cut into 1/4" plywood while the rectangular base was cut into 1/8" plywood. These three pieces fit together using numerous slots and teeth and are secured with wood glue. The two payload locks were manufactured of 3D printed ABS plastic. Once the locks were aligned with the holes in the base, the locks were fastened with four 0.09" diameter screws and nuts. The payload assembly is then epoxied to the inside of the fuselage. The outside face of the bulkheads provide a flat surface for the GPS unit to be attached to. Since the payload is located on only one side of the wood base, there is sufficient room on the opposite side for recovery system U - bolts to be mounted.
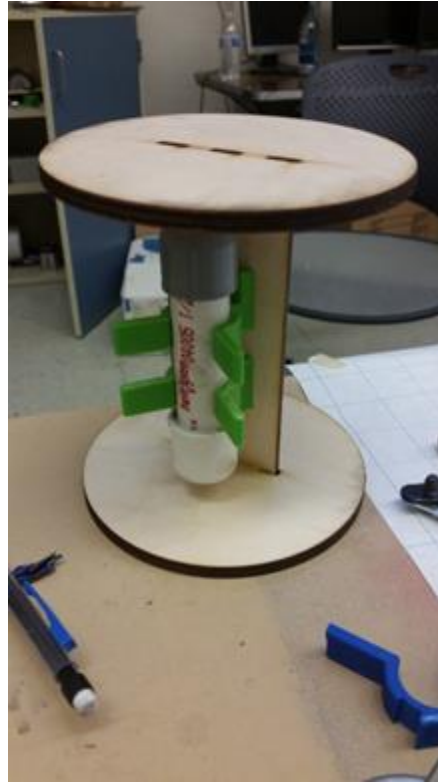
Figure XX: Assembly of Internal Payload Section

3.13. Safety and Failure Analysis

The table below details the safety and failure analysis of the entire launch vehicle during the construction and assembly phase. Safety is of paramount importance during the construction and assembly phase.

Equipment	Hazard	Severity	Likelihood	Mitigation and Control
Batteries	Batteries explode	Burns, skin, and eye irritation	Low	Wear safety glasses and gloves when handling. Make sure no shorts exists in circuits using batteries. If battery begins to overheat, stop its use and disconnect it from any circuits.
Black Powder	Chemical explosive	Explosions, burns, skin,	Medium	Wear safety glasses and gloves when handling.

		and eye irritation		Be careful when pouring black powder. Operate in a static-free environment.
Dremel Rotary Tool	High-power rotary tool	Cuts and scrapes	Medium	Only operate tools with supervision of teammates. Use tools in appropriate manner. Wear safety glasses to prevent debris from getting into eyes.
Power Tools	High-power construction equipment	Cuts, punctures, and scrapes	Medium	Only operate tools with supervision of teammates. Use tools in appropriate manner. Wear safety glasses to prevent debris from getting into eyes.
Epoxy/Glue	Potent chemical adhesive	Toxic fumes, skin, and eye irritation	High	Wear gloves, nitrile for epoxy, face masks, and safety glasses. Work in well ventilated areas.
Exacto/Craft Knives	Knives	Cuts, serious/fatal injuries	Medium	Only use knives with teammate supervision. Only use tools in appropriate manner. Do not cut in the direction towards oneself.
Flammable Objects/Environment	Fire	Burns. serious/fatal injuries	Low	Keep a fire extinguisher nearby. If an object becomes too hot or does start a fire, remove power (if applicable) and be prepared to use the fire extinguisher.
Hammers	Construction equipment	Bruises, serious/fatal injury	Medium	Be aware of where you are when swinging the hammer, so that it does not hit yourself others, or could bounce and hit someone.

Handsaws	Construction equipment	Cuts. serious/fatal injuries	Medium	Only use saws with teammate supervision. Only use tools in appropriate manner. Wear safety gloves to prevent debris from getting into eyes. Wear gloves for hand protection.
Waterjet Cutter	Construction equipment	Cuts, serious/fatal injuries, flying debris	Low	Only operate under supervision of Undergraduate/Graduate Learning Instructors, and with other teammates. Follower proper operating procedures. Wear safety glasses.
Improper Clothing	Dangerous environment	Cuts, serious/fatal injuries	High	Wear closed tied shoes, tie back long hair, do not wear baggy clothing.
Power Supply	High voltage equipment	Electrocution, serious/fatal injuries	Medium	Only operate power supply with teammate supervision. Turn off power supply when working with circuits.

The table below details the potential hazards and failures that may occur during the Launch and/or Recovery phase.

Potential Failure	Effects of Failure	Failure Prevention
Apogee Targeting System (ATS)	Vehicle will not reach target altitude.	Test ATS using subscale launch vehicles.
Body structure	Launch failure, damage to launch vehicle, unable to be reused, and	Test structure to withstand expected forces at launch with a factor of safety.

buckling on takeoff	flying shrapnel towards personnel/crown.	Have proper sized couplers connecting sections.
Drogue separation	Main parachute will deploy at high speed and may rip or disconnect from vehicle. Launch vehicle may become ballistic.	Perform ground and flight tests.
Fins	Fins could fall off, causing unstable flight. Fins break or disconnect from launch vehicle, unable to be classified as reusable.	Test fin at attachment points, using expected forces to ensure strength of attachment method. Do not have fins with sharp pointed edges, ensure parachute is large enough to minimize impact kinetic energy.
Ignition failure	Failure to launch.	Follow proper procedures when attaching igniter to AGSE. Perform subscale launches.
Launch buttons	Launch vehicle will separate from rail, causing an unstable flight.	Ensure launch rail is of proper size to accommodate the buttons. Ensure buttons slide easily into rail.
Main parachute separation	High impact velocity may damage vehicle and make it unrecoverable. Vehicle may become ballistic, causing serious injury or death.	Perform ground and flight tests to ensure veracity of deployment method.
Motor failure	Motor explodes, damaging launch vehicle/AGSE beyond repair.	Follow NAR's regulations. Follow manufacturer's instructions when assembling motor. Assemble motor under supervision.
Motor retention	Motor casing falls out. Lost motor case could damage persons/properties.	Test reliability of motor retention system.
Payload separation	Main parachute may not deploy correctly. Higher impact velocity may damage launch vehicle, or cause personal/property damage.	Perform ground and flight tests to ensure veracity of deployment method.
Thrust plate failure	Motor goes through the launch vehicle, causing damage to the launch vehicle and making it unusable again.	Test plate and attachment method to withstand expected launch forces with a factor of safety.

Potential Failure	Effects of Failure	Failure Prevention
Apogee Targeting System (ATS)	Vehicle will not reach target altitude.	Test ATS using subscale launch vehicles.
Body structure buckling on takeoff	Launch failure, damage to launch vehicle, unable to be reused, and flying shrapnel towards personnel/crown.	Test structure to withstand expected forces at launch with a factor of safety. Have proper sized couplers connecting sections.
Drogue separation	Main parachute will deploy at high speed and may rip or disconnect from vehicle. Launch vehicle may become ballistic.	Perform ground and flight tests.
Fins	Fins could fall off, causing unstable flight. Fins break or disconnect from launch vehicle, unable to be classified as reusable.	Test fin at attachment points, using expected forces to ensure strength of attachment method. Do not have fins with sharp pointed edges, ensure parachute is large enough to minimize impact kinetic energy.
Ignition failure	Failure to launch.	Follow proper procedures when attaching igniter to AGSE. Perform subscale launches.
Launch buttons	Launch vehicle will separate from rail, causing an unstable flight.	Ensure launch rail is of proper size to accommodate the buttons. Ensure buttons slide easily into rail.
Main parachute separation	High impact velocity may damage vehicle and make it unrecoverable. Vehicle may become ballistic, causing serious injury or death.	Perform ground and flight tests to ensure veracity of deployment method.
Motor failure	Motor explodes, damaging launch vehicle/AGSE beyond repair.	Follow NAR's regulations. Follow manufacturer's instructions when assembling motor. Assemble motor under supervision.
Motor retention	Motor casing falls out. Lost motor case could damage persons/properties.	Test reliability of motor retention system.

Payload separation	Main parachute may not deploy correctly. Higher impact velocity may damage launch vehicle, or cause personal/property damage.	Perform ground and flight tests to ensure veracity of deployment method.
Thrust plate failure	Motor goes through the launch vehicle, causing damage to the launch vehicle and making it unusable again.	Test plate and attachment method to withstand expected launch forces with a factor of safety.

4. AGSE Criteria

4.1. AGSE Overview

The Autonomous Ground Support Equipment (AGSE) consists of 3 main subsystems: The Robotic Payload Delivery System (RPDS), the Rocket Erection System (RES), and the Motor Ignition System (MIS). These three subsystems will accomplish the main goals of the AGSE, respectively: capturing and securing the payload, raising the launch vehicle, and inserting the ignition. An Electronics Containment Unit (ECU) will house the electronics used by the AGSE.

The RPDS is a robotic arm that will capture the payload with a gripping claw and then swing the payload into the payload bay of the launch vehicle. The design consists of 4 servo motors and 4 wooden struts. Overall, the arm will have 4 degrees of freedom. The payload bay will have snapping plastic clips inside that will enclose the payload. The RPDS will then close the door of the payload bay with another movement.

The RES will raise the launch vehicle from a horizontal position to a position 5 degrees from the vertical. A base hinge will move along a threaded rod that is turned with our NEMA 23 Stepper motor. As the hinge moves, it pushes an arm rail attached to launch vehicle rail, rotating the launch vehicle into position. As it nears the appropriate angle, a button located on the back of the main axis will be pushed, ending the functions of the RES. Also part of the RES are the support rails. These rails create a wide and rigid base to increase the stability of the system as it performs its actions.

The MIS will insert the ignition into the motor cavity using a rack and pinion system. A Mercury stepper motor will spin a pinion that will translate a rack. An electronic match will be attached to the rail. The rack is secured in a slot so that it can only translate up and down the launch vehicle rail. The rack can move 16 inches into the motor cavity. The MIS will be attached to launch vehicle rail so that it rotates with the launch vehicle. In front of the stepper motor and attached to the launch vehicle rail will be a stop that will keep the launch vehicle from sliding down the rail.

4.2. AGSE Features

4.2.1. RDPS

The RPDS, shown in **figure i**, is composed of a robotic arm with a claw that completes the function of capture and containment of payload.

The arm consists of a shoulder joint, an elbow joint, and a wrist joint, each powered and controlled by a Tower Pro MG-995 servo. Connecting the joints are wood struts that support the arm with required mechanical integrity with light weight and low cost. Ball bearings, shown in **figure ii**, are employed to ensure the smooth relative motion between wood struts and servo mounts on the joints. A claw is installed on the wrist joint. The base of the claw provides mounting points between the claw and wrist joint as well as between the claw and a servo. On the far end of the claw base, a rail is designed for two plastic grips to slide on.

The procedure for RPDS includes picking up a cylindrical payload, safely transporting the payload to the launch vehicle, accurately inserting the payload into the launch vehicle body, and in the end close the door of the payload bay. Several degrees of freedom are needed for the robotic arm to complete these tasks. Rotation about the shoulder joint determines the general motion and direction of the arm. Rotation about the elbow joint accurately places the claw on the desired position. Rotation about the wrist joint direct the claw to the target. The three joints coordinate together to accurately control the motion of the claw, as shown in **figure iii.**

The position of the claw relative to the shoulder joint can be obtained by the following equation:

$$\vec{r} = \begin{bmatrix} cos\alpha & -sin\alpha \\ sin\alpha & cos\alpha \end{bmatrix} \begin{pmatrix} r1 \\ 0 \end{pmatrix} + \begin{bmatrix} cos(\alpha+\beta-\pi) & -sin(\alpha+\beta-\pi) \\ sin(\alpha+\beta-\pi) & cos(\alpha+\beta-\pi) \end{bmatrix} \begin{pmatrix} r2 \\ 0 \end{pmatrix} + \begin{bmatrix} cos(\alpha+\beta+\theta) & -sin(\alpha+\beta+\theta) \\ sin(\alpha+\beta+\theta) & cos(\alpha+\beta+\theta) \end{bmatrix} \begin{pmatrix} r3 \\ 0 \end{pmatrix}$$

Linear translation for the grips along the claw rail enables the gripper to open and close its grasp upon objects. Each of the 3 rotational motion is actuated by a servo installed on the joint, while the linear motion is achieved by connecting the two grips with a disk that rotates with the gear of claw servo, such that the disk translates its own rotation to a linear motion on its edge.
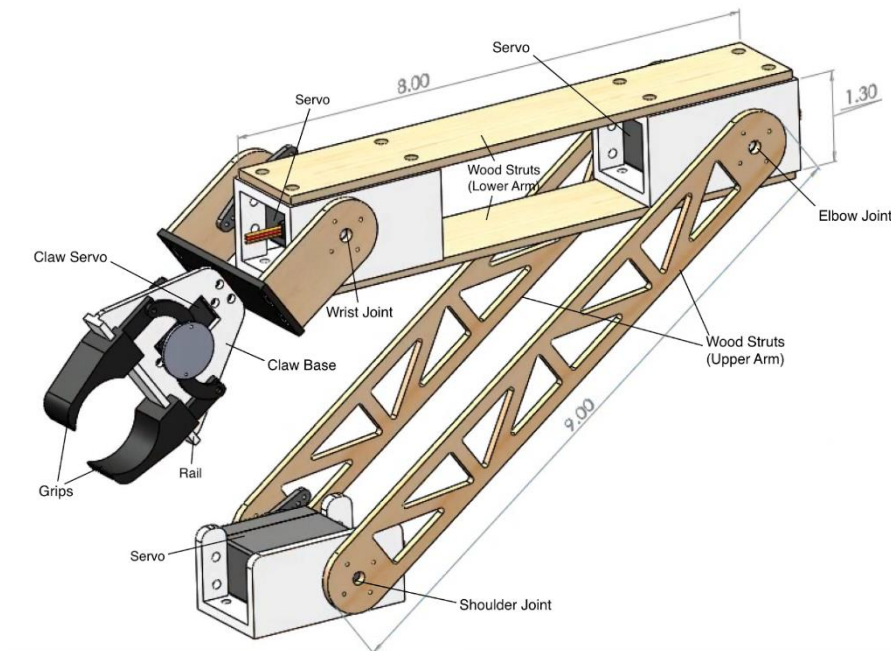
Figure i: RPDS Overview
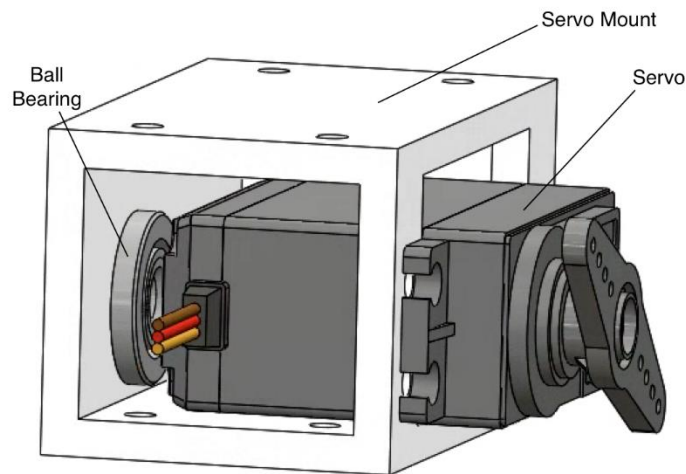
Figure ii: Single Joint
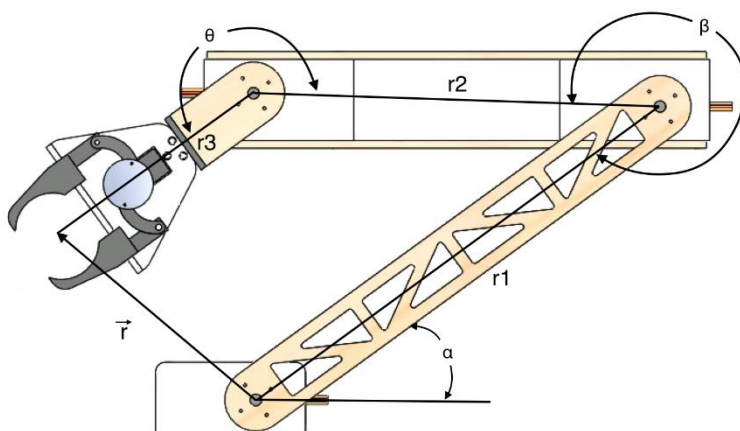
Figure iii: Geometry Analysis
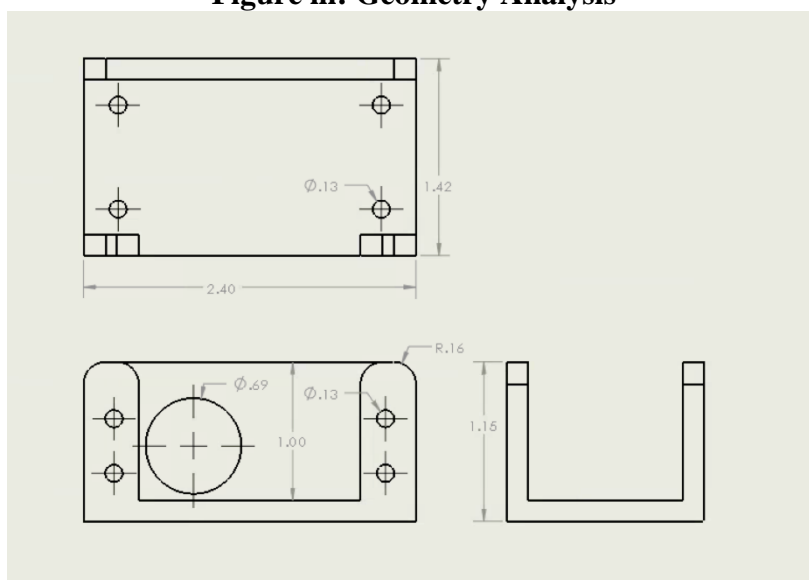
Figure iv: Servo Mount for Shoulder Joint - Drawing
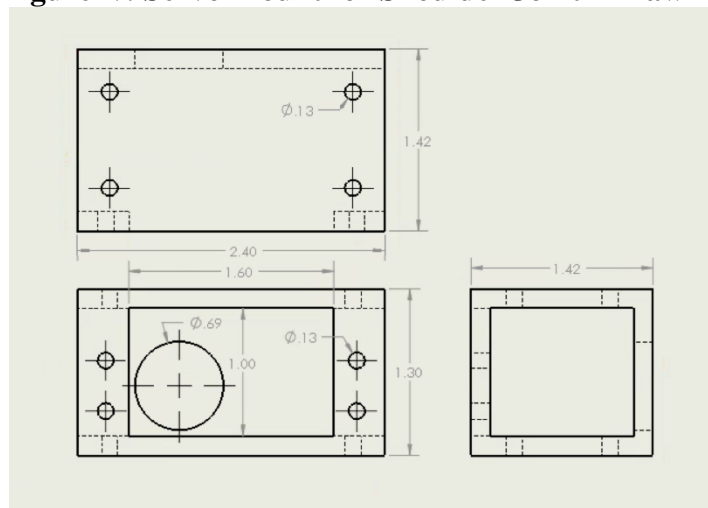
Figure v: Servo Mount for Elbow And Wrist Joint - Drawing
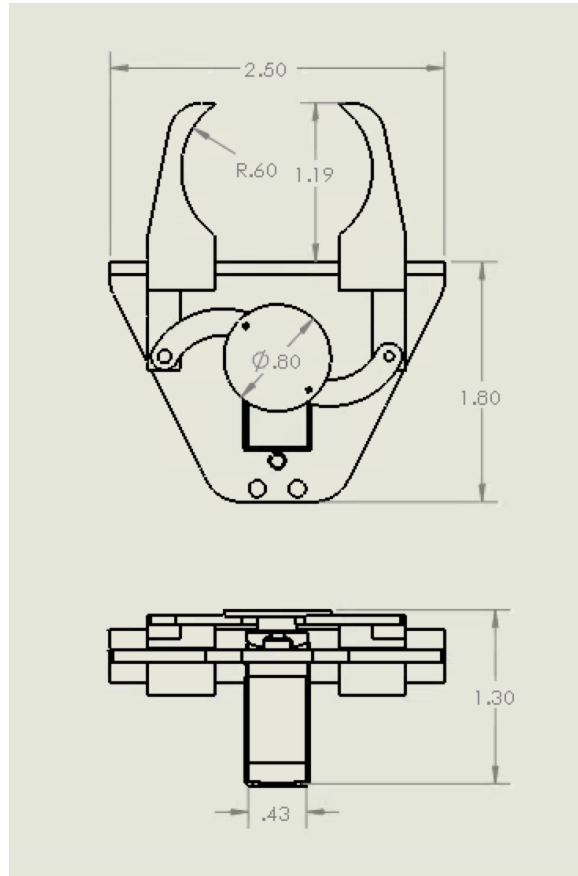
Figure vi: Claw - Drawing

4.2.2. RES

The RES, shown in **FIGURE XX**, utilizes a threaded rod to lift the launch vehicle. A NEMA 23 stepper motor mounted on the base rail spins the threaded rod which pulls a sliding base closer to the motor. The sliding base has a threaded acme cylinder nut attached to it, which allows the base to slide closer to the motor when the threaded rod is turned. The arm rail is attached to the sliding base and the launch vehicle rail. As the sliding base moves closer to the motor, the arm rail pushes up the launch vehicle rail, lifting the launch vehicle into position. The sliding base also features a rod that runs straight through and rests on the wooden rails on either side of the sliding base. This rod, shown in more detail in **FIGURE XX**, supports the load that the arm rail applies to the sliding base instead of the load being applied directly to the threaded rod.

Base Rail

Launch Vehicle Rail

Arm Rail

Angled Supports

Mounted Ball
Bearing

NEMA 23 Stepper Motor

Wooden Rails

Support Frame

Sliding Base

Threaded Rod
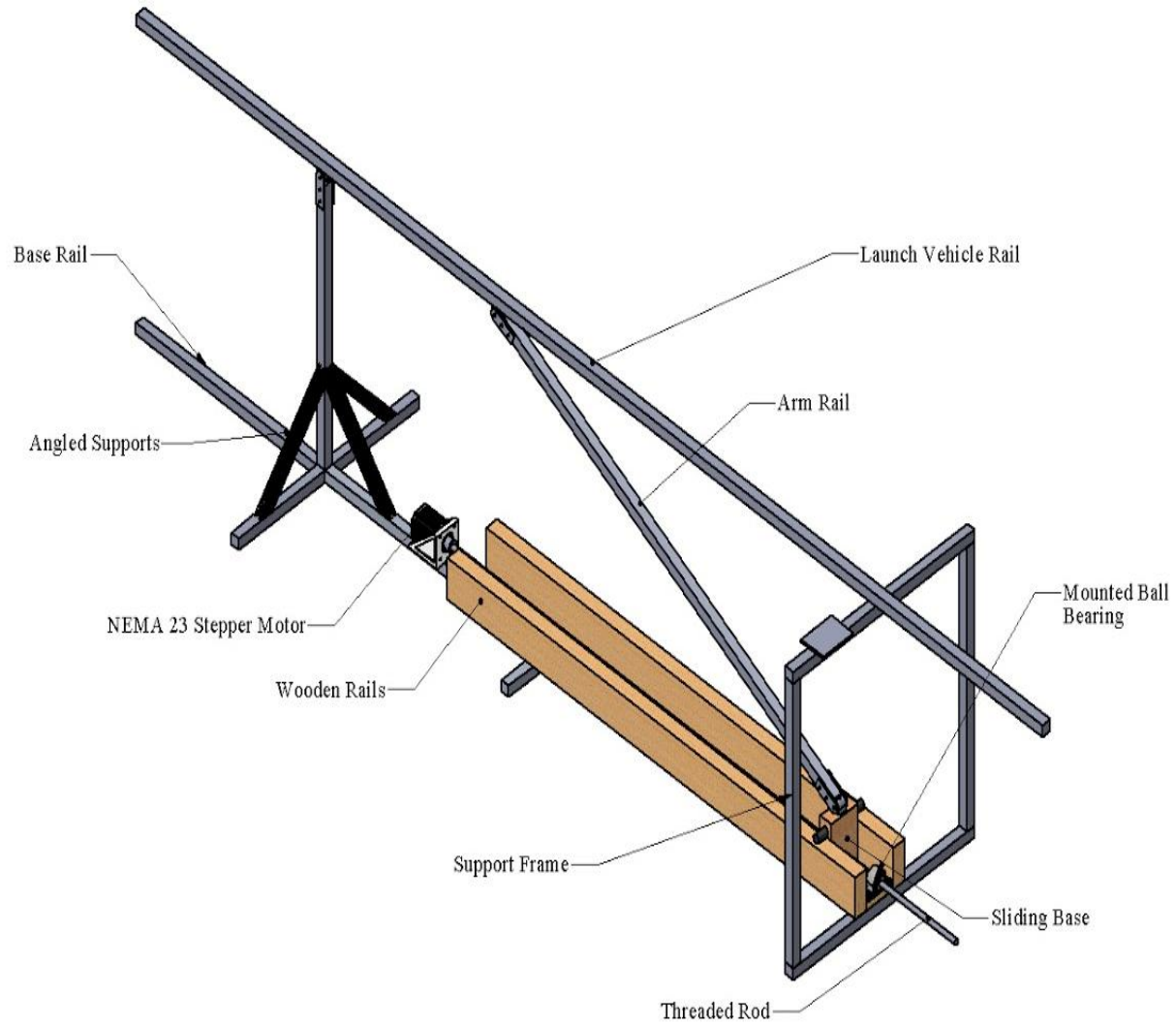
Figure XXXX: RES
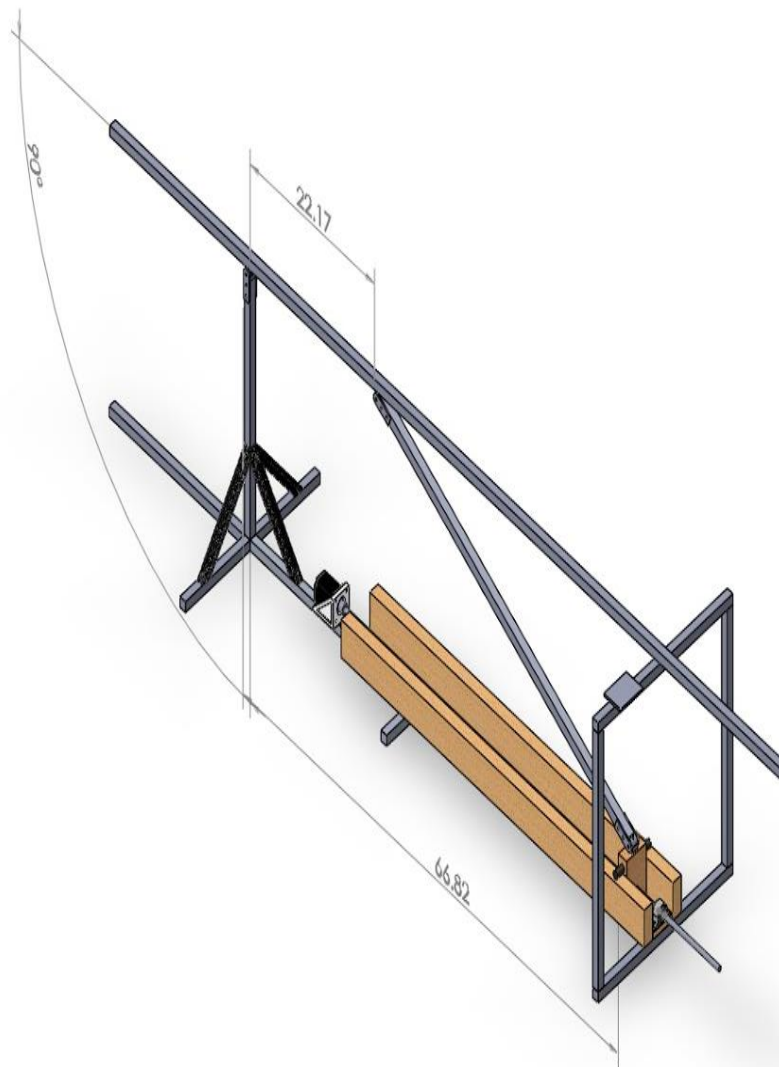
Figure XXXX: RES Initial Position

Figure XXXX: RES Final Position
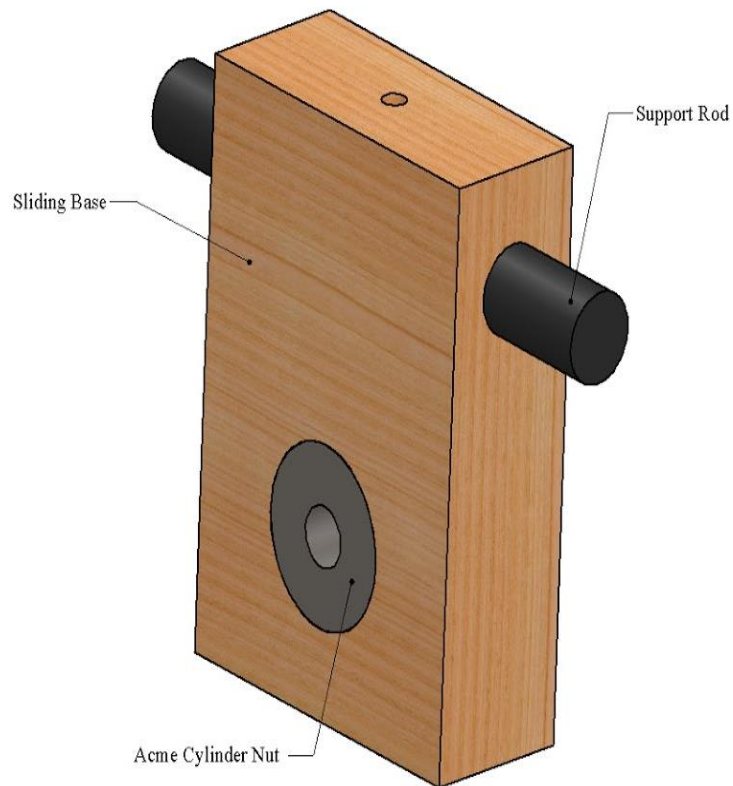
Figure XXXX: Sliding Base - Isometric
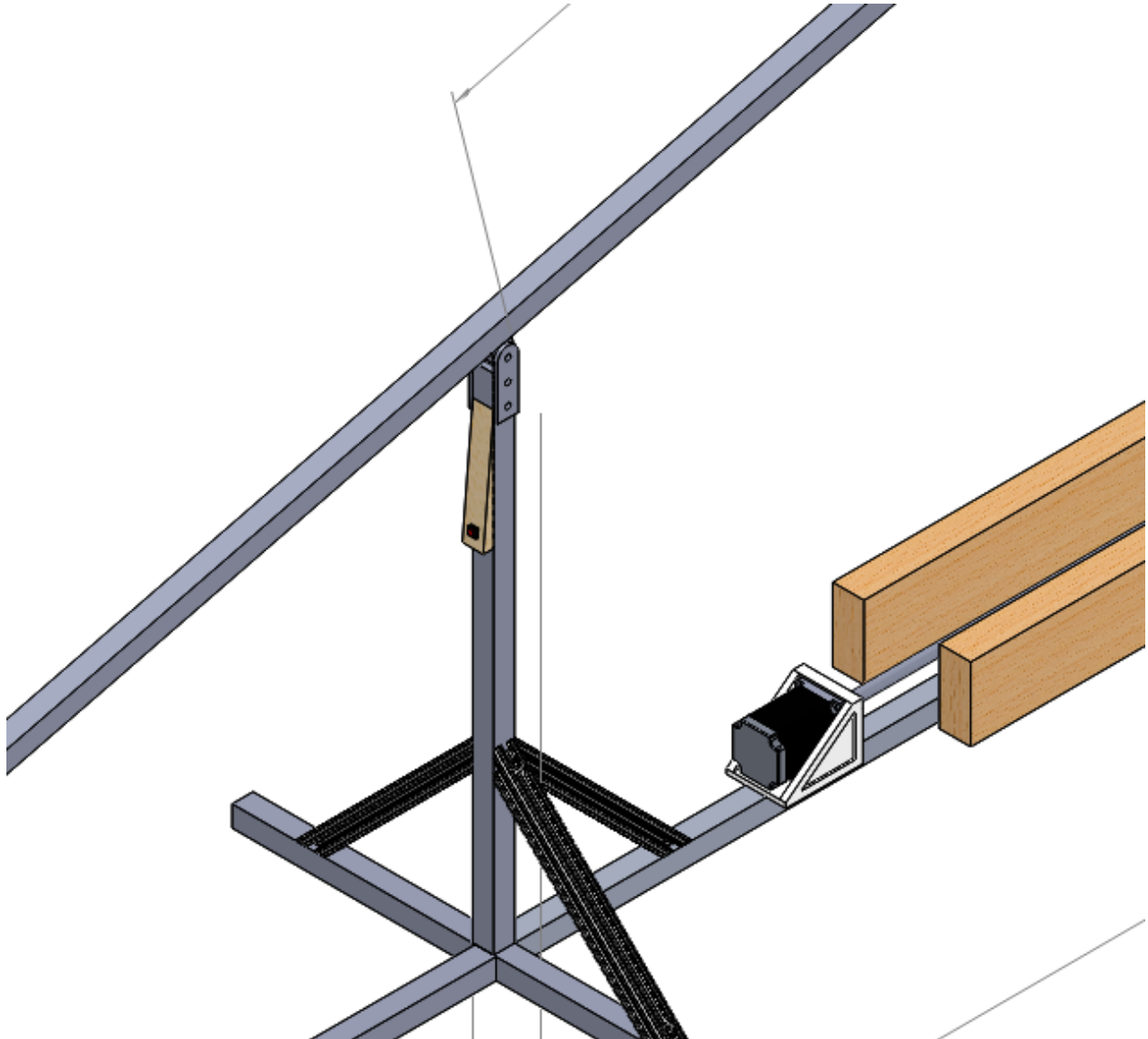
Figure XXXX: RES Stop Button
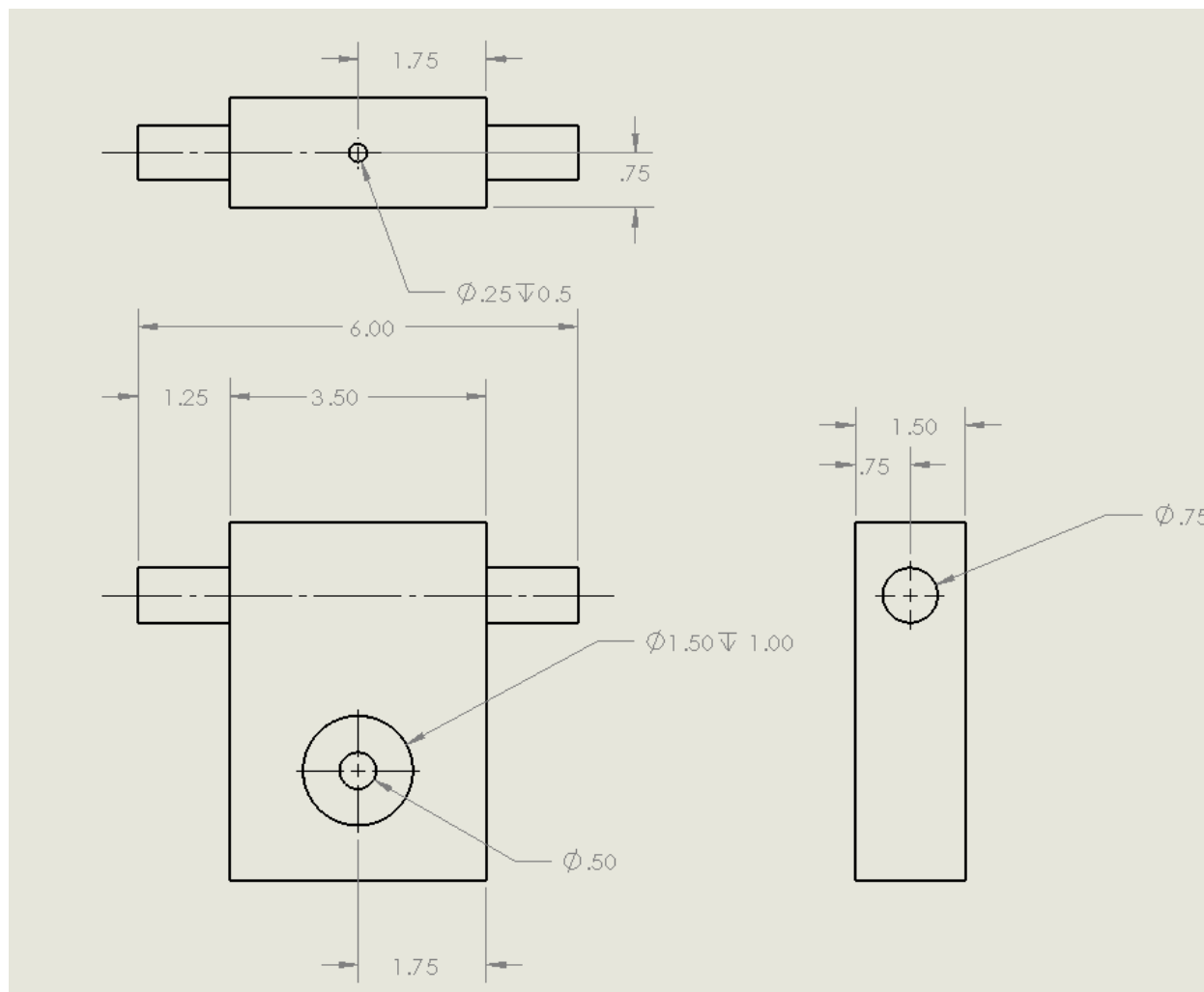
Figure XXXX: Sliding Base - Drawing
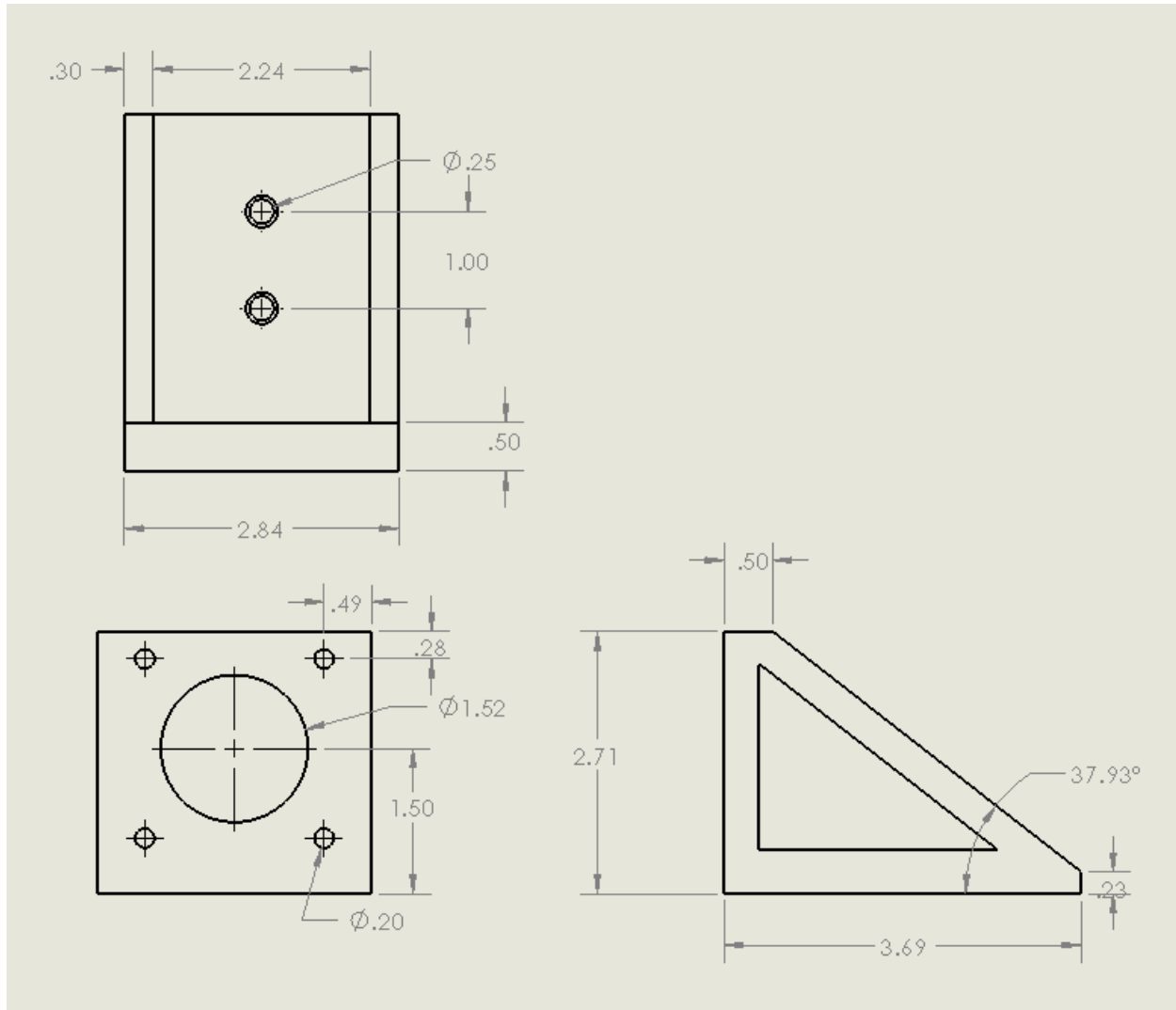
Figure XXX: Stepper Motor Mount

Analysis Results

The RES is able to successfully lift the 10 foot launch vehicle rail without the launch vehicle or any weight on it from 0 degrees to 85 degrees at a safe rate of speed. The launch vehicle rail tends to yaw during erection. It takes about two minutes and twenty seconds to get from horizontal to fully erect. There is a torque on the sliding base in the first five inches of travel, when it is attempting to lift the launch vehicle from the horizontal that prevents it from lifting a load exceeding 10 lbs. This initial lifting torque also causes the threaded rod, vertical support, and angled supports to bow and bend. The current pulled by the stepper motor follows a logarithmic trend that pulls the most amps, about 1.75 amps, at the beginning of the lift and slowly approaches a constant current of about 1.35 amps when the launch vehicle rail passes the 45 degree mark and the torque is lifted off of the sliding base. This is expected, as the most power is required from the

motor during the initial lifting stages. The distance from the motor to the sliding base is linear over the two minutes and twenty seconds it takes to lift the launch vehicle rail without any weight. This shows the motor, threaded rod, and sliding base spin and move smoothly without slippage. The angle data of the launch vehicle rail follows the expected logarithmic trend. Possible errors in the data collection could be attributed to inaccuracies in measurement (incorrect distance measurements) or inaccuracies in our measurement devices (inaccurate power supply readings).

Angle of Launch Vehicle Rail vs. Time
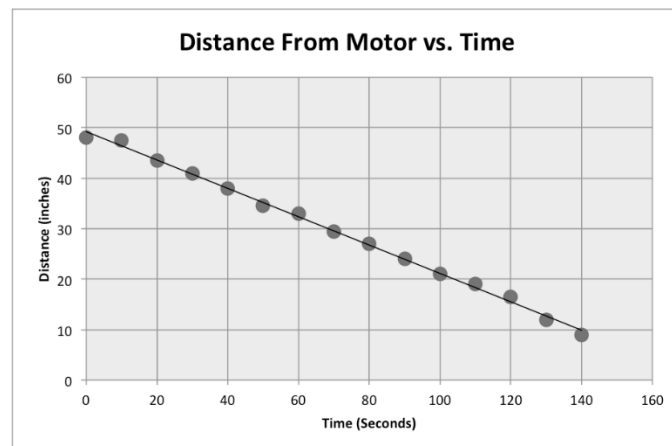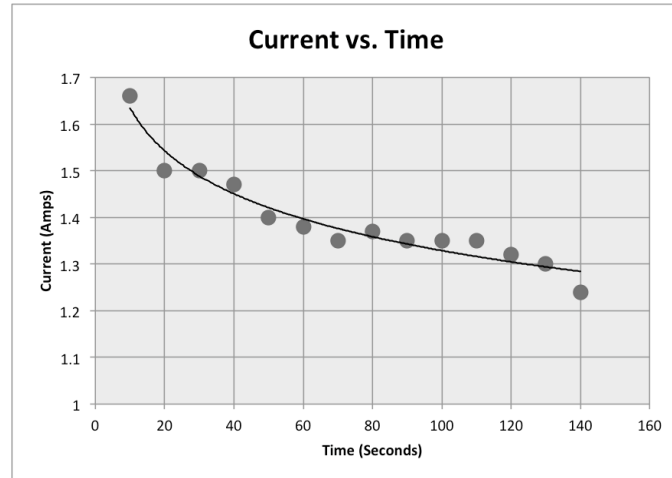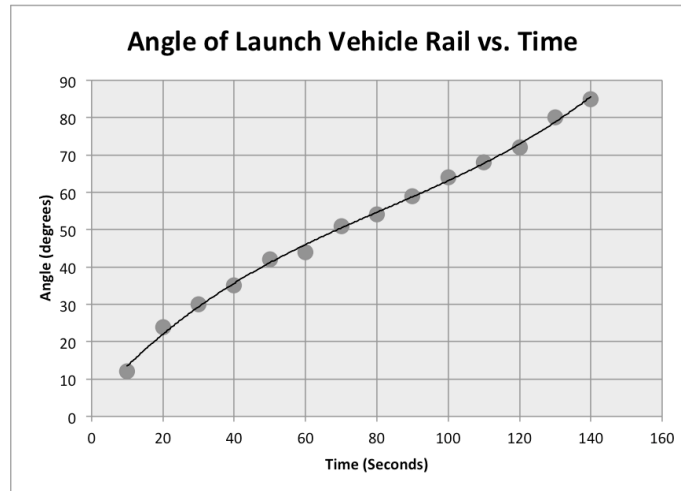
Integrity of Design

Given the results of the testing, the RES design is able to lift an unloaded launch vehicle rail successfully from horizontal 0 degrees to 85 degrees. The motor moves the sliding base down the threaded rod successfully in a linear trend. As expected the motor encounters the most resistance during the first 30 degrees of erection, which is about 5 inches of travel for the sliding base, where an excess amount of torque is subjected to the sliding base. The torque becomes unmanageable to overcome when a load exceeding 10 lbs is added to the RES. After the sliding base passes the 5 inches of excessive torque and resistance, and the launch vehicle rail is over 30 degrees, the RES can successfully erect a loaded launch vehicle rail to 85 degrees. The following changes will be implemented to reduce torque on the sliding base and the threaded rod. The sliding base will be increased in length along the threaded rod to have a longer lever arm to resist torque introduced by the threaded rod. The motor will be moved closer to the sliding base to prevent unused thread rod from bowing under torque. Additionally, the launch vehicle rail has a tendency to slightly yaw during erection. The attachment between the arm rail and the top of the sliding base will be strengthened with a standoff screw used as a threaded drop-down insert to provide a more stable connection to resist torque.

4.2.3. MIS

The MIS, shown in **FIGURE XXXXXXXXX,** utilizes a rack and pinion mechanism to insert an electronic match into the launch vehicle's motor cavity. Overall, the MIS is 1 inch wide, 4 inches tall, and 2 ft long. The whole MIS is secured to the bottom of the launch vehicle rail with t-nut fasteners and rotates with the launch vehicle during the RES stage of the AGSE mission. A Mercury stepper turns a pinion in contact with a rack. As the pinion turns, the rack moves up the launch vehicle rail, 12 inches into the motor cavity. The rack sits on a MDF base so that it can reach into the center of the motor cavity.

Drawings and Specifications:
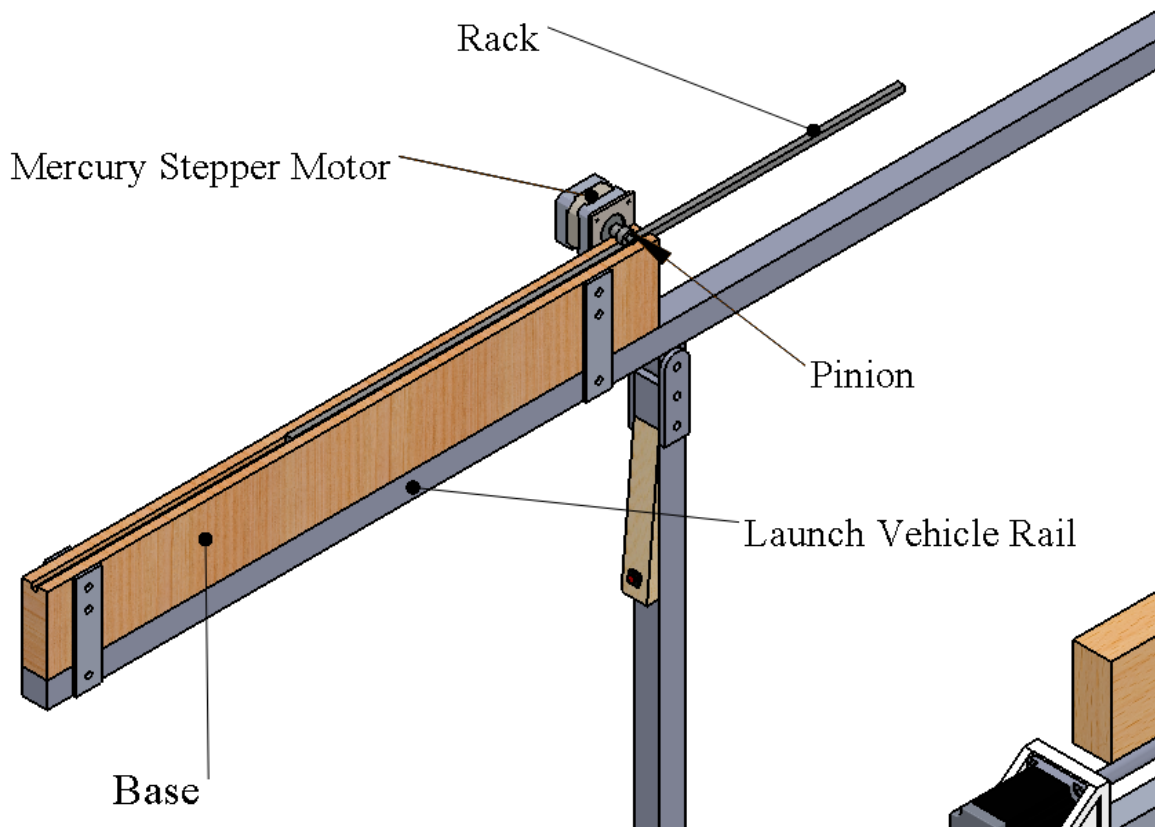
FIGURE XXXXXX: MIS
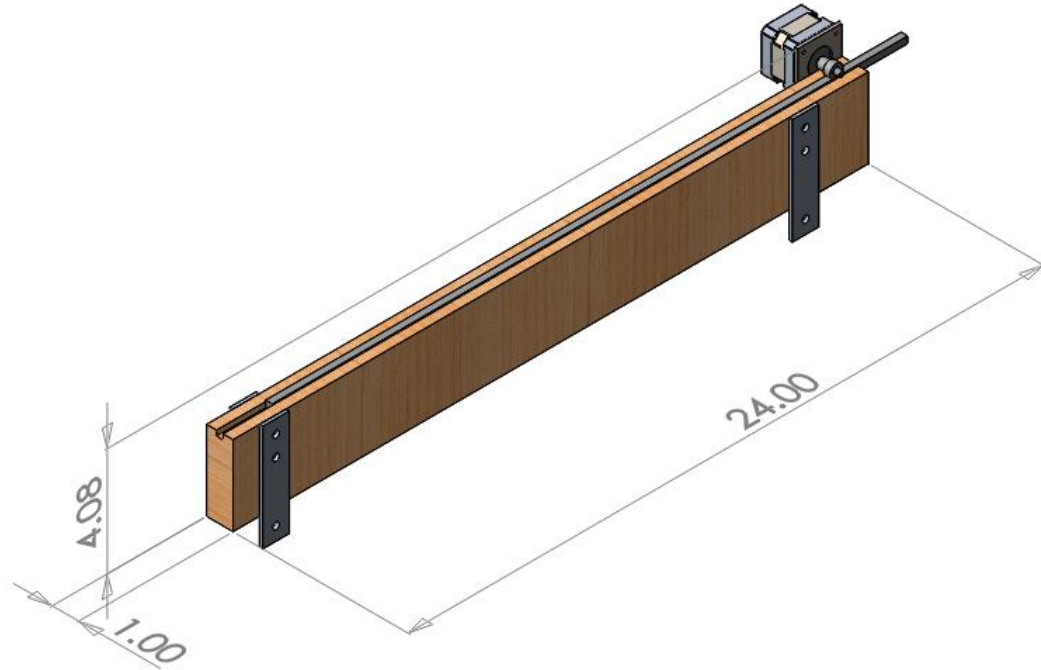
FIGURE XXXXX: MIS Specifications

Analysis Results

The MIS successfully moved the rack 1.5 ft while horizontal. The overall time for accomplishing the task was 14 seconds. As the rack moved towards its final position, the stability of the rack decreased. This is most likely due to the rack moving off the base and having less support. At 85 degrees from the vertical, there was no unexpected motion of the rack. The main concern was that the stepper motor would not have enough static torque to keep the rack upright. This proved not to be an issue. There were a few instances when the pinion did not turn enough and the rack did not reach its full extension. This was attributed to a poor connection between the pinion and the motor shaft. In general, the MIS was able to accomplish its task quickly and reliably.

Integrity of Design

From the testing, the MIS seemed effective at inserting the ignition into the motor cavity. Some troubles may occur from the pinion slipping on the motor shaft. If this happens, the rack will slip down the track. To prevent this, several changes could be implemented. First, the track could be remade to have a tighter press fit around the rack. Also, a better interface between pinion and motor shaft could be made. This could be done with a coupler, set screws, or epoxy. Additionally, the

pinion placement could be lowered to sit deeper in the teeth of the rack to increase contact area. All these changes could reduce the chance of MIS failure drastically.

4.2.4. Electronics
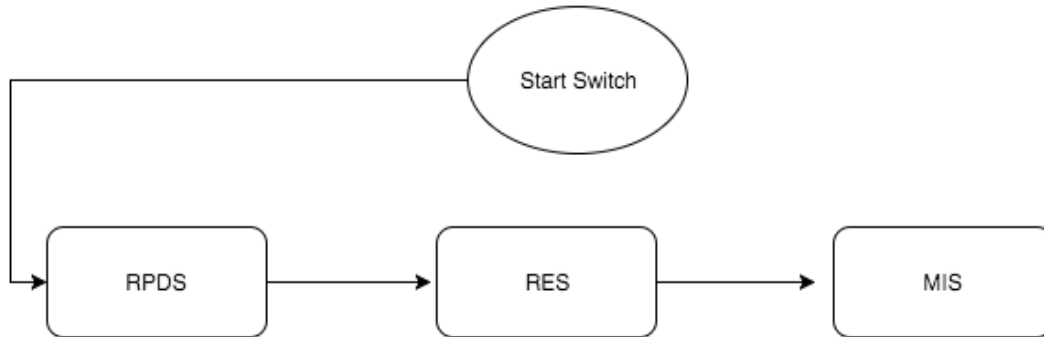
The AGSE electronics primarily consists of 1 unipolar stepper motor, 1 bipolar stepper motor, 4 servo motors, 3 LEDs, 2 pushbuttons, and a safety switch. The entire system will be controlled using an Arduino Uno-R3. The first component of the AGSE is the RPDS, which is composed of 4 servo motors. Each servo motor controls a different degree of rotation for the robotic arm. All the servo motors will be powered with a 6V Battery. Once the RPDS is completed, the RES will be activated. The RES uses a unipolar stepper motor to raise the rocket to 85 degrees. The NEMA-23 unipolar stepper motor requires a ST-M5045 driver, both of which will be powered using a 24V battery. Once the rocket is raised to 85 degrees, the Launch Vehicle Rail will hit a push button that deactivates the RES and starts the MIS. The MIS uses a Mercury-Motor sm-42byg011-25 bipolar stepper motor to raise the ignition system. This motor requires the EasyDriver stepper motor driver to function. Both the motor and the driver will be powered with a 12V battery.

Schematic:
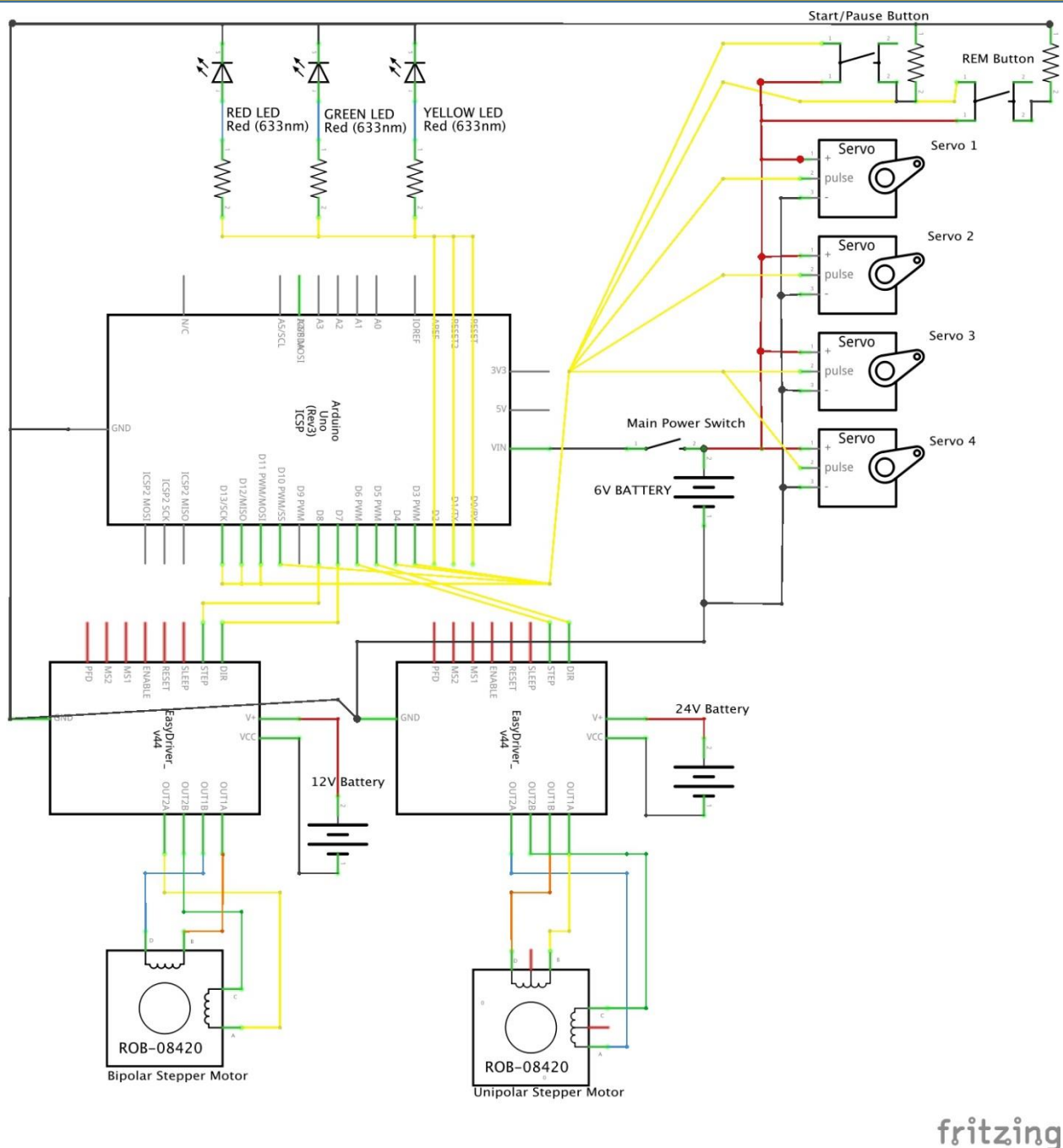
Figure XXXX: Full Schematic of the AGSE electronics

Power:

Battery Energy Levels

Battery	Total Energy
6V	.446 Ah
12V	2.3 Ah
24V	2.3 Ah

Energy Consumption AGSE Components

Component	Quantity	Operating Current	Operating Time	Energy Consumption
Servo Motor	4	400 mA	180 seconds	.02 Ah
NEMA 23 / Driver	1	1600 mA	165 seconds	.073333 Ah
Mercury Motor / Driver	1	330 mA	45 seconds	.004125 Ah
LEDs	3	120 mA	400 seconds	.013333 Ah
Pushbuttons	2	80 mA	400 seconds	.00889 Ah
Arduino Uno-R3	1	100 mA	400 seconds	.01111 Ah

The 6V Battery powers the LEDs, Pushbuttons, Arduino Uno-R3, and the servo motors. The total energy consumption of these 4 components is .05333 Ah. The 6V Battery provides .446 Ah, which is enough to run the 4 components through 8 full runs.

The 12V Battery powers the Mercury Motor and its driver, which consumes .004125 Ah. The 12V Battery provides 2.3 Ah, which is enough to run the motor over 500 times.

The 24V Battery powers the Nema 23 Motor and its driver, which consumes .073333 Ah. The 24V Battery provide 2.3 Ah, which is enough to run the motor about 30 times.

Safety Switches / LEDs:

Each battery will be connected through one main power switch. This safety switch will instantly turn off the entire AGSE, regardless of what component is currently running. There is also a start/pause button that can pause the component of the AGSE that is currently running. While the Arduino is powered on, the green LED will also be on, and while the Arduino is off, the red LED will be on. If the pushbutton is pressed to pause the operation, the yellow LED will be on.

4.3. Mission Success Criteria and Verification

Requirement	Design Feature	Requirement Verification	Success Criteria
Capture the payload	RPDS will locate and grip the payload	The payload is enclosed in the claw	The payload stays in the grip of the claw
Move the payload into the payload bay	RPDS will have 4 DOF controlled by 4 servo motors	The payload moves with the claw	The arm moves with speed and accuracy and the payload stays in the grip of the claw
Secure payload in the payload bay	Plastic clips will snap around the payload from force of RPDS	A snapping sound is heard from the payload bay and the payload is within the clips	The payload does not move inside the bay
Close the payload door	RPDS will flick the door of the payload bay, the payload hatch is sealed magnetically	No excessive gaps are seen on the payload hatch	The payload hatch closes fully
Raise the Launch Vehicle	A threaded rod and acme nut system will pull the guide rail upright	The launch vehicle rail moves to a vertical position, a touch sensor is triggered at the end	The launch vehicle remains on the rail, and is stable throughout the erection
Maintain the Launch Vehicle angle	The threaded rod prevents slipping, and 3 pairs of set screws prevents the threaded rod from moving	The threaded rod does not translate, and only rotates	The launch vehicle does not fall

Insert the igniter	A rack and pinion system will move the electronic match into the motor cavity	The rack moves as the pinion turns	The igniter is inserted 1 ft. into the motor cavity

4.4. Structural Elements

4.4.1. Launch Vehicle Rail

The launch vehicle rail is supported by one vertical support two feet from the back of the rail and by the arm rail 22 inches from the vertical support. In addition, there is a support frame that holds the launch vehicle rail parallel to the ground when lowered. As the launch vehicle rail is raised, all of the weight of the launch vehicle and the rail combined is distributed to the vertical support and the arm rail. At the instant the rocket is raised, the force on the vertical support in the horizontal direction causes the most problems for the design. That horizontal force was calculated to be 91 lbf. This force was calculated by assuming at the initial point of motion, the launch vehicle rail was in static equilibrium and the normal force from the support frame was zero.

$$F = 0, M = 0$$
$$Fx = Rx + F_{ARMCOS} = 0$$
$$Fy = Ry + F_{armsin} - WLV - WR = 0$$
$$M = -WLV(d1) - WR(d2) + F_{armsin} = 0$$

Farm= Force of arm on rail
WLV=Weight of Launch Vehicle
WR= Weight of rail
R= Reaction forces
θ = Angle between arm and rail
d1,d2= distance from axis

After taking into consideration the weight of the launch vehicle and the rail, the horizontal force could be calculated. **FIGURE XXX and XXX** show the results of an FEA test conducted on the vertical support. The maximum displacement of the rail is approximately 0.95 inches. However, this test was conducted without the angled supports factored in. The angled supports should work to reduce this displacement to a more reasonable level. The sliding base also experiences large forces during the erection of the launch vehicle rail.
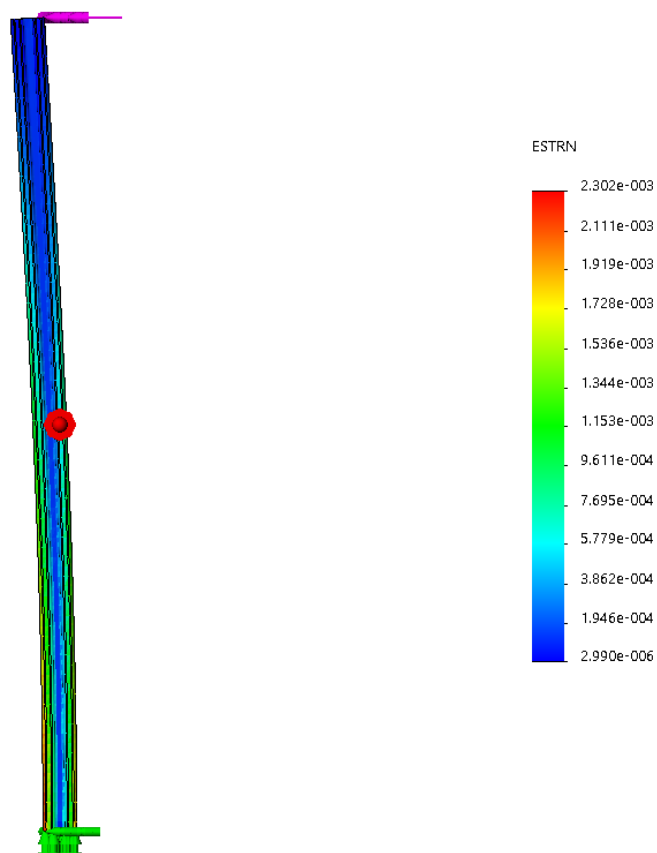
Figure XXXX: Strain in Vertical Support Rail
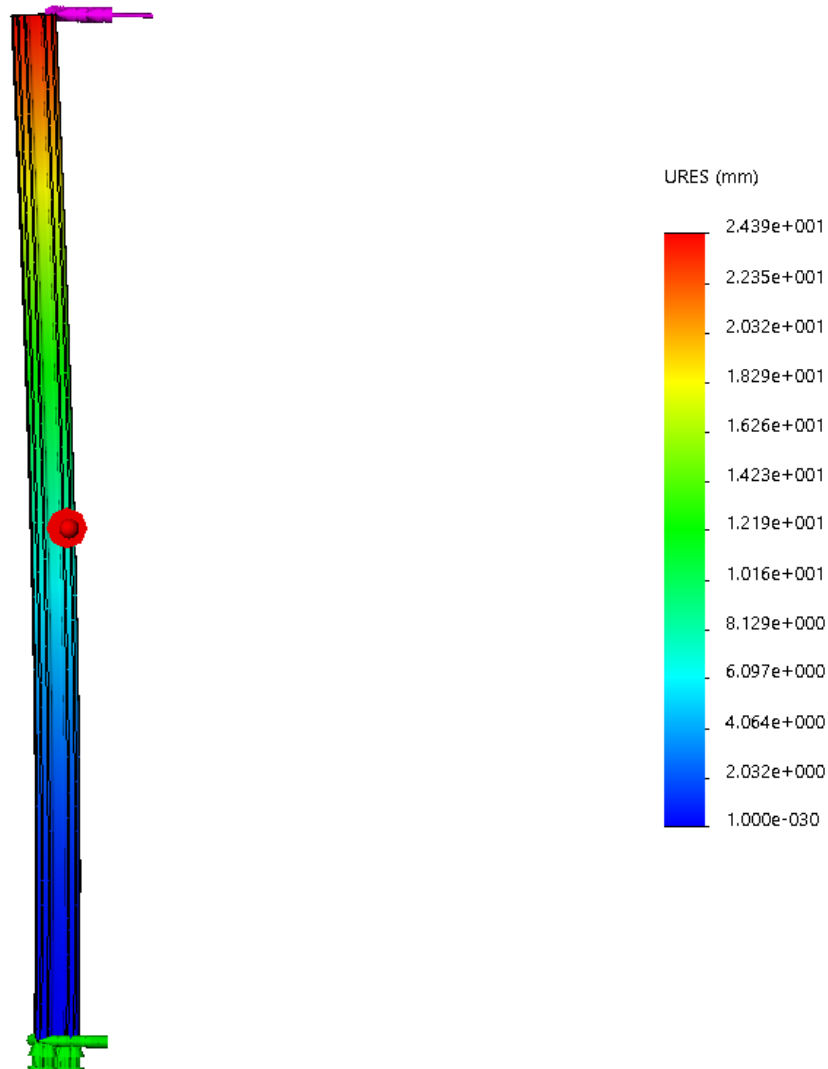
Figure XXXX: Displacement of Vertical Support Rail

4.4.2. Robotic Arm Struts

The two wood struts on the lower arm are supported by the servo mount on the elbow joint. At the far end of the struts, the wrist joint and claw are mounted. When the payload is captured by the arm, the load on the wrist side of the struts becomes a concern for structural integrity of the arm. To analysis the forces on the struts, the lower arm is assumed to be horizontal, as the struts experience the maximum bending moment when they are horizontal. The total weight of the claw and wrist assembly is calculated to be less than 0.3 lbf. The payload weight is given to be 0.25 lbf (4 oz). The following force analysis on one strut is done with the assumption that the wood strut is in static equilibrium.

$F = 0, M = 0$ R = Reaction Forces
$Fy = Ry - 12(Wasm + Wpay) - Wstrut$ Wasm=Weight of Claw-wrist assembly

$M = 12(Wasm(d1) + Wpay(d2)) + Wstrut(12Lstrut) - Ryd3$ Wpay=Weight of Payload

Wstrut=Weight of Wood Strut
Lstrut=Length of Wood Strut
d1,d2,d3=Distance from axis

Figure xxxxx and **figure xxxxxx** shows the result of finite element analysis using Solidworks. The maximum displacement at the wrist end of the wood strut is estimated to be 0.05 inch, which is safely within the design limit of this component. This analysis concerns the horizontal placement of lower arm, when the maximum bending moment on the wood struts occurs. Therefore, during normal operation, the mechanical integrity of the wood strut can be ensured.
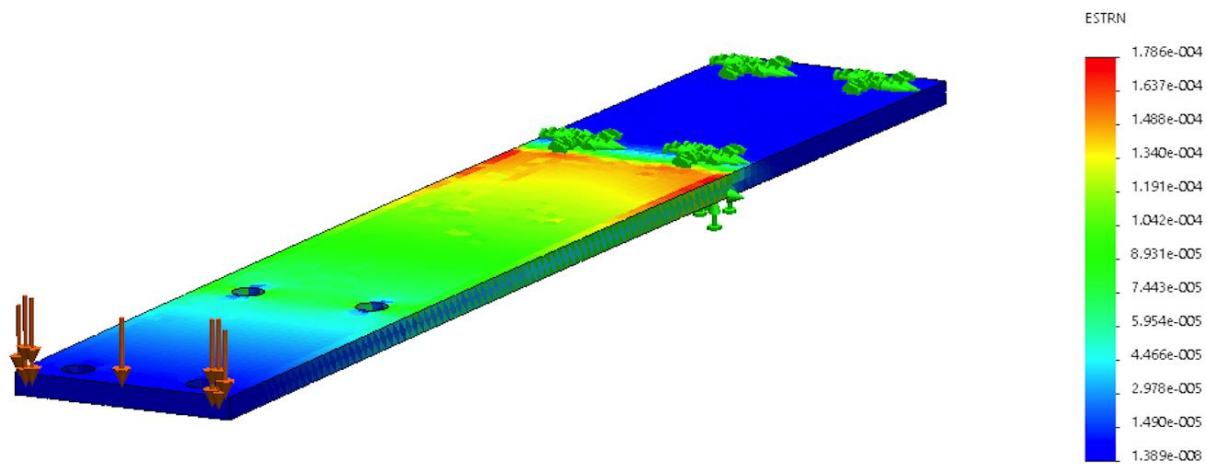
Figure xxxxx: Strain in Lower Arm Wood Strut
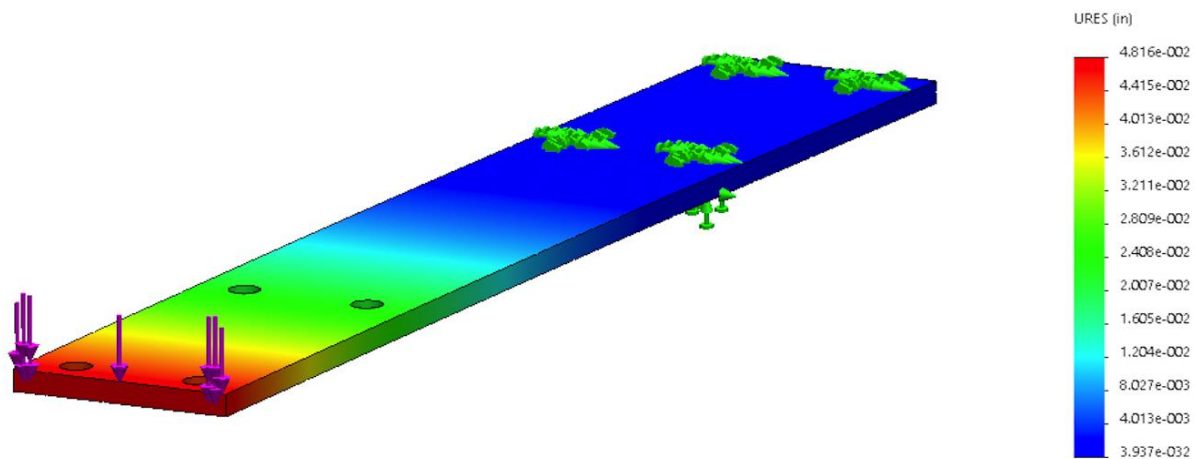
Figure xxxxxx: Displacement in Lower Arm Wood Strut

4.5. Mass Breakdown

Subsystem	Part	Material	Mass (kg)	Amount
RES	80/20 Rails	Aluminum	8.7	38 ft
	2x4 Rails	Wood	3.5	8.5 ft
	Hinges	Aluminum	.4	3
	Brackets	Aluminum	.4	10
	Motor Holder	ABS Plastic	.1	1
	Mounted Ball Bearing	Steel	.2	1
	Support Rod	Steel	.2	1
	Threaded Rod	Steel	1.66	1
	Acme Nut	Steel	.1	1
	Motor coupler	Aluminum	.05	1
	NEMA 23	Electronics	.4	1
MIS	Mercury Motor	Electronics	.2	1
	Base	MDF	.2	1
	Rack	Steel	.2	1

	Pinion	Steel	.05	1
	Motor holder	Plywood	.1	1
	End stop	Aluminum	.2	1
RPDS	Arms	Plywood	.1	4
	Claw	ABS Plastic	.1	1
	Servo Mounts	ABS Plastic	.1	4
	Servo Motors	Electronics	.2	4
ECU	Arduino Uno	Electronics	.1	1
	Sainsmart Driver	Electronics	.2	1
	EasyDriver	Electronics	.1	1
	Buttons	Electronics	.05	2
	LEDs	Electronics	.05	3
	Batteries	Electronics	.5	3

4.6. Electronics Expanded

4.6.1. Arduino Code:

One of the biggest coding challenges was implementing the start/pause button. Because the button has to instantly start and pause the movement of motors, the motors cannot be programmed to move to a single location in a single line of code. Instead, each motor movement is actually a loop that increments the position of the motor until it has reached the final position. Loops allow the Arduino to constantly monitor the state of the button, thereby allowing it to continue from where it left off. The following code is used to start and pause any component using a pushbutton.

```
if (digitalRead(ButtonPin) == HIGH) {
    CurrentState = CurrentState + 1;
    delay(1000);
  }
if (CurrentState % 2 == 0) {
    while (digitalRead(ButtonPin) == LOW) {
    }
    CurrentState = CurrentState + 1;
    delay(1000);
}
```
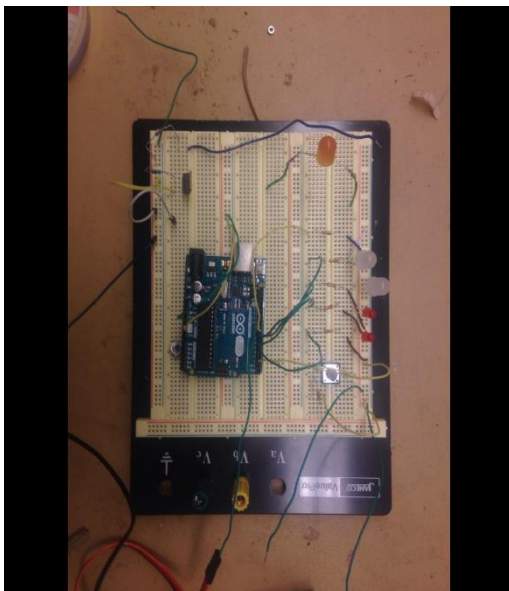

Figure XXXX: Start/Pause Test Setup

A Start/Pause Test was used to see if the button could instantaneously stop and resume a servo motor's movement. Initially, the servo motor was moving to 180 degrees. During the test, when the button was pressed, the servo stopped immediately and resumed moving to 180 degrees on the next press. The code for this test is shown below.

```arduino
for (int pos = 0; pos < 180; pos++) {
  Servo.write(pos);
  if (digitalRead(ButtonPin) == HIGH) {
    CurrentState = CurrentState + 1;
    delay(1000);
  }
  if (CurrentState % 2 == 0) {
    while (digitalRead(ButtonPin) == LOW) {
    }
      CurrentState = CurrentState + 1;
      delay(1000); |
  }
}
```

The same test was applied to the stepper motors. This time, the LEDs were also used in the test. This code applies to both the unipolar and bipolar stepper motors. The only differences are the Arduino pin numbers.

```
for (pos = 0; pos <= 100000; pos+= 1) {
  digitalWrite(8, directionP);
  digitalWrite(9, HIGH);
  delayMicroseconds(del);
  digitalWrite(9, LOW);
  delayMicroseconds(del);
  if (digitalRead(ButtonPin) == HIGH) {
    CurrentState = CurrentState + 1;
    delay(1000);
  }
  if (CurrentState % 2 == 0) {
    while (digitalRead(ButtonPin) == LOW) {
      digitalWrite(Yellow, HIGH);
    }
    CurrentState = CurrentState + 1;
    digitalWrite(Yellow, LOW);
    delay(1000);
  }
  if (digitalRead(ButtonPin2) == HIGH) {
    if (directionP == HIGH) {
      directionP = LOW;
    }
    else {
      directionP = HIGH;
    }
    delay(1000);
  }
}
```

The transitions between components (RES, RPDS, MIS) are hard-coded. For example, the RPDS will have a predetermined motion coded, so the payload must be placed in a specific place. Once the RPDS is finished, the RES starts automatically. But, the MIS does not start until the RES push button is hit. When the Launch Vehicle Rail hits this button, the rocket will be at 85 degrees, so the RES stops.

4.6.2. Electronic Containment Unit
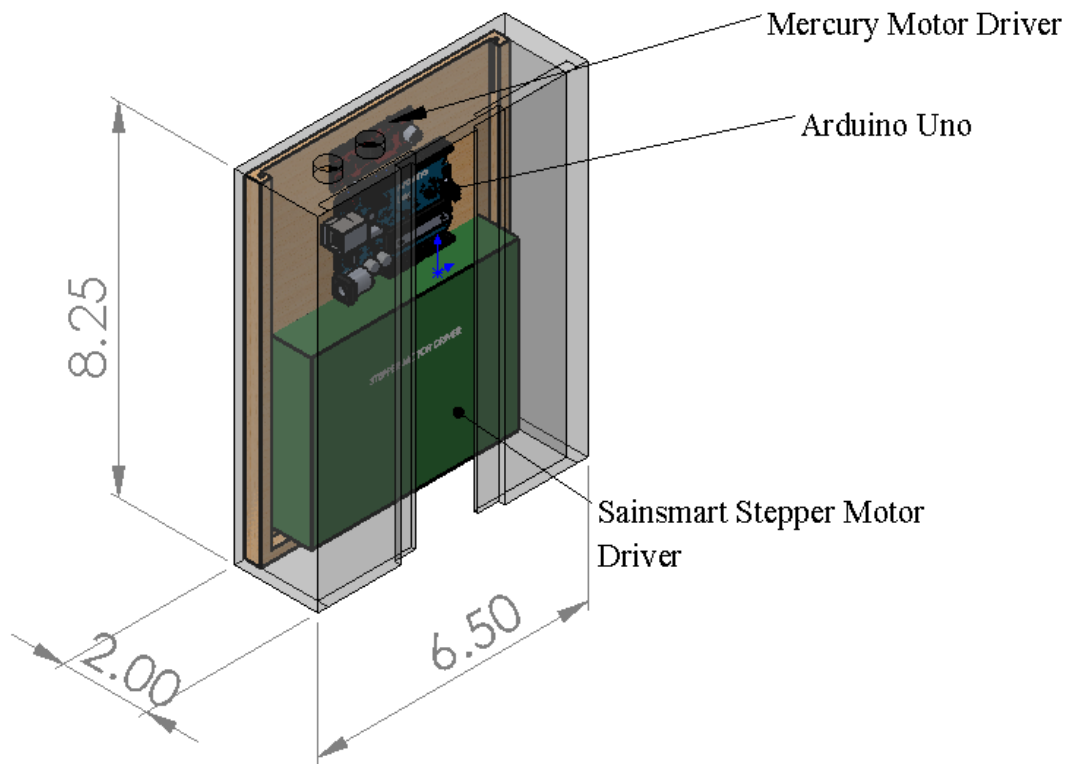
Figure XXXX: AGSE Electronics Containment Unit

All the electronics of the AGSE will be attached to the board shown above. The side that is shown contains the Arduino and the stepper motor drivers. The other side of the board will contain all of the necessary batteries. This setup removes the need for a breadboard, and it keeps the electronics compact and organized.

4.7. Testing

To test the effectiveness of the raising mechanism, we tested the RES with no weight and with weight. For the unweighted tests the total time it took to raise the launch vehicle from horizontal to 85 degrees was recorded. In addition to the distance traveled by the sliding base, the angle of the launch vehicle rail off the horizontal, and current drawn was also recorded. The unweighted test was deemed a success, the RES was able to successfully erect the launch vehicle rail to 85 degrees off the horizontal. The sliding block moved at a nearly constant rate down the threaded rod, and the most current was drawn at the beginning when the torque is at its highest, but slowly

reached a constant current around 30 degrees off the horizontal. However for the weighted test, the RES was unable to lift 10 lbs past the initial high torque mark, and was deemed a failure. To assist the mechanism resist high torques through the initial raising of the launch vehicle, the sliding base will be elongated, the threaded rod will be shortened, the wooden rails will be pressed against the sliding base, and the connection between the arm rail and the top of the sliding block will be strengthened with a steel threaded insert. To view a more detailed outline, please refer to the test plan in Appendix xxxx.

4.8. Workmanship

4.8.1. RPDS

The plastic parts in RPDS, including 2 grips, 2 claw connectors, a claw base, and 3 servo mounts, were 3D printed out of ABS plastic. The rail on the claw base is then sanded and lubricated to reduce the friction of the grips sliding on the rail. All the wooden pieces, including 2 lower arm wood struts, 2 upper arm wood struts, and 2 wrist joint connecting pieces, are laser cutted out of ⅛'' polywood board to meet the required manufacturing precision for smooth joint motion. Different parts in RPDS are all jointed by screw and nut combinations. The size of the screw and mounting points are chosen between ¼'' and 1/32'' based on the available mounting space so that the screws and nuts does not interfere with any other components.

4.8.2. RES

The RES launch vehicle rail, arm rail, vertical support, angled supports, main rail, and support framing are all made out of 1 inch T-slotted which were sawed to the proper length using a miter saw to build the framing necessary. They are joined together using a ¼"-20 x ½" screw and t-nut combination that slides through and fastens to the T-slotted rails. The system uses one perpendicular and two parallel hinges for the arm rail and launch vehicle rail that are attached using the same T-slotted fasteners that join the framing. The RES stepper motor is press fitted and screwed into the motor holder. The motor holder was 3D printed out of ABS plastic to the exact dimensions of the stepper motor and screwed onto the main rail. A threaded rod is inserted into a coupler on the motor arm, and screwed in, to secure it in place. The threaded rod is then lead

through the Acme cylinder nut on the sliding base and then supported on the other side by the mounted ball bearing. The system uses two wooden rails that are in parallel to the main rail and threaded rod. The wooden rails serve as a path for the sliding base's iron support rod to roll down. The two wooden rails are screwed into wooden risers, which are screwed into the T-slotted rails. The wooden risers raise the height of the wooden rails to reach just beneath the sliding base's iron support rod. The sliding base was constructed out of a piece of wooden 2" by 4". The wooden block was drilled with holes for the Acme cylinder nut, cylinder nut support screws, arm rail hinge screw, and iron support rod. The bottom of the sliding base was sanded and the components mentioned above were screwed in, besides the iron support rod which was just inserted to allow to spin freely.

4.8.3. MIS

The MDF base of the MIS was first cut to size using a table saw to 1 in. by 3 in. and 2 ft. long. Then, a slot was milled into the top face using a ¼" end mill bit. The slot is then lightly sanded so that the rack can move smoothly through the rack. On the bottom face, opposite of the slot, 4 ¼" holes are drilled to a depth of .35 inches. Screws that will fix the MIS on the launch vehicle rail are inserted in these holes. The metal supports are cut from the water jet out of ⅛" aluminum plates. The metal supports are fastened to the MDF base using screws. The whole assembly is then slid onto the bottom of the launch vehicle rail and secured using appropriate fasteners.

4.8.4. Electronics

All of the batteries will be recharged to full capacity before the final run. All wire connections will be taped to prevent any broken connections. The wires for the MIS will run through a PVC pipe that runs parallel to the base rail to protect the wires. Every button and LED will be connected through a pull-down resistor to ensure that the logical signal is near 0 volts when the button is not being pressed. By adding resistors, it not only saves power, it also improves the performance of the LEDs and buttons. The REM-button will be used to stop the REM to provide the best accuracy for the final angle when the rocket is being raised.

4.9. Safety and Failure Modes Analysis

Phase	Description	Failure Mode	Hazard
Construction	Each component has its own construction process that is detailed in sections 4.2.1 (RPDS), 4.2.2 (RES), and 4.2.3 (MIS).	One or more components of the AGSE fail.	Flight with a faulty AGSE may cause rocket to fall unpredictably, possibly causing damage to persons/properties.
Assembly	The Robotic Payload Delivery System, Rocket Erection System, and Motor Ignition System comprise the AGSE.	One or more components of the AGSE fail.	See Construction Hazard
Launch	The Robotic Payload Delivery System (RPDS) will deliver and secure the payload inside the payload bay. The Rocket Erection System (RES) will raise the launch vehicle. The Motor Ignition System (MIS) will insert the igniter.	Servo motor failure(s) resulting in failure to deliver and secure the payload. Bipolar stepper motor failure, resulting in failure to raise the launch vehicle. Failure of the unipolar stepper motor or failure of the rack and pinion system, resulting in failure to insert igniter.	See Construction Hazard
Recovery	-	-	-

The table below details the potential hazards and failures that may occur during the Launch and/or Recovery phase for the AGSE.

Potential Failure	Effects of Failure	Failure Prevention
Payload is not secured in bay.	Payload will bounce inside the payload bay, disrupting flight.	Test various plastic clip dimensions to find best fit.

RPDS is stuck inside the payload bay.	Payload bay will not close and RPDS will be destroyed by raising the launch vehicle.	RES will be started by a signal from the RPDS after it has completed its task.
Launch Vehicle moves uncontrollably on the rail.	Could disrupt the performance of other subsystems.	More support along the launch rail to keep the disruptive movement of the launch vehicle at a minimum.
RES is not stable while raising.	Rocket will not be raised, and motors may potentially be broken.	Test subsystem, add counterweights to reduce necessary force from motor and add more framing to increase stability.
RES is not stable at full extension.	Launch vehicle could tip over.	Increase the weight to lower the center of gravity. Increase the base width. Add more supports to the launch rail.
RES does not stay upright.	Launch vehicle will fall unpredictably.	Perfect ratchet system, ensure tension in steel cable.
RES stepper motor does not stop.	Tension will continue to increase in the cable leading to failure.	Emergency stop button in place that activates when rail is at maximum angle.
MIS stepper motor does not stop.	Rack will move further into motor cavity, possibly damaging rotor.	Emergency roller switch in place that activates when rack passes a certain distance.
Electronics short circuit or are overloaded.	System will lose control.	Fuses will protect electronics, subscale testing will prevent short circuits and overload.

5. Electrical Subsystem

5.1. Flight Systems Overview

The current flight system features versatile connections on the printed circuit board. This allows easy connections with the entire rocket. Only three sensors are used: two altimeters and one accelerometer. All of the power supplies for the motors, sensors, and microcontroller will be within the avionics bay. All of the components and their functions are shown below.

Part	Function
Stratologger SL100	Altimeter - used to receive and record altitude
MMA8452Q	Accelerometer - used to receive and record acceleration
mbed LPC 1768	Microcontroller - used to receive sensor data to compute and control the ATS
Eggfinder TX/RX Module	GPS module - used to track the rocket in real time
9V Alkaline Batteries	Used to power all Avionics components and ATS

5.2. Flight System Features
5.2.1. Launch Vehicle

The electrical subsystem onboard the flight vehicle has several purposes including: deployment of parachutes, acquisition of data for post-flight analysis, and control of the flaps in order to reach the desired apogee of one mile.

Data acquisition and parachute deployment are accomplished by the altimeter solely, but control of the rocket flaps calls for a more elaborate flight software, a microcontroller flight computer, and the use of an added sensor: the accelerometer. Both the altimeter and the accelerometer output sensed values into an Mbed microcontroller, which then filters noise from the sensors according to the kalman filter specifications. The filtered values are then compared to flight simulation data generated via Simulink, and the control algorithm makes the difference between sensed and simulation values go to zero as time gets larger. The control algorithm works based on an equation, shown in Figure XX, that relates the change in height to the change in velocity.

```
s = (lambda * delta_h) + delta_v;
*control = (sign(s) + 1)/2;
```

Figure XX. The equation that describes control of the rocket.

5.3. ATS

The ATS function will be controlled by the 32-bit ARM microcontroller, which is being used as the flight computer. Based on the flight systems software's control algorithm, a PWM out (pulse-width modulated) will be sent to the 4 servo motors telling them whether to actuate the flaps or not. If the output of the microcontroller to a motor is a '1', then the servo motor will actuate a flap. If the output is '0', then a motor will retract a flap.

5.4. Workmanship

All of the sensors, motors, and microcontroller will share a common ground in order to function. The motors will be connected to the microcontrollers through header pins shown in Figure ZZ. The wires that connect the motor and microcontroller will be slip-connectors, that way, when the parachutes deploy, the wires can comfortably separate once the rocket splits. All of the components on the breadboard will be soldered.

5.5. Flight Systems Software

The onboard flight software was designed to be modular in order to maximize performance while also making it easy for the team to work on it cooperatively. The main () code loop can be described simply: the software waits for a sensed acceleration on the rocket which exceeds 2Gs, and then the code begins to run a scheduling function. The scheduling function determines the frequency at which each block of the 4 code blocks runs. The flight software consists of four main blocks of code, each is its own function. The functionality of the software is shown in Figure XX.
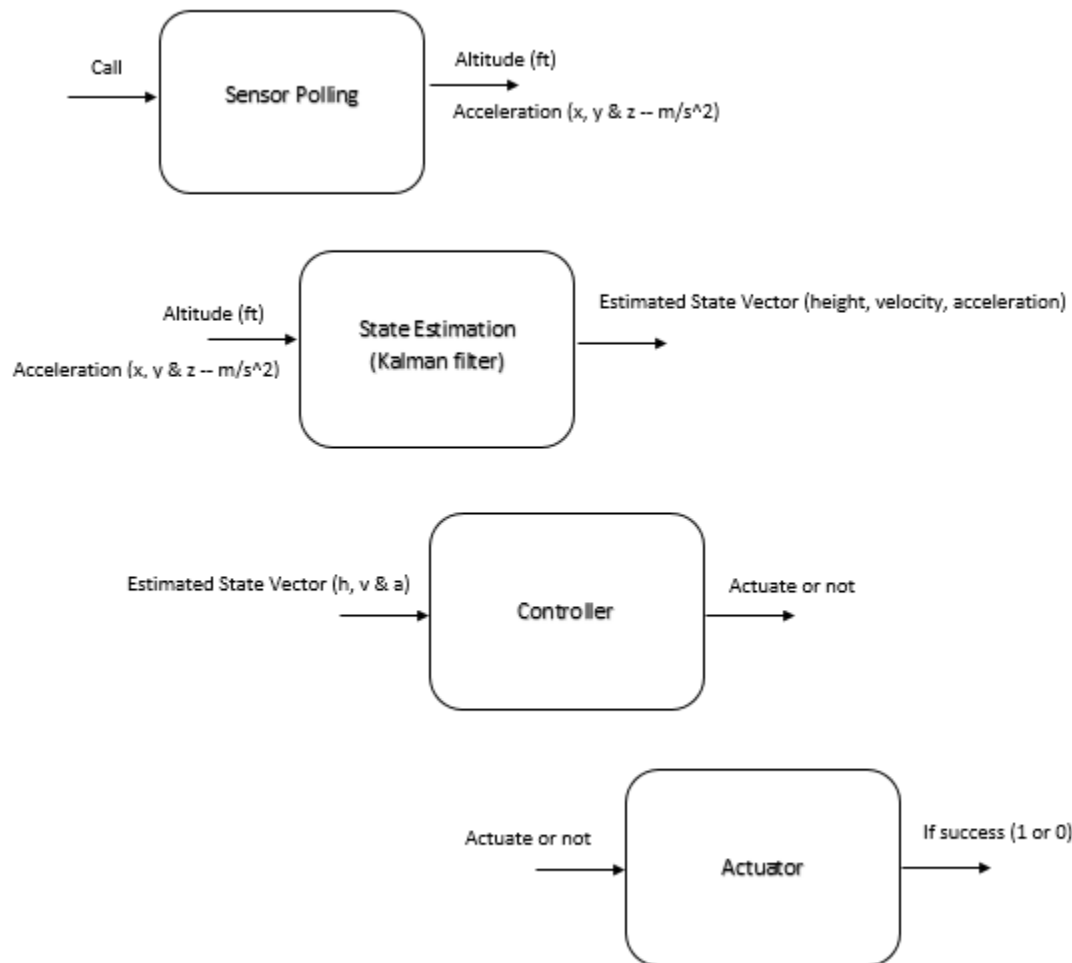
Figure XX. A flowchart which describes the functionality of the flight software's four main functions: Sensor Polling, State Estimation, Controller, and Actuator.

The process of scheduling the blocks of code begins with polling the sensors. This code block outputs an altitude and acceleration vector which is then input into the State Estimation block. The State Estimation block runs five times for every single time the sensors are polled. This process allows the State Estimation block to compare the sensed data to the ideal path of the rocket, which has been created via simulation. This process continues 20 times before the controller code block is scheduled. Based on the estimated state, the Controller block outputs whether to actuate or not. The Controller, and thus the Actuator, block runs every 100th time the state is estimated and every 20th time the sensors are polled.

The scheduling process allows the team the opportunity to choose how often the ATS is triggered as well as how much data is gathered before adjusting flight path. The altitude and acceleration data gathered during the sensor polling code block ultimately drive the decisions made throughout the rest of the code and lead to the decision of whether to correct flight path or not.

5.6. Flight Systems Verification

5.6.1. Mission Success Criteria and Verification

Requirement	Design Feature to Satisfy Requirement	Requirement Verification	Success Criteria
The vehicle shall not exceed an apogee of 5,280 feet	Drag from the ATS system	Full-scale flight test	Apogee within 1% of target
The vehicle will be tracked in real- time to locate and recover it	GPS module will be used in the vehicle and base station	Full-scale flight test	The vehicle will be located on a map after it lands for recovery
The data of the vehicle's flight will be recorded	Sensors will save data	Full-scale flight test	The data will be recovered and readable after flight

5.7. Safety and Failure Analysis

6. Launch Operations Procedure

Launch procedures will proceed from pre-launch to launch and conclude with post-launch. Each phase of the launch procedures has its own checklist that details the necessary steps to have a successful launch.

6.1. Launch Checklist

PRE-LAUNCH		
Checklist	**Performer**	**Inspector**
Pack all necessary equipment/supplies the night before team leaves for the launch site.		
On the morning of departure, check to make sure all necessary equipment/supplies have been stored in a secure manner.		
LAUNCH		
Checklist	**Performer**	**Inspector**
Prepare Payload Bay		
Ensure the batteries and switches are properly connected to the altimeters.		
Ensure the batteries, power supply, switches, data recorders, and pressure sensors are properly wired.		
Install and secure new batteries into the battery holders.		
Insert the altimeter and payload into the payload bay.		
After connecting the appropriate wires, verify that the payload powers are turned on and working properly. If the payload power does not work, check the wiring schematics. Turn off payload power afterwards.		
Arm the altimeters to verify the jumper settings. Check the battery voltage and continuity once the altimeters have been armed.		

Disarm the altimeters afterwards.		
Assemble Charges		
Test e-match resistance and make sure it is within specifications.		
Remove protective cover from e-match.		
Measure the required amount of black powder that was determined during testing.		
Place e-match on tape with the sticky side facing up.		
Pour the black powder over the e-match and seal the tape.		
Retest the e-match resistance.		
Check Altimeters (Figure 1 for configurations)		
Ensure altimeters have been properly disarmed.		
Connect charges to the ejection wells/altimeter bay.		
Turn on altimeters and verify continuity. Disarm altimeters afterwards.		
ALTIMETER 1		
ALTIMETER 2		
Pack Parachutes		
Connect drogue shock cord to booster section and altimeter.		
Fold excess shock cord so it does not tangle.		
Add Nomex cloth to ensure only the Kevlar shock cord is exposed to ejection charge.		
Insert altimeter bay into drogue section and secure with shear pins.		
Pack main chute.		
Attach main shock cord to payload bay.		
Assemble Motor		
Follow manufacturer's instruction.		

Use the necessary safety equipment needed such as gloves and safety glasses.		
Be careful not to get any grease on propellant or delay grain.		
Do not install the igniter until at launch pad.		
Install motor in launch vehicle.		
Secure motor retention system.		
Final Preparation		
Turn on payload via a switch and start stopwatches.		
Install skin.		
Inspect the launch vehicle. Verify the CG in order to make sure it is in safe range. Add nose weight if necessary.		
Bring launch vehicle to the range safety officer (RSO) table for inspection.		
Bring launch vehicle to pad, install on pad, and verify that it can move freely.		
Install igniter in launch vehicle.		
Touch igniter clips together to make sure they will not fire igniter when connected.		
Make sure clips are not shorted to each other or blast deflector.		
Arm altimeters via switches and wait for continuity check for both.		
Connect shock cord to nose cone, install nose cone, and secure with shear pins.		
Launch		
Stop the stopwatches and record time from arming payload and launch.		
Watch flight so launch vehicle sections do not get lost.		

POST-LAUNCH

Checklist	Performer	Inspector
Recovery		
Recover launch vehicle, document landing.		
Disarm altimeters if there are any unfired charges.		
Disassemble launch vehicle, clean motor case, other parts, and inspect for damage.		
Record altimeter data and download payload data.		

Figure 1. Altimeter On/Off Configurations.

7. Project Plan

7.1. Budget Plan

The projected project budget is approximately $5.872.38 – below the projected fundraising goal by just over 11%. This cost was derived using the actual project costs from the 2015-2016 NASA SLI competition cycle and a 15% margin was added to the Launch Vehicle and Flight Systems costs during the previous project cycle. The project budget breakdown is listed numerically in Table XY: Budget Summary and graphically in Figure Xy2.

Section	Cost
Avionics	$700.00
AGSE	$808.60
Launch Vehicle	$963.78
Motors	$1,000.00
Operations	$300
Outreach	$1,250
Total Budget	$5,022.38

7.2. Funding Plan

In order to fund the 2015-2016 competition cycle, Team ARES have sought sponsorships from academic and industry sources. The current sponsors of Team ARES and their predicted contributions can be found in Table XX. Additionally, the Team has also received a dedicated room in which the Team can construct and store their launch vehicle, payload, and other non-explosive components. All explosive components (i.e. black power) are properly stored in Fire Lockers in either the Ben T. Zinn Combustion Laboratory or the Ramblin' Rocket Club Flammable Safety Cabinet. Furthermore, the Georgia Tech Invention Studio and AE Maker Space will support all fabrication needs of the Team.

Sponsor	Contribution	Date
Georgia Space Grant	$1,200	Nov 2015

2014-2015 Unused Funds	$1,000	Jan 2016
Daniel Guggenheim School of Aerospace Engineering	(est. $1,000)	March 2016
Corporate Donations	(est.) $2,000	March 2016
GT Student Foundation	$1,295.00	Feb 2016
Orbital ATK Travel Stipend	Est $400	Feb 2016

7.3. Timeline

Team ARES project is driven by the design milestones set forth by the NASA SLI Program Office.

Deadline	*Date*
Team Formation	20 AUG
Proposal	11 SEPT
Web Presence Established	6 NOV
PDR Documentation	9-20 NOV
PDR Teleconference	15 JAN
CDR Teleconference	19-29 JAN
AGSE, Flight Systems, and Launch Vehicle Testing	29JAN – 20 FEB
Full Scale Testing and Launching	12 MAR
FRR Documentation	14 MAR
FRR teleconference	14 MAR
Competition	12-16 APR
PLAR Documentation	29 APR

The design milestones are listed in Table XX. The project Gantt chart for Project Hermes –contains only high-level activities due to the unique launch vehicle and payload designs. A more detailed Critical Path chart is located in Section XX.

 Critical Path Chart: CDR to PLAR

The critical path chart illustrated below demonstrates the highly integrated nature of Project

Hermes. The critical path chart identifies:

• High Risk Tasks – red boxes

• Low-Moderate Risk Tasks – pink boxes

• Earned Value Management (EVM) Goal Tasks – gold boxes

• Nominal Tasks – grey boxes

• Critical Path – green arrow

• Non-Critical Path – black arrows

• Current Place on the Critical path – blue outline

       7.3.1. Gantt chart

       7.3.2. Critical Path

7.4. Educational Engagement Plan and Status

       7.4.1. Overview

The goal of Georgia Tech's outreach program is to promote interest in the Science, Technology, Engineering, and Mathematics (STEM) fields. Team A.R.E.S. intends to conduct various outreach programs targeting middle school Students and Educators. Team A.R.E.S. will have an outreach request form on their webpage for Educators to request presentations or hands-on activities for their classroom. The team plans to particularly encourage requests from schools in disadvantaged areas of Atlanta, with the goal of encouraging students there to seek careers in STEM fields.

       7.4.2. Atlanta Maker's Faire

Team ARES had a booth at the Atlanta Makers Fair, a fair in which various craftsman from the community and Georgia Tech assemble to show off their accomplishments. The intent of this program is to give clubs, organizations, and other hobbyists the opportunity to show others their unique creations and skills. The event is open to the entire Atlanta community and had a large attendance this year. The Team ARES booth had a display of our various rockets, as well as a

station for children to use stomp rockets. Our booth had 45-60 middle school aged children attend and participate in the stomp rocket activity across the two days.

7.4.3. CEISMC GT

The Center for Education Integrating Science, Mathematics, and Computing (CEISMC) is a partnership uniting the Georgia Institute of Technology with educational groups, schools, corporations, and opinion leaders throughout the state of Georgia. Team ARES is dedicated to the enhancement of STEM education and will look forward to partnering with CEISMC and their events in the near future.

8. Safety

Team A.R.E.S. is dedicated to maintaining safe operating conditions for all team members and anyone involved in competition activities. Team A.R.E.S. will undergo rigorous safety training to ensure the integrity and safety of the entire team and equipment is constant. During manufacturing, fabrication, and testing of the launch vehicle and AGSE components, it is important to follow safety procedures and protocols in order to prevent accidents, personal injuries or injuries to others, and damage to all competition hardware.

When working with construction equipment, team members are instructed to work in minimum team sizes of two. This ensures that at least one team member is always available to provide immediate assistance should an incident occur while using any construction equipment. The Invention Studio at Georgia Tech houses a multitude of necessary equipment for manufacturing and fabrication. Many of these equipment's are used to construct the launch vehicle as well as the AGSE. In order to use the equipment, all team members have been briefed on the proper protocols and procedures of using the lab equipment. Risk identification and mitigation techniques are used to assess the dangers of tools and activities to personnel, and how they may create safe operation conditions. The studio has first aid kits, safety goggles, fire extinguishers, as well as expert supervision at all times.

Personal injuries can occur at any given time throughout the entire project. Each individual should be aware and alert at all times when working on the launch vehicle and/or AGSE. Warning labels on hazardous materials should be thoroughly read. Equipment should only be used with authorized personnel present. Each team member should be familiar with the safety hazards and prevention methods listed in this document as well as in the safety handbook provided by NASA. Every team

member understands that the safety guidelines and procedures outlined must be followed at all times. Failure to do so may result in injury and/or death.

The team understands that building a rocket requires the use of many equipment and/or materials throughout the entire design process. Despite the complexity of building a rocket, the environment must be taken into account at all times. Hazardous materials must be properly disposed of. Launches may only take place on authorized days and times. The Material Safety Data Sheet (MSDS) for each material used must be thoroughly read by each team member. Team ARES will do its best to ensure that the negative impact on the environment is at a minimum while designing the launch vehicle.

8.1. Launch Vehicle

Key points on launch vehicle safety include proper construction and assembly of both the launch vehicle itself and the launch vehicle recovery subsystem. The majority of dangers/failures can be dealt with during assembly and construction. As long as team members follow all safety guidelines while constructing the launch vehicle, proper construction of the launch vehicle and its recovery subsystem can be ensured. Proper construction will result in a successful launch. A successful launch will include successful recovery as well as no injuries whatsoever to any team member.

8.2. AGSE

Key points on AGSE safety include proper construction, assembly, and testing of the AGSE and its electrical subsystem. Team members must ensure no one gets injured while the AGSE is assembled. Testing to check the strength and support capability of the AGSE must be done with other group members as well as an authorized personnel present. When constructing the electrical subsystem, team members must be aware of potential hazards when dealing with batteries, wires, and electronics.

8.3. Safety and Quality Assurance

Safety is of paramount importance to Team A.R.E.S. All team members must be aware of all safety guidelines during all phases of the project. Each phase (construction, assembly, launch, and recovery) has its own safety guidelines and hazards that must be taken seriously. Team

A.R.E.S.'s safety goal is to have no injuries occur to any team member. With proper training and guidance, all team members will have a safe and knowledgeable project experience.

9. Conclusion